

Effects of apoptotic inhibitor addition to cell viability prolongation of suspended bench-scale CHO culture and analysis of Raman spectra in off-line bioreactor samples

By

Juan Carlos Rosario

A thesis submitted in partial fulfillment of the requirements for the degree of

Master of Science

in

Chemical Engineering

University of Puerto Rico at Mayagüez

2010

Approved by:

Lorenzo Saliceti Piazza, Ph.D.
President, Graduate Committee

Date

Juan Carlos Sáez, Ph.D.
Member, Graduate Committee

Date

Walter Silva, Ph.D.
Member, Graduate Committee

Date

Rodolfo Románach, Ph.D.
Member, Graduate Committee

Date

Jaime E. Ramírez-Vick, Ph.D.
Representative of Graduate Studies

Date

David Suleiman, Ph.D.
Chairperson of the Department

Date

Abstract

The productivity of suspended mammalian cell cultures plays a major role in the overall manufacturing costs of biotechnology products. Upstream cell culture product variability can lead to problems in downstream purification and even in the quality of the final product. Amino acids and carbohydrates are the major raw substrates of mammalian cell metabolism. Knowing the ways in which the cells use these nutrients, researchers can gain a better understanding of what factors contribute to productivity, variability and apoptosis in cell culture processes. To achieve this knowledge, Raman spectroscopy can be used to develop a non-invasive, in-line tool to monitor and better understand the mammalian cell growth process in real-time. Our work is focused in implementing this analytical method as a way to monitor off-line cell metabolism and death under different culture conditions, such as two levels of temperature set points and presence or absence in the culture medium of an apoptosis inhibitor (Cytochrome C inhibitor). Techniques such as HPLC and biochemical analyzers were used as reference methods to validate the Raman spectra as a routine measurement in suspended mammalian cell culture processes and to monitor metabolic pathway changes. It is expected that the implementation of this methodology in-line will result in a better comprehension of mammalian cell culture in real-time and an improvement of productivity in such systems, as well as a tool towards implementation of process analytical technologies (PAT).

Eight batches of suspended cultures of Chinese hamster ovary (CHO) cells were performed under four different conditions. The best parameters were a temperature shift of 35-33°C in 2.5 days with addition in the media of the apoptotic inhibitor (Cytochrome C inhibitor). In this case, twelve run days were achieved with viability between ninety and eighty percent with a substantial increment in L-lactate of approximately 35% as a secondary metabolite and a constant cell density on the entire runs. In addition to this condition a cell viability decay rate was observed. For conditions with temperature shift of 37-33°C in 2.5 days and over-expression or addition of the anti-apoptotic molecule, data obtained show that even though a higher viability was achieved, the run days could not be extended, an increment of approximately 35% on L-lactate production was also observed and the cell density decay rate was faster.

This increment shows the possibility of double inhibition by the over-expression of the apoptotic inhibitor. As a consequence, these simultaneous inhibitions affect the cell metabolism and avoid the normal process of gluconeogenesis as published by Centocor with the use of another apoptotic inhibitor. These present increments on L-lactate provoke the use of more base in the process to stabilize and maintain pH measurements among the runs showing increments in osmolality values too.

The proposed use of Raman to monitor cell metabolism and apoptosis was assayed in an off-line mode providing promising results for cell metabolism monitoring (secondary and primary metabolites). The case of cell viability identification is still a matter of study. Peaks of some intracellular components were identified and they would constitute a subject of study to model any increase that could be associated with cellular survival or death.

Resumen

La productividad de los cultivos suspendidos de células mamíferas juega un rol importante en el costo de la manufactura de productos biotecnológicos. La variabilidad en esta parte del proceso puede propiciar problemas en etapas subsiguientes, como lo es la purificación; provocando posibles cambios negativos en la calidad del producto final. Amino ácidos y carbohidratos son la mayor fuente principal de sustratos en el metabolismo celular de un mamífero. Comprendiendo las maneras en que las células utilizan estos nutrientes los investigadores pueden obtener una mayor comprensión de que factores contribuyen a la productividad, variabilidad y la apoptosis en los cultivos celulares.

Para alcanzar este entendimiento, la espectroscopía Raman puede ser utilizada para desarrollar una herramienta no invasiva en línea para monitorear y comprender mayor el crecimiento celular mamífero en tiempo real. Nuestro trabajo se enfoca en implementar este método analítico como una manera de monitorear fuera del cultivo (off-line) el metabolismo celular y la muerte celular bajo diferentes condiciones operacionales en el cultivo. Dos parámetros con dos niveles cada uno fueron estudiados. Rangos de temperatura entre 35-33° C y 37-33 °C y la presencia de el inhibidor de apoptosis (inhibidor de citocromo C) en el medio. Técnicas tales como el HPLC y analizadores bioquímicos fueron usados como métodos de referencia para validar los espectros de Raman obtenidos para ser usados como medidas de rutina en cultivos celulares suspendidos de células mamíferas y de una vez analizar y observar los cambios en rutas metabólicas si alguno.

Se espera que la implementación de esta metodología en línea y tiempo real resulte en una mayor comprensión de los cultivos celulares en tiempo real y un mejoramiento en la productividad de estos sistemas, así también como una herramienta para la implementación de técnicas de análisis de procesos.

Ocho lotes de cultivos de células de un hámster chino fueron hechos bajo cuatro condiciones distintas. Los mejores parámetros o condiciones fueron aquellas con el rango de temperatura de 35-33°C con la sobre expresión en el medio del inhibidor apoptótico. Para ese caso, doce días de cultivo fueron alcanzados con un por ciento de viabilidad entre noventa y ochenta con un

incremento substancial en L-lactato como metabolito secundario y una densidad celular constante en las corrida completa. En el caso de los lotes con las condiciones de rango de temperatura de 37°C y descendiendo a 33°C en un término de dos días y medio con sobre expresión del inhibidor, la data obtenida demuestra que aunque un porcentaje de viabilidad alto fue alcanzado, los días de la corrida no fueron extendidos y un incremento en L-lactato fue también observado.

Este incremento demuestra la posibilidad de una doble inhibición por la sobre expresión del inhibidor apoptótico. Como consecuencia, estas inhibiciones simultáneas afectan el metabolismo de la células y evitan el proceso normal de gluconeogenesis; esto también es resaltado en un artículo publicado por Centocor con el uso de otro inhibidor apoptótico. El uso de Raman propuesto para monitorear el metabolismo celular y la apoptosis fue estudiado de manera invasiva extrayendo muestra y analizándola diariamente, proveyendo resultados prometedores para monitorear el metabolismo celular (mayormente metabolitos secundarios y primarios). En el caso de identificar o detectar cambios en la viabilidad todavía se está estudiando. Picos de algunos componentes intracelulares fueron identificados y deben ser estudiados para modelar cualquier incremento que pueda estar asociado con la supervivencia o muerte de las células.

Dedicated to My Lord and Savior Jesus who gives me the strength every day to wake up and be grateful; my mom Ana Sylvia Borrero and my beloved wife Madeline Del Valle, who are my inspiration and support every day.

Acknowledgements

In my time as graduate student at the University of Puerto Rico several persons and institutions collaborated directly and indirectly with my research and my personal development. Without their support it would be very difficult for me to finish this work and by consequence my degree. This section is dedicated to any person and institution that influenced my career in certain positive ways.

I want to begin expressing my gratitude to my advisor and president of my graduate committee, Dr. Lorenzo Saliceti Piazza. The opportunity and the liberty to create and think that he gave me opening the doors to do what I did in mammalian cell culture shows that with God, good will, the encouragement and help of intellectual people like him, everyone can reach higher in the world of science, but most importantly in life. We became the first academic research laboratory in Puerto Rico developing a reproducible bench-scale upstream process to study mammalian cell culture in suspended cells. We tried and we did it, this thesis is proof of that.

I also want to thank Dr. Walter Silva for his support, encouragement and guidance, his ideas brought form to this work in the first place. I also thank Dr. Rodolfo Romañach and his research group, for the hours of guidance and training in the use of Raman spectroscopy, without that this thesis would not be completed.

I also want to thank one department and one institution, respectively. The Industrial Biotechnology Program for letting me use a great infrastructure such as the Industrial Biotechnology Learning Center, better known as IBLC; 3M company and the GEM fellowship, for their monetary support, guidance and encouraged me to pursue a Master of Science in Chemical Engineering. Finally, I really want to thank Dr. Juan-Carlos Sáez for his support and direction in one of the goals for this work which was the identification of intracellular molecules with Raman Spectroscopy and the people of Abbott Biotechnology who gave me the opportunity to learn the basics on this field and encourage me in the pursuit of focus in my career.

Table of Contents

ABSTRACT.....	i
RESUMEN.....	iii
ACKNOWLEDGEMENTS.....	vi
TABLE OF CONTENTS.....	vii
LIST OF TABLES.....	ix
LIST OF FIGURES.....	x
1. INTRODUCTION.....	1
1.1 OBJECTIVES.....	2
1.1.1 General Objectives.....	2
1.1.2 Specific Objectives.....	3
1.2 REFERENCES	3
2. LITERATURE REVIEW.....	5
2.1 HISTORICAL BACKGROUND.....	5
2.2 UNDERSTANDING APOPTOSIS IN MAMMALIAN CELLS	6
2.3 METABOLISM IN MAMMALIAN CELL CULTURE AND ITS LINK WITH APOPTOSIS	10
2.3.1 Glucose as a Primary Substrate.....	10
2.3.2 Hexokinase Link with Apoptosis.....	11
2.4 PAT IMPLEMENTATION IN MAMMALIAN CELL CULTURE BIOPROCESSES	12
2.5 RAMAN SPECTROSCOPY HISTORY AND FUNDAMENTAL THEORY	14
2.6 APPLICATION OF RAMAN SPECTROSCOPY IN MAMMALIAN CELL CULTURE MONITORING.....	17
2.7 STATISTICS APPROACH IN BIOPROCESS-FACTORIAL DESIGNS, MULTIPLE RESPONSE FUNCTIONS, AND FUNCTIONS ALONG TIME.....	19
2.8 CHINESE HAMSTER OVARY CELL CULTURE AT BENCH AND MANUFACTURING SCALES	25
2.9 REFERENCES	27
3. MATERIALS AND METHODS	31
3.1 CELL LINE	31
3.2 INOCULUM PREPARATION	32
3.3 BENCH-SCALE BIOREACTOR BATCH EXPERIMENTS AND SET-UP.....	34
3.4 APOPTOSIS INHIBITOR ADDITIONS	35
3.5 DETERMINATION OF GLUCOSE AND L-LACTATE CONCENTRATIONS	36
3.6 DETERMINATION OF CELL VIABILITY AND CONCENTRATION	37
3.7 OSMOLALITY DETERMINATION.....	38
3.8 RAMAN EQUIPMENT PROCEDURE AND ANALYSIS.....	39
3.9 CHINESE HAMSTER OVARY CELLS UPSTREAM PROCESS SIMULATION.....	40
3.10 REFERENCES	42
4. EXPERIMENTAL RESULTS AND DISCUSSION.....	43
4.1 CELL CULTURE RESPIRATION PROFILE	43
4.2 DETERMINATION OF GLUCOSE, L-LACTATE, OTHER METABOLITES AND INTERNAL CELL MATERIAL USING RAMAN SPECTROSCOPY	45
4.2.1 REGIONS OF SPECTRAL ANALYSIS	52
4.2.2 DESCRIPTION OF THE PRIMARY DATA SETS	52
4.2.3 RAW DATA EVALUATION.....	55
4.3 DETERMINATION OF GLUCOSE AND L-LACTATE USING THE HPLC AND THE BIOCHEMICAL ANALYZER (YSI 2300).....	55
4.4 SUITABLE FITS OF X/Y VARIABLES FOR GLUCOSE AND L-LACTATE	58
4.5 PREDICTIONS AND VALIDATION	65
4.6 DETERMINATION OF VIABILITY USING RAMAN SPECTROSCOPY	72

4.7 REFERENCES	75
5. CONCLUSIONS AND RECOMMENDATIONS.....	77
5.1 HIGH VIABILITY PROLONGATION VIA CYTOCHROME C INHIBITION AND BEST OPERATIONAL CONDITIONS ...	77
5.1.1 CONCLUSIONS	77
5.1.2 RECOMMENDATIONS AND FUTURE WORK	78
5.2 DETERMINATION OF GLUCOSE AND L-LACTATE USING RAMAN SPECTROSCOPY	79
5.2.1 CONCLUSIONS	79
5.2.2 RECOMMENDATIONS AND FUTURE WORK	80
5.3 DETERMINATION OF INTRA CELLULAR MATERIAL AND VIABILITY USING RAMAN SPECTROSCOPY; A POSSIBLE WAY OF MEASURE CELL HEALTH AND BY CONSEQUENCE CELL VIABILITY	80
5.3.1 CONCLUSIONS	80
5.3.2 RECOMMENDATIONS AND FUTURE WORK	81
APPENDIX	81

List of Tables

Tables	Page
Table 2.1 Optimization Values obtained using the function “optimizer” in Minitab for the cell density ad viability responses.....	25
Table A.1 Viability for all runs with the respective cell diameters per run.....	83
Table A.2 Cell Density as a function of time.....	83
Table A.3 Specific growth rate and cell doubling time.....	84
Table A.4 Glucose, L-lactate and osmolality.....	84

List of Figures

Figures	Page
Figure 2.1 Apoptosis central activation cascade (mitochondria).....	9
Figure 2.2 Glucose metabolic pathways in mammalian cells.....	11
Figure 2.3 Different Raman scattering models.....	17
Figure 2.4 Two-factor factorial experiment used in this work.....	20
Figure 2.5 Viability coefficients.....	23
Figure 2.6 Cell density coefficients.....	24
Figure 2.7 L-lactate coefficients.....	24
Figure 3.1 2 mL cryo-vial with 1.5×10^7 cells from Invitrogen.....	32
Figure 3.2 first stages of inocula.....	32
Figure 3.3 Second and third stage of the inocula phase.....	33
Figure 3.4 Autoclavable 3L Applikon bioreactor.....	33
Figure 3.5 YSI 2300 (biochemical analyzer).....	37
Figure 3.6 Shimadzu HPLC.....	37
Figure 3.7 Auto T4 cell counter, Nexcelom Company.....	37
Figure 3.8 Fiske 3320 Micro-osmometer.....	38
Figure 3.9 Raman spectroscopy of samples for eight cell culture batches (first and last day of each run).....	39
Figure 3.10 P&ID of CHO cell upstream process using Super Pro designer software.....	40
Figure 3.11 Grant chart schedule for the CHO cell upstream process as generated by Super Pro designer software.....	41
Figure 4.1 Cell density measurements as a function of time, with or without inhibitor at 35-33°C temperature range (a) and with or without inhibitor at 37-33°C temperature range (b). Duplicate batch runs shown.....	46

Figure 4.2 L-Lactate concentrations as a function of time monitored with the YSI 2300, a biochemical analyzer. The HPLC was used for the cases in which the anti-apoptotic molecule was over-expressed.....	47
Figure 4.3 Glucose consumption as a function of time, measured using the YSI 2300 analyzer.	48
Figure 4.4 Sample measurements for all conditions and their replicate for cell viability as a function of time with or without inhibitor at 35-33°C temperature range (a) and with or without inhibitor at 37-33°C temperature range (b).....	49
Figure 4.5 Cell viability as a function of time at both temperatures ranges (a) and L-lactate concentrations at both temperatures ranges (b).....	50
Figure 4.6 Raman spectra for suspended CHO cells culture system as seen in SIMCA Plus software. Culture days 1-9 of condition 1: 35-33°C and no inhibitor present in the media.	53
Figure 4.7 Raman Spectra for suspended CHO cells culture system as seen in SIMCA Plus software. Culture days 1-9 of condition 4: 37-33°C and no inhibitor present in the media.	53
Figure 4.8 Raman Spectra for suspended CHO cells culture system as seen in SIMCA Plus software. Culture days 1-9 of condition 3: 35-33°C and the inhibitor present in the media.....	54
Figure 4.9 Raman Spectra for suspended CHO cells culture system as seen in SIMCA Plus software. Culture days 1-9 of condition 2; 37-33 °C and the inhibitor present in the media.....	54
Figure 4.10 A representative example of Raman spectra obtained for day 1 and day 9 for each of the eight-batch culture performed. Graph shows Raman intensity in Absorbance Units (A.U.) as a function of the Raman shift in cm^{-1}	56
Figure 4.11 A representative chromatogram of a CHO cell culture sample using the HPLC reference method.....	57
Figure 4.12 A fit suggested for the cases 1-3-5-7 shown as A; that the components (glucose and L-lactate) find the direction in X space which get better the X-data description and provide a good correlations with the Y residuals.....	60
Figure 4.13 A fit for L-lactate suggests a correlation between the observed values and model predicted values obtained with the Raman spectral data.....	60
Figure 4.14 A fit is also observed for L-lactate in two of the three analyses performed for cross-validation at ranges of 700-800 cm^{-1}	61
Figure 4.15 Score t_1 versus t_2 for experiments 1, 3, 5, and 7 (A) using PCA analysis.....	62

Figure 4.16 Score t_1 versus t_2 for experiments 2 and 8 (B) using PCA analysis.....	63
Figure 4.17 Hotelling T2 range plots of glucose and L-lactate components containing experiments 1, 3, 5, and 7 (A) at a range of 1000-1100 cm^{-1}	63
Figure 4.18 Hotelling T2 range plots of L-lactate and glucose containing Experiments 1, 3, 5, and 7 (A) from range 500-600 cm^{-1}	73
Figure 4.19 Hotelling T2 range plots of L-lactate and glucose containing experiments 1, 3, 5, and 7 (A).....	64
Figure 4.20 Relationship between observed and predicted values for experiments 1 & 5 (a), 2 & 8 (b), 3 & 7 (c) and 4 & 6 (d) at a 1000-1100 cm^{-1} suggested range to determine glucose concentration.....	67
Figure 4.21 Relationship between observed and predicted values for experiments 1 & 5 (a), 2 & 8 (b), 3 & 7 (c) and 4 & 6 (d) at a range of 500-600 cm^{-1} to determine L-lactate concentration.....	69
Figure 4.22 Relationship between observed and predicted values for experiments 1 & 5 (a), 2 & 8 (b), 3 & 7 (c) and 4 & 6 (d) at 700-800 cm^{-1} to determine L-lactate concentration.....	71
Figure 4.23. Raman spectra of four experimental conditions. Aromatic amino acids and lipid regions are marked. Clear broadening and increase in peaks is also shown.....	74

1. Introduction

Apoptosis is a cellular process wherein mammalian cells initiate a series of events that lead to their ultimate death. It is a phenomenon as important to cell life cycle regulation as well as to growth processes such as mitosis. Normal cells use apoptosis to insure appropriate development and protection against anything that may threaten cell integrity. Abnormal cells lose the ability to properly regulate themselves through apoptosis. When there is not enough apoptosis, cells will grow out of control as demonstrated in cancerous disease states.

There are three mechanisms by which cells may initiate apoptosis: the intrinsic pathway, the extrinsic pathway, and the apoptosis-inducing factor (AIF). In the intrinsic pathway, the apoptotic process is triggered by internal cellular signals. On the contrary, the extrinsic pathway is due to an external signaling mechanism. Independent of the intrinsic and extrinsic pathways, some cells require a specific protein, AIF, to trigger apoptosis.

Regardless of the mechanism by which apoptosis occurs, there are a series of morphological changes that are detectable and considered to be the standard to define the mode of cell death [1]. Some of the changes include cell shrinkage, cell surface blebbing, nuclear chromatin condensation, and apoptotic body formation. Typically, using simple techniques such as microscopy, cytometry and imaging, morphological changes can be detected.

The morphological changes of cells during the apoptotic process are due to underlying biochemical and molecular events. These events are more difficult to determine because they typically require complex cellular assays that are usually tedious, unreliable, or lead to results that in certain ways are difficult to interpret. For example, Annexin V is a common cellular assay to confirm apoptosis. Apoptotic cells lose their ability to regulate the composition of their lipid membranes and phosphatidylserine, which is located on the internal plasma membrane in normal cells, and it is externalized and expressed on the outer plasma membrane of apoptotic cells [2].

Annexin V is a protein that binds to phosphatidylserine (PS) and is used as a fluorescent marker to label PS in several commercially available apoptosis assay kits. Even though Annexin V is a current method to detect apoptosis, challenges remain in the interpretation of the results from this type of assay [3].

There is a need to be able to detect the biochemical changes (metabolites and cell health) in cells in real-time without a reagent-based, multi-step cellular assay. Raman spectroscopy and chemometrics offer an opportunity to implement such techniques, providing specific molecular information in-line and in real-time with no need to collect samples and risk the bioreactor aseptic condition. The question that we are going to address in this work is whether Raman spectroscopy and Raman chemical imaging can be used to measure relevant biological changes in suspended cultures of Chinese hamster ovary (CHO) cells.

Previous Raman spectroscopy assessment of cell and tissue samples has been demonstrated in the literature on a broad group of cells and tissues [4-10], but not for detection of apoptosis in suspended culture of CHO cells.

1.1 Objectives

Our research objectives could be classified as general or specific.

1.1.1 General Objectives

- To monitor off-line in a batch culture of suspended mammalian cell culture:
 - Cell growth (viability, cell density and mean diameter),
 - substrate concentration,
 - by-product concentration and production,
 - osmolality.
- To test an operating temperature range for a better operational condition and the use of an apoptosis inhibitor to prevent any damage and maintain cell density and viability.
- To test an off-line Raman spectroscopy sampling method as a further process

analytical technology (PAT) tool to monitor metabolites and cellular components that could indicate apoptosis in suspended mammalian cell culture at batch mode in real-time.

1.1.2 Specific Objectives

- To implement multivariate analysis such as partial least squares (PLS) to create and validate models to monitor substrates and metabolites in a suspended mammalian cell culture using Raman spectroscopy with HPLC and membrane-immobilized enzyme analytical tests (YSI) as reference methods.
- To use chemometrics to correlate Raman spectra with Cytochrome C inhibitor dynamics.

1.2 References

- [1] Yin, Xiao and Dong, Zeng. 2001. Essential of Apoptosis, Humana Press, 300 pp.
- [2] Desagher, S. and Martinou, J. 2000. Mitochondria as the central control point of apoptosis. *Trends Cell Biol.* **10**:369-377.
- [3] Darzynkiewicz, Z. , Huang, X. , Okafuji, M. , and King, M.A. 2004. Cytometric methods to detect apoptosis. *Methods in Cell Biology* **75**:307-341.
- [4] Kuypers, F., Lewis, R., Hua, M., Schott, A., Discher, D., Ernst, J. and Lubin, B. 1996. Detection of altered membrane phospholipids asymmetry in subpopulations of human red blood cells using fluorescently labeled Annexin V. *Blood* **87**(3):1179-1187.
- [5] Gatti, R., Belletti, S., Orlandini, G., Bussolati, O., Dall'asta, V., and Gazzola, G. 1998. Comparison of Annexin V and calcein-AM as early vital markers of apoptosis in adherent cells by confocal laser microscopy. *J. Histochem. Cytochem.* **46**(8):895-900.

- [6] Shafer-Peltier, K., Haka, A., Fitzmaurice, M., Crow, J., Myles, J., Dasari, R., and Feld, M. 2002. Raman microspectroscopic model of human breast tissue: implications for breast cancer diagnosis *in vivo*. *Journal of Raman Spectroscopy* **33**(7):552-563.
- [7] Haka, A., Shafer-Peltier, K., Fitzmaurice, M., Crowe, J., Dasari, R., and Feld, M. 2002. Identifying micro calcifications in benign and malignant breast lesions by probing differences in their chemical composition using Raman spectroscopy. *Cancer Research* **62**(18):5375-5380.
- [8] Mahadevan-Jansen, A., Mitchell, M., Ramanujam, N., Malpica, A., Thomsen, S., Utzinger, U., and Richards-Kortum, R. 1998. Near infrared and Raman spectroscopy for in vitro detection of cervical precancers. *Photochemistry and Photobiology* **68**(1):123-132.
- [9] Richards-Kortum, R., Ramanujam, N., Mahadevan, A., and Follen Mitchell, M. 1997. Optical method and apparatus for the diagnosis of cervical precancers using Raman fluorescence spectroscopies. U.S. Patent No. 5,697,373.
- [10] Nijssen, A., Bakker, T., Schut, F., Heule, P., Caspers, D., Hayes, M., Neumann, H. and Puppels, G. 2002. Discriminating basal cell carcinoma from its surrounding tissue by Raman spectroscopy. *Journal of Investigative Dermatology* **119**(1): 64-69.

2. Literature Review

2.1 Historical Background

The past decade witnessed an unprecedented number of new arrivals to the biopharmaceutical market, the majority of these being complex therapeutic proteins produced in mammalian cell lines. Mammalian hosts have an innate capacity to perform post-translational modifications; in particular, glycosylation is of special interest as it influences the functionality and immunogenicity of such therapeutics. Several glycoproteins and monoclonal antibodies with relatively high production needs are being identified as new drug candidates. Consequently, the capacity for manufacturing these products in mammalian cell cultures, which nowadays reaches titers of 5 g/L, will remain a challenge [1].

Once a biopharmaceutical has been approved based on a given process, any significant deviation from the production protocol may require new clinical trials to test the safety of the resulting product (“process defines the product”). Since clinical trials are very expensive, process improvements are made under very hard constraints. Therefore, production processes are normally run far below their potential maximum performance. This concern, together with the fact that still a lot of batches cannot be used or have to be reprocessed for quality reasons, has led pharmaceutical companies to re-evaluate their future requirements in terms of bioprocess analysis and some of them are beginning to embrace process analytical technologies (PAT).

PAT is an initiative launched by FDA in 2004 (www.fda.gov/cder/ops/), encouraging the companies producing biopharmaceuticals to adopt modern bioprocess monitoring tools based on on-line or at-line analysis of key variables in all stages of the manufacturing processes. This will allow for early fault detection and thus to maximize the probability

of obtaining good product quality at the end of the process. A good example is the control of glycosylation during reactor operation, which is the most sensitive quality-related feature in recombinant proteins production [3]. The concentration of glucose, ammonia and dissolved oxygen as well as the culture temperature and osmolality are some of the variables that have been reported to determine glycosylation patterns in different recombinant proteins by *Andersen et. Al.* [3]; hence, their monitoring and control are essential for final product quality assurance. PAT is pushing for easy-to-use process analyzers, mathematical integration tools for data analysis and feedback control methods to perform process adjustments as necessary [4]. The major driving force for the penetration of PAT in the industrial environment is the possibility of using the continuous information collected to justify proposals for post approval process changes.

Apoptosis and metabolic controls are other important subjects with high relevance and their study has been very limited between decades in this kind of suspended cell culture. A clear knowledge of the phenomenon is still a matter of study and several works have been reviewed in the last decade, bringing more relevance and importance of these subjects to the field [5].

2.2 Understanding Apoptosis in Mammalian Cells

Currently, the production of therapeutic recombinant proteins relies heavily on the large-scale culture of eukaryotic cells that secrete the protein of interest into the media. It has been recognized that programmed cell death, or apoptosis, may pose a significant hurdle to maximum productivity in such systems. With a greater understanding of the molecular events causing apoptosis, alterations can be made to the cells and culture conditions to prevent or slow down apoptosis and enhance the bioreactor volumetric productivity [6]. This role that apoptosis (programmed cell death) plays in limiting culture performance has only relatively recently begun to be considered.

Apoptosis has evolved as a critical pathway in the development of multicellular organisms and has been shown to occur in essentially every commercially relevant cell type (hybridoma, myeloma, Chinese hamster ovary (CHO), baby hamster kidney (BHK),

and insect cells [5]. Programmed cell death is frequently a barrier to maintaining viable suspended cultures with high cell densities, and the prevention of apoptosis should, at least in theory, contribute to increase the production of recombinant proteins in bioreactor processes.

The ability to apply current knowledge about the apoptotic process and sub-cellular signaling pathways to industrial scale cell culture will contribute to the development of production systems where apoptosis is limited.

In general, cells undergoing apoptosis have received a death stimulus that is translated into an organized destruction of the cell. Transmission of this stimulus results in the activation of a family of cysteine proteases called caspases. Each caspase recognizes a characteristic consensus sequence of four amino acids and cleaves specific substrates after the C-terminal aspartic acid residue of the recognition sequence. Cleavage of these substrates results in activation or destruction of key molecules that coordinate cellular deconstruction.

The consequences of the apoptotic pathway require it to be tightly regulated. The best understood regulatory mechanism involves the Bcl-2 family of proteins. This family has both anti-apoptotic and pro-apoptotic members, many of whom are associated with the mitochondria. For example, anti-apoptotic Bcl-2 and Bcl-xL prevent the release of Cyt *c* from the mitochondria and can be found in the mitochondrial membrane. Members of the pro-apoptotic Bax subfamily are associated to cause Cyt *c* release.

Regulation at multiple points in the pathway is required to ensure that the apoptotic pathway is not initiated accidentally. The challenge for the biochemical engineers and biotechnologists is to apply this wealth of information to enhance large-scale cell-culture processes by identifying triggering events and modifying the culture environment or the cell itself.

To fully understand apoptosis in cell culture, it is important to consider the effects that may initiate the cell-death program. In spite of best efforts to maintain a uniform and optimal environment, cells in suspended culture are constantly exposed to changing conditions. Non-optimal conditions can produce cell death via one of two mechanisms: severe acute effects, such as a collision with the bioreactor wall, result in necrosis (accidental death); whereas chronic effects, such as nutrient depletion, typically result in apoptosis.

Another way to induce apoptosis in most cell types is serum withdrawal; however, there is a strong drive within the biotechnology industry towards the development of serum-free and protein-free manufacturing processes. Besides the cost and potential to interfere with the purification process, the relatively undefined nature of serum raises issues of lot-to-lot variability and, more seriously, the potential of introducing pathogenic impurities such as viruses. It is possible to adapt, or manipulate (engineer) cells to grow in serum-free medium while retaining good growth and productivity characteristics. Typically, such cells remain susceptible to apoptosis from other effects. Even though it has been reported that the re-addition of serum can protect serum-free adapted cells from apoptosis due to nutrient depletion either as a result of altered glucose metabolism or reduced abortive proliferation, this possibility is not well seen by the industry.

A common solution to the issue of nutrient depletion is the use of fed-batch culture processes, which involve a feeding strategy utilizing completely defined media to account for nutrient depletion. Nevertheless, these cultures are still susceptible to apoptosis, just at a later time point than their batch counterparts. Thus, a critical unidentified nutrient would be still missing and driving apoptosis in these fed-batch cultures.

Another potential candidate to induce apoptosis is the accumulation of toxic metabolites in the culture media. It has been shown that both ammonia and lactate can negatively impact cell growth rate and that increasing concentrations of ammonia can indeed cause apoptosis. Recently, the ability of hepatocytes (cells that make up 70 to 80% of the liver mass cells) to remove ammonia from the media has been employed in an interesting co-

cultivation strategy to improve the productivity of a CHO cell culture process.

Even though many causes of apoptosis in eukaryotic cells have been discussed in this short exposition, many others are in constant development at this moment. A correlation between causes and possible solutions to apoptosis is still unfinished. Clearly, many proteins are involved in this process and a combination of modifications in the expression of a number of these proteins will be required to achieve the desired outcomes of increased cell density, viability and productivity. A typical way of release is shown below in Figure 2.1 [41], Cytochrome C (Cyt. C) can be released by cellular stresses, such as DNA damage, heat shock, and oxidative stress, resulting in an increase in the permeability of the outer mitochondrial membrane. Upon release into the cytosol, Cyt. C binds to the apoptotic protease activating factor-1 (Apaf-1). Cytochrome C binding, in association with ATP results in a conformational change in Apaf-1 that promotes oligomerization. Pro-caspase 9 molecules can then bind to each Apaf-1. This high molecular weight complex is called the apoptosome and its formation promotes caspase-9 activation and finally, activation of the other caspases participating in the apoptotic cascade.

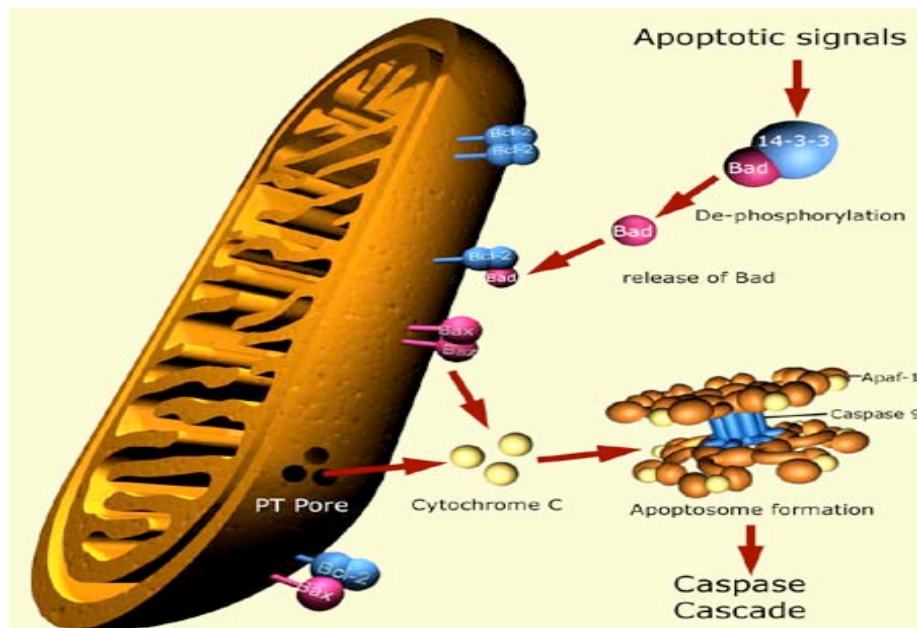


Figure 2.1. Apoptosis central activation cascade (mitochondria)[41].

Another important topic inside apoptosis is the ability to regenerate damaged tissues as a common characteristic of multicellular organisms. Why is this related? Some researchers recently reported a role for apoptotic cell death in promoting wound healing and tissue regeneration in mice [40]. Apoptotic cells release growth signals that stimulate the proliferation of progenitor or stem cells. Key players in this process are caspases 3 and 7, proteases activated during the execution phase of apoptosis that contribute to cell death. In this report, mice lacking either of these caspases were deficient in skin wound healing and in liver regeneration. Prostaglandin E2, a promoter of stem or progenitor cell proliferation and tissue regeneration, acted downstream of the caspases. The term proposed by the authors to denominate the pathway by which executioner caspases in apoptotic cells promote wound healing and tissue regeneration in multicellular organisms is the “Rising Phoenix” pathway [40].

2.3 Metabolism in Mammalian Cell Culture and its Link with Apoptosis

2.3.1 Glucose as a Primary Substrate

The primary metabolic substrate for industrial cell culture is glucose, which is maintained in media at concentrations of 20–25 mM. Glucose serves dual purposes in rapidly proliferating cells. The sugar can be metabolized to generate ATP and metabolic intermediates through glycolysis, the citric acid cycle, and oxidative phosphorylation [5]. Alternatively, glucose may be oxidized to provide precursors for nucleic acid and protein synthesis and NADPH for reducing power in biosynthetic reactions. The glucose metabolism pathway relies upon transport proteins (e.g., glucose transporter and VDAC) and metabolic enzymes (e.g., hexokinase, aldolase) to ensure glucose levels can meet the energy demands of a proliferating cell [6].

The glucose metabolism pathway begins with the transport of glucose into the cell from the medium through specific transport proteins, such as the GLUT-1 glucose transporter (Figure 2.2). Then, glucose is phosphorylated by hexokinase in the initial step of glycolysis and further broken down through the remaining nine steps of this pathway. Pyruvate, the main product of glycolysis (the others being ATP and lactate), enters the mitochondria matrix for utilization in the citric acid cycle. The citric acid cycle provides

precursors for the production of ATP via oxidative phosphorylation, and ATP exits the mitochondria through specific transporters for use within the cell. This is just a brief of the process, it is not the intention to fully describe all the metabolic pathways. The main purpose is to bring and briefly explain the relevance of glucose in the metabolic pathways but to explain the relevance of this step in our study. Finally, it is important to notice that even though apoptotic and metabolic pathways are distinct within cells, both converge on a shared set of proteins such as the BCL-2 family, hexokinase and GLUT-1 membrane protein, among others.

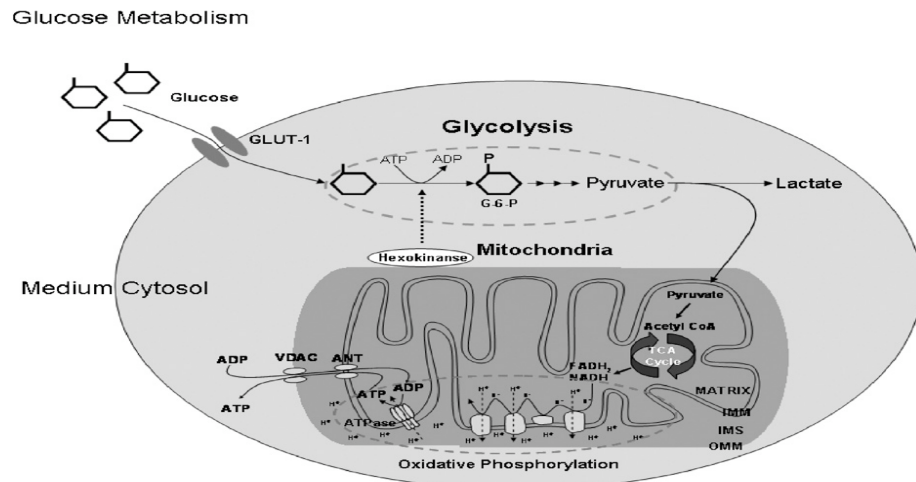


Figure 2.2. The glucose metabolic pathway in mammalian cells [6].

2.3.2 Hexokinase Link with Apoptosis

Hexokinase is the initial enzyme in the glycolysis pathway that catalyzes the irreversible reaction of glucose to glucose-6-phosphate. Hexokinase can be rate-limiting in some cells; hence, cell-engineering strategies that utilize hexokinase may free a cell from this glycolysis limitation, thereby increasing ATP production to maintain cell energy levels and potentially inhibit apoptosis. Through its gateway role in glucose metabolism and its interaction with both pro- and anti-apoptotic proteins at the mitochondria, hexokinase may serve as a key link between metabolism and apoptosis and is an ideal target to increase both the growth and viability of production cell lines [7].

Similar to GLUT-1, the protective effects of hexokinase against cell death have long been observed in tumor cells. The anti-apoptotic phenotype in tumor cells with elevated expression of hexokinase is due at least in part to an increased rate of glycolysis from increased hexokinase activity [7]. In addition, hexokinase II, the second isoform of hexokinase, is up regulated under the hypoxic conditions found in rapidly growing tumors as suggested by *Mathupala et al.*, in 2001. The ability to maintain glucose flux and ATP generation through glycolysis during the hypoxic conditions that prevent oxidative phosphorylation promotes tumor cell survival in environments most cells cannot tolerate.

Through both increasing catalysis of glycolysis and prevention of mitochondria permeabilization, hexokinase represents an important but underutilized anti-apoptotic protein for inhibition of PCD. Beyond the anti-apoptotic effects of hexokinase, the increased flux of glucose into glycolysis may provide increased energy needed for the production of recombinant proteins in a suspended mammalian cell culture system.

2.4 PAT Implementation in Mammalian Cell Culture Bioprocesses

The ability to develop improvements in bioprocess control and optimization strategies is directly linked to the capacity to devise relevant real-time analytical instrumentation. The necessity for rapid monitoring techniques is being driven by several factors such as: the need to construct better process models; a general desire for improved control of feed strategies and other process parameters; a requirement to develop robust, transferable, operator-independent processes; and finally, the necessity of complying with FDA's process analytical technology (PAT) guidance [8].

Bioprocess monitoring techniques can be classified with respect to their level of invasiveness, ranging from off-line and at-line employment of analytical instrumentation to on-line or in-line integration of analyzers. Some in-line configurations are available, including direct sensor insertions as well as sample loops with *in-situ* analyzers.

Ideally, small *in-situ* electronic sensors would meet the monitoring requirement for each process parameter of a bioreactor control system. Process parameters such as temperature, dissolved oxygen and pH have long been readily measured using *in-situ* sensors [9]. Now the optical sensors are rapidly evolving, which hold great promise for bioprocess applications by means of technology that generally supports non-invasive, continuous and simultaneous substrate and product monitoring. However, at this time no comprehensive and practical optical detection system has been developed.

On the other hand, process parameters such as cell density, viability, and medium component concentrations have historically been monitored in laboratories that were physically remote from manufacturing sites (off-line). However, analytical instrumentation for bioreactor process monitoring and control is currently in a phase of rapid development. At least some important factors must be examined when considering new analytical systems in bioprocess applications: the specific values of key process parameters, the required accuracy and reproducibility, the available technical principles of such sensors, their qualification and validation requirements, and the speed of data acquisition and processing are crucial when discussing the development in this type of field [10].

The highest goal of the PAT initiative is that the process engineers and scientists must develop a solid understanding of their product's critical quality attributes and which critical process parameters affect them. Practical differences in biotechnology products are that they are generally produced using a cell culture system in a bioreactor, which is usually more complex and dynamic than chemical reactors for small-molecule systems and the products are susceptible to potential degradation events during manufacturing and storage, just to mention some of the big issues.

Given the complexity and nonlinearity of processes occurring in a bioreactor, increasing the number of process variables being monitored can only contribute to a better understanding of the bioprocess in general, to identify the relationships between specific operational activities and critical product attributes, to correlate process variables with

product quality and to improve reproducibility of manufacturing operations. The PAT guidance also defines the value of automated monitoring and control devices. Such efforts provide information that could or will be an existing part of an integrated data management system when the applicability and demand for it emerges during subsequent stages of development, scale-up and product manufacturing.

It is wide comprehended by the scientific community working with PAT that such important field should be improved to achieve the final goal to have a better understanding of each bio-pharmaceutical and pharmaceutical process.

2.5 Raman Spectroscopy History and Fundamental Theory

Even though Raman scattering was discovered in 1928, this kind of analytical technology has become a convenient and available technique only in the last two decades. The weakness of the Raman signal with respect to other optical signals makes acquiring spectra a difficult task. The current state-of-the-art equipments allow Raman spectroscopy to be not only possible, but also affordable and convenient. These technological improvements have allowed for a proliferation of Raman spectroscopic techniques and applications, making the field the subject of many research papers.

Resonantly enhanced Raman techniques take advantage of the dramatically enhanced Raman signal that occurs when the wavelength of the incident laser coincides with an optical absorption arising from fundamental internal excitations in the material. Under these circumstances, the intensity of Raman scattering can increase by a factor of 10^6 .

The new optical design developments have enabled lower power (and lower cost) UV lasers to become candidates for use with materials that are transparent at visible wavelengths. Further signal improvement can be obtained using surface enhanced resonance Raman scattering (SERRS) techniques. Over the years these have proved difficult to use in a quantifiable way because of a lack of understanding of the bonding interactions occurring at the interface of the sample material and the substrate.

Results can also vary, depending upon the surface roughness of a metallic substrate or the consistency of a colloidal substrate, for example. However, in recent meetings it has been indicated that most of the polarized views relating to the theoretical background are coming together. It is believed that this could become an important application area in the future. For example, it has been demonstrated that novel SERRS techniques can detect certain drugs and explosives in remarkably low quantities, and there are DNA related applications, too.

Interfacing of Raman systems to other instrumentation has also been a major feature of recent work. For example, one major advantage of the new technology over well-established IR absorption methods is the use of a microscope with spatial resolutions of less than 1 mm using visible excitation, on relatively easily prepared samples. This compares with spatial resolutions of 5–10 mm using microscope based IR techniques. Prior to 1990, microscopes were attached to Raman systems using standard monochromators without optimization of the optical design. These proved to be reasonably successful, although extremely cumbersome and expensive to start up and maintain. They were suitable for use only in advanced research laboratories. The University of Leeds/Renishaw approach began with the premise that the optical design should start at the microscope and work backwards through the Raman system. This led, for example, to the employment of infinity-corrected optics in the microscope, resulting in greater flexibility for linking to the spectrometer and permitting the insertion of additional sampling options.

Raman spectroscopy takes advantage of Raman scattering, discovered by C.V. Raman in 1928. Raman scattering also referred as inelastic scattering, is caused by the interaction between the optical oscillations of light with the vibrational motion of molecules. To explain Raman scattering, consider the case of a monochromatic beam of light with energy $h\nu_0$, when the light comes into contact with a group of molecules much smaller than the wavelength of the light, most of the light will scatter elastically, an effect called Rayleigh scattering. A much smaller amount of light anywhere through 10^{-6} to 10^{-10} of the

total scattered light will scatter off of the particle with energy $h\nu_1 \neq h\nu_0$. The incident photon with energy $h\nu_0$, excites vibrational motion in the molecule with energy h_f , causing some of the energy to be given to the molecule, while the rest of the energy is scattered off as a new photon. In this case, the scattered photon has a lower energy, $h\nu_1$.

$$h\nu_1 = h\nu_0 - h_f$$

As seen in Figure 2.3, when the scattered light has less energy than the incident light ($h\nu_1 < h\nu_0$) it is referred to as Stokes Raman scattering. The opposite case is referred to as anti-Stokes Raman scattering. Since anti-Stokes requires that molecules begin in an excited state, it is generally much weaker. In general, all spectroscopies can be viewed as ways of observing a mechanism by which the incident radiation interacts with the molecular energy levels of a sample. In infrared spectroscopy, like Raman spectroscopy, the mechanism is molecular vibration. Unlike Raman, however, infrared probes the vibrations directly. For vibrational Raman spectroscopy the mechanism is the interaction of radiation with a polarizable electron cloud, modulated by molecular vibration. Raman scattering can also be modulated by rotational changes in the excited molecules, but these are lower in energy than vibrational transitions [11].

A number of factors can affect the intensity of a Raman signal; in theory all the factors could be summarized with the simple equation [12]:

$$I_R = I_0 \sigma_j D dz$$

Where I_R is the intensity of the Raman signal, I_0 is the intensity of the excitation light at the sample; D is the number density of the scatterers, dz is the path length or depth of field of the laser in the sample, and σ_j is an empirically determined cross-section of Raman scattering. In the literature, Raman intensities are often expressed in terms of the differential cross-sections to facilitate repeatability [12].

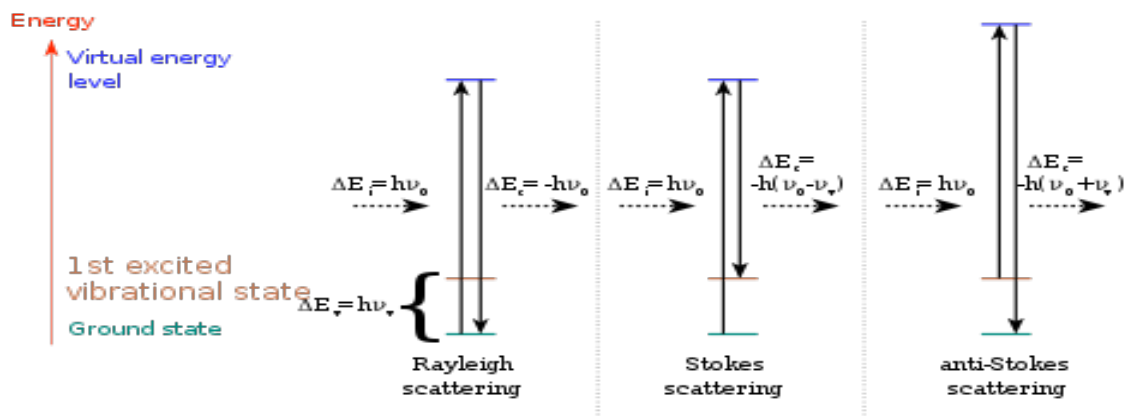


Figure 2.3 Different Raman scattering models[12].

2.6 Application of Raman Spectroscopy in Mammalian Cell Culture Monitoring

Advantages over the standard IR techniques commonly used in these areas, are that minimal sample surface preparation is now required (i.e. no polishing or vacuum), and improved high spatial resolution can distinguish between incipient and excipient in powdered compacts. The measurement is wholly nondestructive. Owing to the low laser powers that can now be used, spectra can be obtained within cells without damage to the cell wall. Raman techniques are now being investigated to combat cancer, and to control the quality (and possible patent violations) of drug composition. Many biomedical samples will be immersed in or contain water and these can be easily measured while IR absorption measurements are very difficult in presence of water [13]. In mammalian cell culture this is not an exception, most of the culture media used to culture these cells are based on water (i.e. aqueous solutions), which is why Raman spectroscopy is one technique that should be given serious consideration.

Many techniques have been proposed for interrogation and measurement of biological response of cellular sensors. Changes in cell behavior, cell-cell and cell-substrate contact, metabolism, or induction of cell death following exposure of cells to toxic agents can be measured and used to detect the presence and identification of the toxic agents. Optical methods offer a significant advantage as light can be used non-invasively to probe cells.

Variations in the intensity of the intrinsic light emitted by bioluminescent bacteria can be used to detect toxic chemicals such as polycyclic aromatic hydrocarbons and phenols [14]. Various fluorescent labels have been developed to monitor cellular functions and a large number of techniques have been implemented for high-throughput screening [15]. Neurotoxic chemicals can be detected by monitoring active neuronal networks using microelectrode arrays [16]. Changes in the spontaneous electric activity (e.g. burst duration, frequency) can be measured when neurons are exposed to various neuroactive drugs and toxins. Similar methods using cardiac myocytes have also been reported for studying pesticides and metals toxicity [17].

The extracellular potential of other electrically active cells, such as osteoblasts, can also be measured and related to presence of various toxic agents [18]. Measurement of pH using microelectronic sensors to monitor the acidity of culture media in the vicinity of living cells has also been used to monitor the behavior of living cells [19]. Cells exposed to toxins known to inhibit membrane ionic pumps show small decreases in the pH which can be detected using integrated microelectronics. Changes in the pH caused by exposure of genetically engineered bacteria to express various enzymes have also been used for the detection of organophosphate toxins, such as nerve agents [20]. Confluent layers of endothelial cells grown on ion-selective membranes were able to detect various concentrations of histamine in the culture medium due to increased permeability caused by cell-cell contact alteration and formation of gaps [21]. Impedance measurements of cellular arrays have been used to determine the behavior of various cell types, such as fibroblasts [22] and endothelial cells [23].

The main challenge faced by all biosensing techniques is the ability to discriminate between diverse toxic agents. Although the information regarding general toxicity may be useful for classification of a potential agent, identification and quantification are also desirable. With the possible exception of the neuronal network type systems, it has proven difficult to identify and quantify different toxic agents with many of the approaches described. The main reason is that the interrogation of the cellular component results in readouts with limited biological information and thus results in similar changes in the detected signal for many different toxic agents. Additionally, many of these techniques require invasive methods of cell sampling, complex cellular modifications or use cell types that are difficult to establish in reliable cell lines. Such methods limit considerably the time-dependent biological responses of cells, which often are indicative of the type and dose of the toxic agent.

Raman spectroscopy is a powerful analytical technique, which has been widely used in the study of biological samples during the last two decades [24]. Raman microspectroscopy can provide useful biochemical information regarding live cells, which can be related to the interaction with toxic agents or drugs, disease, cell death and differentiation [24]. In addition to conventional non-resonant Raman spectroscopy, there have been numerous reports on using resonant Raman (RS) spectroscopy [25], surface enhanced Raman spectroscopy (SERS) [26] and coherent anti-Stokes Raman spectroscopy (CARS) [27] for studying live cells. These methods are based on various effects to enhance the Raman signal of specific molecules found in cells [28]. These techniques have been widely used for developing sensors and biosensors [29].

The potential of non-resonant conventional Raman spectroscopy as an interrogation method of cells is based on the fact that different toxic chemicals have different effects on living cells and induce specific time-dependent biochemical changes related to cell death mechanisms. The Raman spectrum of a cell represents a “fingerprint” with rich information rich of the overall biochemical composition of the cell, thus different toxic agents that initiate different cellular responses and biochemical changes should produce distinct changes in the Raman spectra. In addition, time-course Raman spectra can be acquired from live cells maintained in physiological conditions and without need of invasive procedures. The information obtained is related to the intrinsic molecular composition of the cell, thus no labels or other contrast enhancing chemicals need to be used. The detection of time-dependent biochemical changes of cells has the potential to provide the additional level of information needed for quantification and discrimination of a wider range of toxic agents. Conventional non-resonant Raman spectroscopy has a great potential as an interrogation method for cell-based biosensors.

2.7 Statistics Approach in Bioprocess-Factorial Designs, Multiple Response Functions, and Functions Along Time

2.7.1 Factorial Designs

Many experiments involve the study of the effects of two or more factors and generally factorial designs are the most efficient to elucidate these types of experiments. By factorial designs we refer that in each complete trial or replication of the experiment all possible combinations of the levels of each factor are investigated. That means if there

are x levels for factor X and y levels for factor Y , each replicate contain all x and y level combinations. When factors are set in a factorial design it means that they are crossed. The effect of a factor is defined to be the change in response made by a change in the level of the factor. For example, in our case, there are two factors affecting the process. The first is the temperature change which is 35-33°C (low level part) and 37-33°C (high level part). The second one is over-expression of the apoptotic inhibitor in the media (high level part) or no over-expression of the apoptotic inhibitor in the media (low level part). Each factor, combined or alone, affects the responses, which are the primary (substrates) and secondary (by-products) metabolites. In Figure 2.4, an example of the factor design used in this work is shown. In our case, both factors do not interact among them, given the fact that one of the factors cannot be measured quantitatively, but qualitatively.

As part of the explanation, temperature range will be factor A and over-expression of the apoptotic inhibitor factor B .

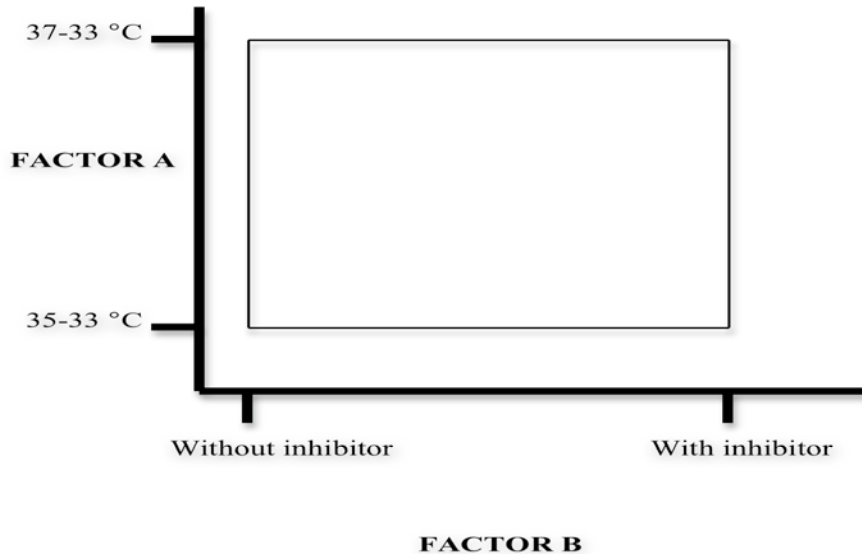


Figure 2.4 Two-factor factorial experiment design used in this work.

2.7.2 Robustness and Multiple Responses

Typically, in the analysis of industrial data for process optimization, there are many response variables that are under investigation at the same time. Robustness is also an important concept in industrial optimization. Here, robustness means that the responses are not sensitive to the small changes of the input variables. However, most of the recent work in industrial optimization has not dealt with robustness, and most practitioners follow up optimization calculations without consideration for robustness. In many practical situations, it is quite common that several responses are observed for each setting of a group of input variables. When there are several responses, the problem of multi-response optimization is an important issue, which becomes more complicated with the increase in the responses and factors. Response surface methodology (RSM) is a well-known tool for optimization using design of experiments.

RSM has been introduced as an important tool in modern quality engineering. Box and Wilson [30] first introduced the concept of RSM, which changed the way engineers and statisticians considered design of experiments. Many other recent publications such as Khuri and Cornell [31], Park [32], Myers [33], Myers and Montgomery [34] work this subject too. The basic idea of RSM is to first fit a model for the response variable and then find the various settings of interest for the process variables.

As mentioned by *Zhen et al.* [35], much of RSM was focused on finding the optimal operating condition for the process variables (multiple variables), which resulted in a maximum or minimum response. For multi-response optimization, the objective is to determine a set of process variables to optimize several responses simultaneously. It is worth emphasizing that both robustness and optimization are two important and useful concepts in statistical procedures. Our job was mostly to focus here in showing and demonstrating another alternative to know more, in a qualitative way rather than a quantitative, industrial bioprocess behavior and patterns through time. This kind of approach could be improved and continued to expand our knowledge in each individual bioprocess.

It is important to mention and maintain clear that each individual process has its own behavior and patterns. Factors such as the by-products (molecule of interest secreted or any other secondary metabolite), primary metabolites (such as substrates) or even operational conditions (change in temperature, air and carbon dioxide flow, and level of agitation) could completely change behavior patterns in growth, viability and metabolic pathways. Last one mentioned could be inferred by the use of such an advance qualitative tool as Raman spectroscopy. Most of these systems (biotechnological processes) require the continuous monitoring of multiple responses over time as we mentioned, but as if this was not difficult, most of these responses are recorded through time and for statistical experts these still remain a matter of deep study and comprehension. That is mostly because all of the statistical approaches and tools available were developed to analyze patterns with mostly one response at certain amount of time, and not for multiple responses that over time would become functions with respect to time. In the meantime, tools such as multiple linear regression and RSM are being used to explain the process behavior statistically, giving a “ball park” understanding of the process, but not an accurate description and analysis of any multivariate process.

2.7.3 Responses as Functions of Time (Multiple Regression Analysis)

In statistics, regression analysis includes many techniques to model and analyze many variables. The focus could be on the relationship between a dependent variable and one or more independent variables. This analysis helps to explain how the typical value of the dependent variable changes when any one of the independent variables is varied, while the other independent variables are fixed [36]. Frequently, regression analysis estimates the conditional expectation of the dependent variable given the independent variables. In the majority of cases, the estimation target is a function of the independent variables called the regression function. On the other hand, the estimation target could also be several functions over time reduced to one to obtain one coefficient per function over time and try to explain, analyze, and predict the behavior at certain time or until the solution or coefficients become unstable.

A good example of this raw method proposed by several scientists is this case, in which several responses through time (cell density, viability and primary and secondary metabolites concentrations) that will be changing or become unstable and make the statistical analysis and modeling very difficult. An example on how this method would work and could describe and predict in a "qualitative" way such cases is shown in Figures 2.5-2.7. For each condition studied without replicates, coefficients were calculated and extracted from functions of the responses over time.

In the particular case of cell viability behavior (Figure 2.5), a pattern or good prediction was clearly obtained for the first six days of both coefficients calculated (temperature- β_1 and inhibitor- β_2), but at days 7 to 9 prediction and behavior became unstable. For the other two cases studied, such as cell density (Figure 2.6) and L-lactate production and consumption (Figure 2.7), it is clearly evident that the behavior or pattern modeling could not be achieved by the instability observed in the coefficients values. In order to summarize our attempts using this method to describe and predict the behavior of at least three of our responses (viability, cell density, and L-lactate concentration), Table 2.1 shows time (days), solutions for cell density and viability, respectively, and their composite using the "optimizer" function in Minitab which optimizes the coefficient value, but our case is still far off the reality for the system.

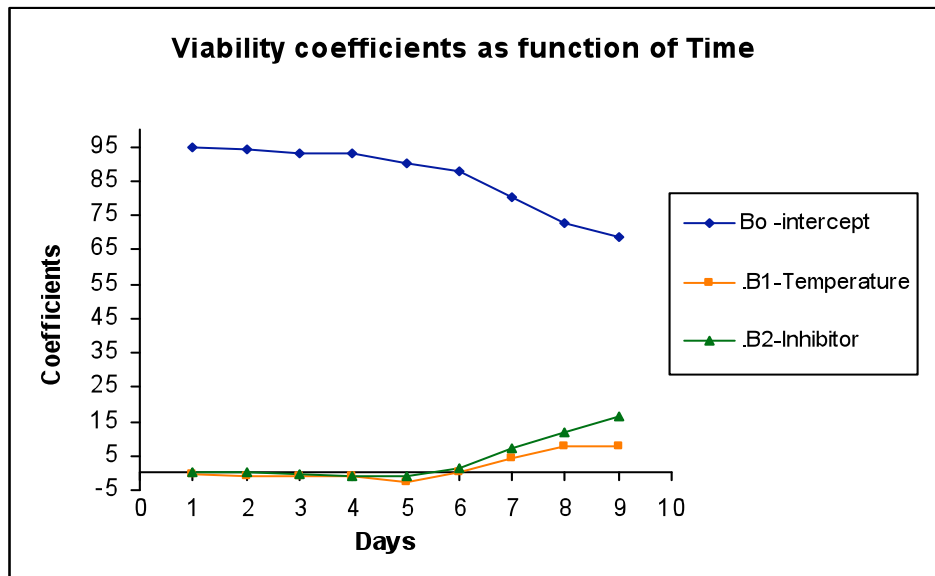


Figure 2.5 Cell viability coefficients variation over time.

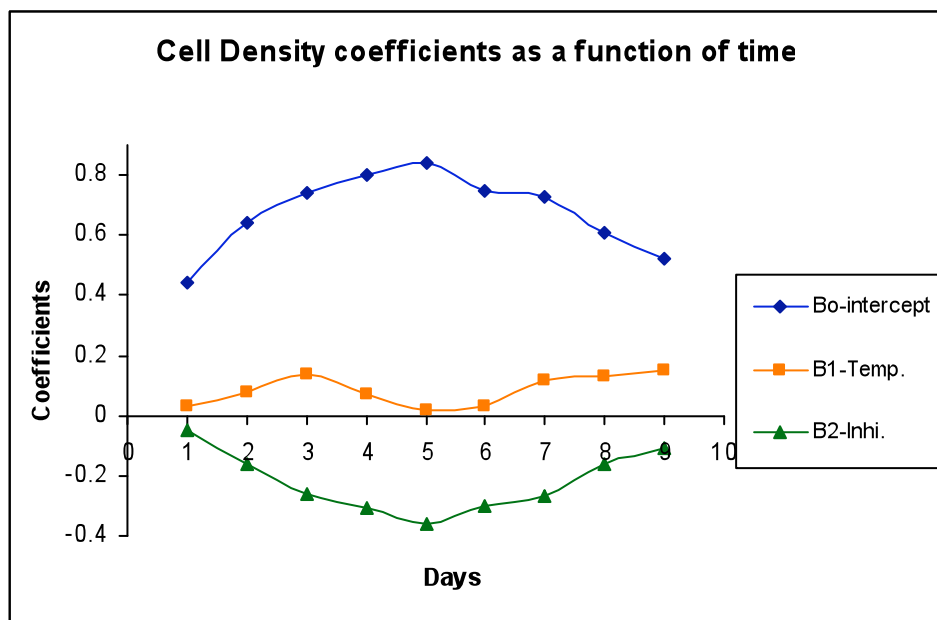


Figure 2.6 Cell density coefficients variation over time.

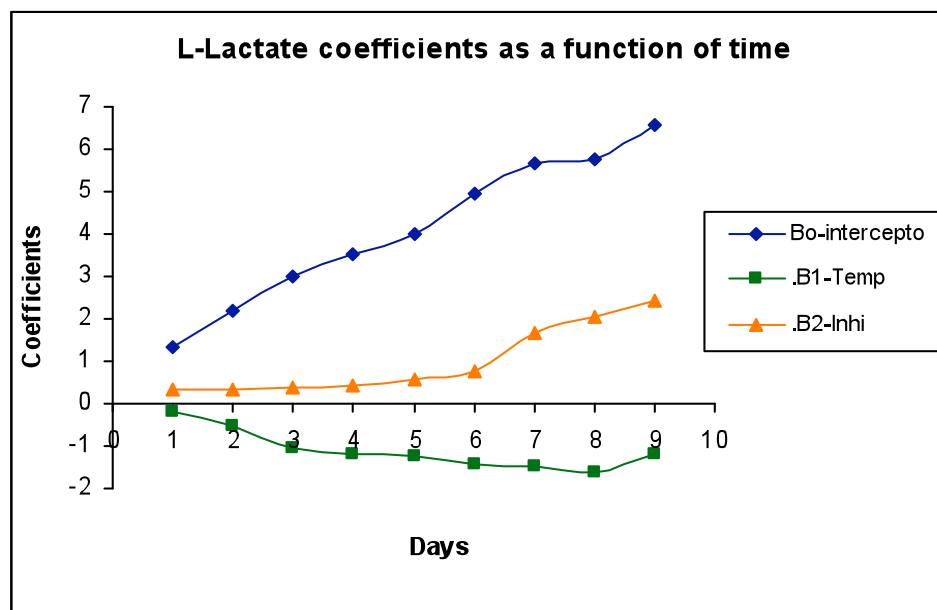


Figure 2.7 L-lactate coefficients variation over time.

Table 2.1. Optimization values obtained using the function “optimizer” in Minitab for the cell density and viability responses.

Days	Solution A (Cell density)	Solution B (Viability)	Cell Density Desirability	Viability Desirability	Composite (A and B) Desirability
1	0.7374	-0.4747	0.9997	0.9282	0.9752
2	-0.3655	0.8492	1.00	1.00	1.00
3	-0.9394	0.8384	0.9819	0.9983	0.9874
4	-1	1	0.9500	0.7500	0.8780
5	-0.9634	-1	0.1638	0.2274	0.4249
6	-1	0.8969	1.0	0.8789	0.9579
7	-1	1	0.9500	0.5300	0.7821
8	-1	1	0.7000	0.2900	0.5218
9	No opt.	No opt.	No opt.	No opt.	No opt.

2.8 Chinese Hamster Ovary Cell Culture at Bench and Manufacturing Scales

Recombinant proteins are synthesized by large-scale cultivation of genetically engineered host cells, which harbor the genes encoding the target proteins [37]. Demand for production of recombinant proteins for biopharmaceuticals has been increasing rapidly. Production of recombinant proteins by pharmaceutical companies will serve a global market worth \$70 billion by 2010 [4]. The increasing demand for recombinant therapeutic proteins has placed significant pressure on the biopharmaceutical industry to develop high-yielding mammalian cell-based production systems. Mammalian cells are the most appropriate host cells for the production of biopharmaceuticals if complex protein structures such as monoclonal antibodies must be synthesized in their native form. Current efforts to increase the supply of recombinant protein from mammalian host cells have been directed toward increasing the scale of production rather than increasing the stability of systems for long-term production [38].

However, increasing long-term system stability is advantageous because it saves the time normally used to produce seed cultures for large-scale bioreactors. The growth of mammalian cells is slower than that of microorganisms. The process of large-scale cultivation of mammalian cells usually involves thawing the frozen seed cells, activating cells in spinner flasks, cultivating cells in bioreactors of increasing sizes and finally cultivating cells in the production-scale bioreactor. In other words, the majority of the time spent for one batch is used to produce the seed cells used for inoculation of the main culture. A 1,000-L production scale bioreactor requires at least 100 L of seed cells and it usually takes more than two months to produce seed cells (cell thawing, cultivation in various sizes of spinner flasks and various sizes of bioreactors up to 100 L) for inoculation and subsequent production by batch or fed-batch cell culture at scales above 1,000 L. These numbers imply that using the lot-to-lot batch cultivation method; only five batches can be produced from five frozen vials with the same sets of bioreactors in a year. Therefore, establishing a repeated batch culture system that would operate for much longer would enable the same practical production-scale reactor to produce, say, five lots of batch culture from only one vial of frozen cells in three months. This saves both time and money (in terms of the number of frozen vials) and ensures product consistency. In a practical production plant, repeated batch culture is very important because it would save both the time and money required to prepare fresh seed cultures. As the frozen vials are generally prepared as pre-assessed and guaranteed master cell banks, they are extremely expensive. Thus, it is very important to reduce the number of frozen vials used.

CHO cells remain stable during cultivation, with relatively rapid cell proliferation that yields viable cells at high density. However, there are no published reports, assessing the stability of antibody production using CHO cell lines in large-scale (i.e., practical-level) culture. Barnes, et al. reviewed published information on the stability of protein production in hybridoma, CHO, and NS0 cell lines [39]. According to this review, several reports on the instability of protein production from recombinant cell lines exist, but the cause of this instability is yet unknown. Recently, Kaneyo, et al. addressed this subject in their research project and brought out some knowledge to this unknown subject

[2]. Proposing that a decrease in cell-specific productivity was associated with an increase in the rate of cell proliferation and by consequence helping in the cell instability.

2.9 References

- [1] Laken, H.A. and Leonard, M.W. 2001. Understanding and modulating apoptosis in industrial cell culture. *Current Opinion in Biotechnology* **12**:175-179.
- [2] Kaneko, Y., Sato, R., and Coyaja, H. 2010. Evaluation of Chinese hamster ovary cell stability during repeated batch culture for large-scale antibody production. *Journal of Bioscience and Bioengineering* **109**(3):274-280.
- [3] Andersen, D.C. and Krummen, L. 2002 Recombinant protein expression for therapeutic expression. *Current Opinion in Biotechnology*, **13**:117-123.
- [4] Whitford, W. and Julien, Ch. 2007. Analytical Technology and PAT. *Biopharma International* **1**:532-545.
- [5] Nelson, D.L. and Cox, M.M. 2007. Principles of Biochemistry, Wiley-Intersciences.
- [6] www.nature.com/nrc/journal
- [7] Xiao-Ming, Y. and Dong, Z. 2003. Essential of Apoptosis, Humana Press.
- [8] Pitt, G.D., Batehelder, D.N., and Bennett, R. 2005. Engineering aspects and applications of the new Raman instrumentation. *Meas. Technol.* **152**(6):241-318.
- [9] Jayapal, K., Wleschin, K., and Wei-Shou, H. 2008. Recombinant Protein Therapeutics from CHO cells- 20 years and counting. SBE special edition, *AIChE Journal* S40-S48.
- [10] Kansakoski, M., Kurkinen, M., and Weymam, N. 2006. Process Analytical Technology needs and applications in the bioprocess industry. VTT Technical Publications. 1-100.
- [11] Gil, G.A. 2006. Online Raman Spectroscopy for Bioprocess Monitoring. Master of Engineering Thesis. MIT.
- [12] McCreery, R.L. 2001. Raman spectroscopy for Chemical Analysis. *Measurements Science and Technology* **12**:653-654.

- [13] Verbier, S., Nottingher, I., Polak, J.M., and Hench, L.L. 2003. *In situ* Monitoring of Cell Death using Raman Spectroscopy. *Biopolymers* **74**:157-162.
- [14] Zeiri, L., Bronk, P.V., Shabtai, Y., Eichler, J., and Efrima, S. 2004. Surface-enhanced Raman Spectroscopy as a tool for probing specific bio-chemical components in bacteria. *Applied Spectroscopy* **58**(1):33-40.
- [15] Stark, E., Hizmann, B., Schurgel, K., Scheper, T., Furchs, C., Koster, D., and Markl, H. 2002. *In situ*-fluorescence probes: A useful tool for non-invasive bioprocess monitoring. *Advances Biochemical Engineering* **74**:21-38.
- [16] Nottingher, I., Selvakumaran, J., and Hanch, L.L. 2004. New detection system for toxic agents based on continuous spectroscopic monitoring of living cell. *Biosensors and Bioelectronics* **20**(4):780-789.
- [17] Natarajar, A., Molnar, P., Sieverades, K., Jamshidi, A., and Hickman, J.J. 2006. Microelectrodes array recordings of cardiac action potentials as a high throughput method to evaluate pesticides toxicity. *Toxicology in Vitro* **20**(3):375-381.
- [18] Ronconi, L. and Saddler, P.I. 2008. Applications of heteronuclear NMR spectroscopy in biological and medicinal inorganic chemistry. *Coordination Chemistry Reviews* **252**(21):2239-2277.
- [19] Bardallo, I. and Jiménez-Jorquera, C.D. 2009. Microelectrodes for measurement of cellular metabolism. *Procedia Chemistry* **1**(1):289-292.
- [20] Pourciel, M.L., Sant, W., Humenyuk, I., Malaquin, L., Dollat, X., and Temple-Boyer, P. 2004. Development of pH-ISFET sensors for the detection of bacterial activity. *Sensors and Actuators B: Chemical*, **103**(1):247-251.
- [21] Cheran, L.E., Cheung, S., Wang, X., and Thompson, M. 2008. Probing the bio-electrochemistry of living cells. *Electrochimica Acta* **53**(23):6690-6697.
- [22] Asphanai, F., Thein, M., Veisch, O., Edmondson, P., and Kosai, R. 2008. Influence of cell adhesion and spreading on impedance characteristics of cell-based sensors. *Biosensors and bioelectronics* **23**(8):1307-1313.
- [23] Rumenapp, C., Remm, M., Wolf, B., and Gleich, B. 2009. Improved method for impedance measurements of mammalian cells. *Biosensors and Bioelectronics* **24**(9):2915-2919.

- [24] Baena, J.R. and Lendl, B. 2004. Raman spectroscopy in chemical bio-analysis. *Current Opinion in Chemical Biology* **8**(5):534-539.
- [25] Teixeira, A.P., Oliveria, R., Alves, P.M., and Carrondo, M.J.T. 2009. Advances in on-line monitoring and control of mammalian cell culture: Supporting the PAT initiative. *Biotechnology Advances* **27**(6):726-732.
- [26] Scalfi-Happ, C., Jauss, A., Ibasch, W., Hollricher, O., Fulala, S., and Harusen, C. 2007. Confocal Raman microscopy as a diagnostic tool for investigation of living neuroblastoma tumour cells. *Medical Laser Application* **22**(3):157-164.
- [27] Eliasson, C., Loren A., Engelbrektsson, J., Josefson, M., and Abrahamsson, J. 2005. Surfaced-enhanced Raman scattering imaging of single living lymphocytes with multivariate evaluation. *Spectrochimica Acta Part A: Molecular and Bio-molecular Spectroscopy* **61**(4):755-760.
- [28] Li, L., Wang, H., and Cheng, J.X. 2005. Quantitative Coherent Anti-Stokes Raman Scattering Imaging of Lipid Distribution in Co-existing Domains. *Biophysical Journal* **89**(5):3480-3490.
- [29] Velasco-García, M.N. 2009. Optical biosensors for probing at the cellular level: A review of recent and future prospects. *Seminars in Cell and Developmental Biology* **20**(1):27-33.
- [30] Box, G.E.P. and Wilson, K.B. 1951. On the experimental attainment of optimum conditions. *J. Royal Statistics Society B* **13**:1-45.
- [31] Khuri, A.I. and Cornell, J.A. 1996. Response Surfaces, Second Edition.
- [32] John-Chul, P., Dong-Myeong, H., and Moon-Gab, K. 1996. Modified response surface methodology for phase equilibrium-theoretical background. *Korean Journal of Chemical Engineering* **13**(2):115-122.
- [33] Myers, W.R. 2003. Response Surface Methodology. Encyclopedia of Biopharmaceutical Statistics.
- [34] Myers, H. and Montgomery, D. 1995. Response Surface Methodology: Process and Product Optimization Using Design of Experiments.
- [35] Zhen, H., Jing, W., Jinho, O., and Sung, H.P. 2009. Robust optimization for multiple responses using response surface methodology. *Applied Stochastic Models in Business and Industry* **26**(2):151-171.

- [36] Mardia, K.V., Kent, J.T., and Bibby, J. 1979. Multivariate Analysis. Academic Press.
- [37] Matesci, M., Hacker,D.L., Balali,L., and Wurm, F.M. 2008. Recombinant therapeutics protein production in cultivated mammalian cells: current status and future prospects. *Drug Discovery Today Technologies* **5**(2):37-42.
- [38] Costa, R., Rodrigues, E., Henriques, M., Azeredo, J., and Oliveira, R. 2010. Guidelines to cell engineering for monoclonal antibody. *European Journal of Pharmaceutics and Biopharmaceutics* **74**(2):127-138.
- [39] Barnes, L.M., Bentley, C.M., and Dickson, A.J. 2006. Stability of Protein Production from Recombinant Mammalian Cells. *Biotechnology and Bioengineering* **81**(6):631-6.
- [40] Fang, L., Qian, H., Jiang C., Yuanlin, P., Roop, D., and Chuan, L. (2010) Apoptotic cells activate the “Phoenix Rising” Pathway to promote wound healing and Tissue Regeneration. *Sc. Signal.*, 3(**110**): 1-20.
- [41] <http://www.sgul.ac.uk/depts/immunology/~dash/apoptosis/mito2.jpg>

3. Materials and Methods

3.1 Cell Line

The cell line used in this research work was CHO-S cells, Serum Free Adapted (Cat. No. 11619-012, Invitrogen). These CHO-S cells are a clonal isolate, derived from the original Chinese hamster ovary (CHO) cell line isolated by Puck [1]. The CHO-S cells are adapted to serum-free suspension culture in CD CHO medium (Cat. No. 10743-029, Invitrogen) supplemented with L-glutamine for transient or stable expression of recombinant proteins. The CHO-S parental cell line was selected for growth and transfection efficiency. CHO cells have historically been grown in serum-supplemented medium. The use of serum-free media offers ease of downstream purification of expressed product, reduced risk of viral contamination and better lot-to-lot consistency. The CD CHO medium is a chemically defined, protein-free medium formulated with no components of animal or human origin by Invitrogen. Its composition has not been published and remains in proprietary knowledge. These cells were prepared from low-passage cells with documented lineage (20 to 25 passages serum-free) by Invitrogen. Cells were provided as a frozen stock with approximately 1.5×10^7 total cells in a 2-mL cryogenic vial (Figure 3.1).

These cells can be thawed and used directly in suspension culture for rapid expansion of cell stocks, or they can be cultured in monolayer for transfection using Lipofectamine™ 2000 Reagent.

3.2 Inoculum Preparation

Inocula were prepared using a three-stage process. In the first stage, one cryo-vial of CHO-S cells SFM adapted (Figure 3.1) was thawed at 37°C and then seeded in a 250-mL sterile vented cap Erlenmeyer flask with 40 mL of CD CHO Serum Free Media (SFM), for a total volume of 41 mL. Immediately, this first stage was inserted in an orbital shaker at 120 rpm inside a carbon dioxide incubator at 37°C, 150 ccm of CO₂ (6% CO₂) and 3 lpm of air as operational conditions (Figure 3.2). Two to three days were allowed to reach an optimal cell density ($2-3 \times 10^6$ cells/mL) to transfer into the second stage.

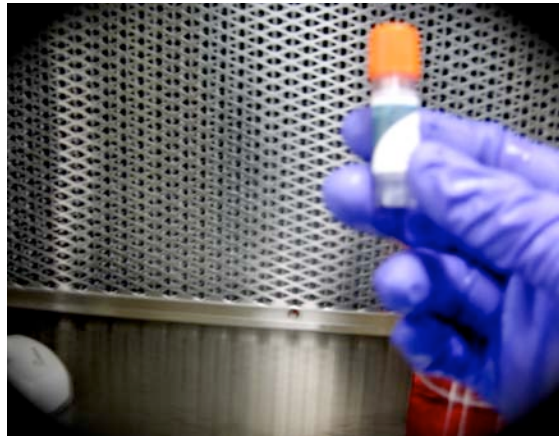


Figure 3.1. Cryogenic vial with $\sim 1.5 \times 10^7$ cells from Invitrogen.



Figure 3.2. First stage of inoculum.

At the second stage of the inoculum, cells were constantly monitored for cell density, viability and glucose and L-lactate consumption and production, respectively. When the optimal cell density was achieved at the first stage, then cells were transferred to a new sterile 500-mL Erlenmeyer vented cap flask with 120 mL of fresh medium (CD CHO SFM) to a final working volume of 155 mL, approximately (cell with fresh media, Figure 3.3). The same operational conditions were maintained in the CO₂ incubator, except for the rpm of the orbital shaker (150 rpm). Between two or three days took place to achieve the optimal cell density ($2-3 \times 10^6$ cells/mL) for passing to the third and last stage of the inoculum preparation.

Finally, at the third and last stage of the inoculum process, approximately 150-160 mL (depending on the cell density) of fresh CD CHO SFM was added to complete 300 mL. Two to three additional days were necessary for cell culture development. Operational conditions were still the same as in the CO₂ incubator (Figure 3.3), except that the orbital shaker was operated at 170 rpm instead of 150 rpm. The entire three-phase inoculum process, took six to nine days to finish before passing to the fourth and last phase, which was the final batch suspended cell culture in the bench-scale bioreactor.

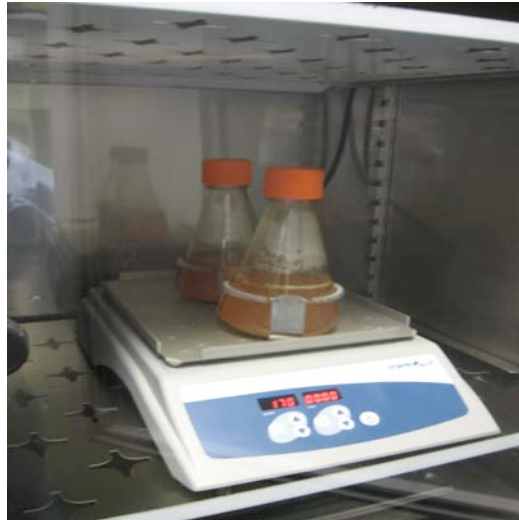


Figure 3.3. Second and third stages of the inoculum phase.

3.3 Bench-Scale Bioreactor Batch Experiments and Set-Up

Inocula cultured as described above were aseptically transferred into a 3-L autoclavable Applikon bioreactor with 1.2 L of fresh media, for a final working volume of 1.5 L. In all eight runs, the pH was monitored using an Applisens pH probe and was controlled with a PID (proportional-integral-derivative) control system with a starting pH set point of 7.10 using carbon dioxide and a 0.5 N sodium hydroxide solution. A pH cascade mode was always used establishing 7.10 as the starting set point and ending in the third batch day with a pH 6.99.

Before inoculation, the sterile bioreactor containing fresh media was aerated until 100% oxygen saturation to calibrate the Applisens Dissolved Oxygen (DO) probe. DO was then measured and controlled with a PID controller at a set point of 30% oxygen saturation by air enrichment with air gas addition. Temperature was monitored using a resistance temperature detector (RTD) and was controlled at a starting set point of 37°C or 35°C (depending on the operational condition studied at the moment of the run) by an electrically heated jacket as the heat source (Figure 3.4). Temperature was set to a 33°C ending set point with the purpose to induce hypothermia for additional secondary metabolite production and mitochondrial apoptosis cascade activation. Bioreactor contents were mixed at 150 rpm using a marine blade impeller.

After the inoculation, the process was monitored and the run was finished by either one of the following conditions occurring first: 50% of viability or a maximum of 10 days accomplished.

Since the beginning of the batch, samples were collected every day for cell count (Auto T4 cellometer), HPLC analysis (Shimadzu), biochemical analyzer (YSI 2300), osmolality (Fiske 3320 Osmometer) and Raman (Kaiser Optical System, Inc.) assays. As a part of one of the two operational conditions studied, 20 mg of the over-expressed apoptosis inhibitor (Apoptosis Inhibitor II, NS3694 from CALBIOCHEM, Cat. No. 178494) was

added into the media when the viability started to reach 90% for each case (approximately at the third day of the experiment). The following are the four operational conditions studied:

1. 35-33°C temperature range with apoptosis inhibitor addition.
2. 35-33°C temperature range without apoptosis inhibitor addition.
3. 37-33°C temperature range with apoptosis inhibitor addition.
4. 37-33°C temperature range without apoptosis inhibitor addition.

Duplicate suspended CHO cell cultures were performed for each condition above, in a random pattern.



Figure 3.4. Autoclavable 3-L Applikon Bioreactor.

3.4 Apoptosis Inhibitor Additions

For the two operational conditions with inhibitors described above, an apoptosis inhibitor, known as NS3694 with a molecular weight of 462.16 g per mol soluble in DMSO from Calbiochem was used. This molecule is a cell-permeable diarylurea that specifically prevents the active apoptosome complex formation (~700 kDa) triggered by

Cytochrome C release, thus blocking apoptosome-mediated caspase activation and cell death [2].

The over-expression or addition of this compound was as follows: 20 mg of the inhibitor were diluted in 20 mL of CD CHO SFM (containing DMSO) fresh media and mixed until entirely dissolved. This solution was filtered and added to the bioreactor (culture broth) when cell viability reached its early 90%, usually on the third day of the bioreactor batch culture.

3.5 Determination of Glucose and L-Lactate Concentrations

Glucose and L-lactate concentrations were determined using high performance liquid chromatography (HPLC, Figure 3.5) and a biochemical analyzer (YSI 2300, Figure 3.6). Bioreactor samples were collected and centrifuged using a Spectrafuge centrifuge system (16 M). The supernatant was filtered using a 0.22 μ m Cole-Parmer nylon membrane and was then analyzed using high performance liquid chromatography with a BioRad HPX-87H, 300- mm x 7.8 mm organic acids column (BioRad Labs, CA) operating at 55°C. A refractive index detector was used for compound detection. Dilute sulfuric acid (0.1 N) at a flow rate of 0.6 mL/min was the mobile phase. Mixed component concentration verification standards containing glucose and L-lactate were periodically injected to the HPLC to verify calibration accuracy (a similar procedure was reported by Sáez Miranda, et al.,) [3]. For the YSI 2300 (Figure 3.6) calibration membrane integrity (FCN solution) and linearity tests (glucose and L-lactate standard) were periodically ran through to verify the instrument calibration.



Figure 3.5. Shimadzu HPLC.



Figure 3.6. YSI 2300 biochemical analyzer.

3.6 Determination of Cell Viability and Concentration

Cell concentration was determined using an AUTO T4 Cellometer from Nexcelom Company (Figure 3.7). Two mL of whole culture broth sample were mixed (10 seconds) using a vortex mixer. 100 microliters of vortexed culture broth were collected from the 2-mL vial and mixed with 100 microliters of 0.2% of trypan blue tint solution from Invitrogen. At this moment the cells were loaded into the counting film (approximately 20 microliters at each side), and finally inserted into the cellometer auto T4 chamber (Figure 3.7).



Figure 3.7. Auto T4 Cell Counter, Nexcelom Company.

3.7 Osmolality Determination

The major components of the Model 3320 Micro-Osmometer (Figure 3.8) are: a test sampler, an operating cradle, a cooling system with a sample port to precisely position each sample for the osmolality test, a high precision thermistor probe, measurement and control circuitry, a power supply, and a user interface which includes the message display panel. For the sample test the following procedure was used. A sample tip was placed on the sampler and approximately 15 microliters were extracted from the 2-mL vial containing the cell culture broth sample. The sample was inspected visually for any large voids or bubbles in the fluid. The sides of the loaded sampler tip were wiped with a kimwipe to remove any clinging droplets.

After the chamber was cleaned with a cleaning tip the sample was inserted into the chamber. The operating cradle was pushed in until reaching a positive stop. Finally, the instrument automatically ran the test for approximately one minute and displayed the result. Results were recorded for each day. Each sample was discarded and the chamber cleaned with a chamber cleaning tip.



Figure 3.8. Fiske 3320 Micro-Osmometer.

3.8 Raman Equipment Procedure and Analysis

Raman spectra were collected using a Raman probe immersed in 4 mL of bioreactor samples collected off-line. Before sample analysis, calibration was performed with a cyclohexane standard. Samples were analyzed with ~15 exposures and ~17 accumulations. GRAMS software was used for the data acquisition. Figure 3.9 shows representative Raman spectra of samples collected from a suspended CHO cell culture run.

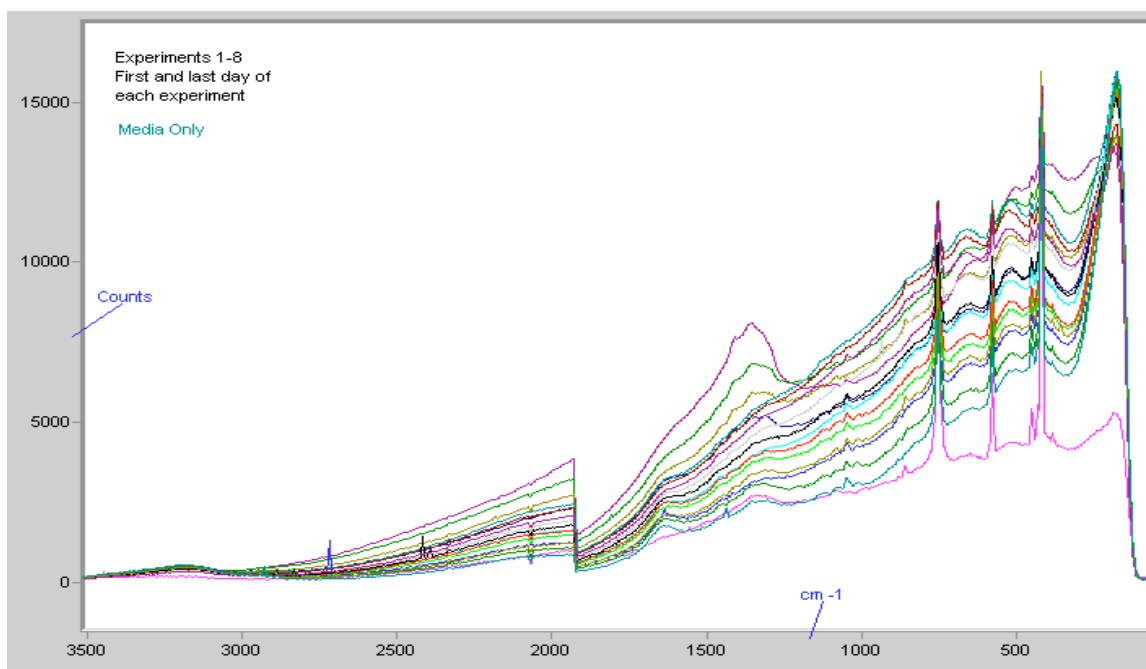


Figure 3.9. Raman spectra of samples from the eight cell culture batches (first and last day of each run).

In these experiments different types of components were monitored using different reference techniques such as HPLC and a biochemical analyzer (YSI 2300). Some of these techniques are time consuming. To speed up the process of sample analysis, Raman combined with multivariate data analysis was performed using SIMCA-P software. Mostly, the software used to analyze the data, involves steps such as defining the project, preparation of data, model fitting and identifying possible outliers, among other tasks.

3.9 Chinese Hamster Ovary Cells Upstream Process Simulation

For this work, Super Pro Designer software was used to simulate the CHO cell suspended culture process, which is a replicate of an industrial upstream manufacturing process for CHO. This software is used mostly to facilitate process optimization, cycle time and cost reduction, among others. Figure 3.10 shows the Process and Instrumentation Diagram (P&ID) for the upstream process (inocula to harvest). Finally, Figure 3.11 can help to visualize the time schedule schematic as a Gantt chart for the process.

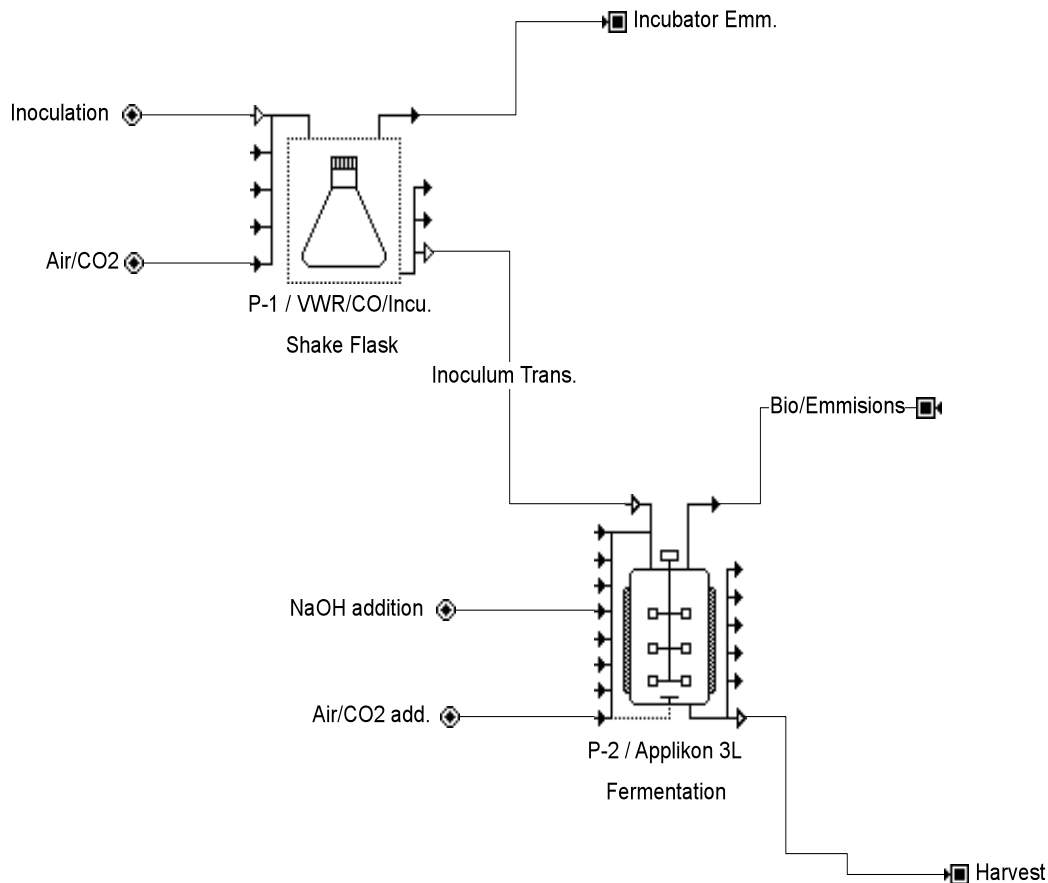


Figure 3.10. P&ID of the Chinese Hamster Ovary Cell upstream process generated using Super Pro Designer Software.

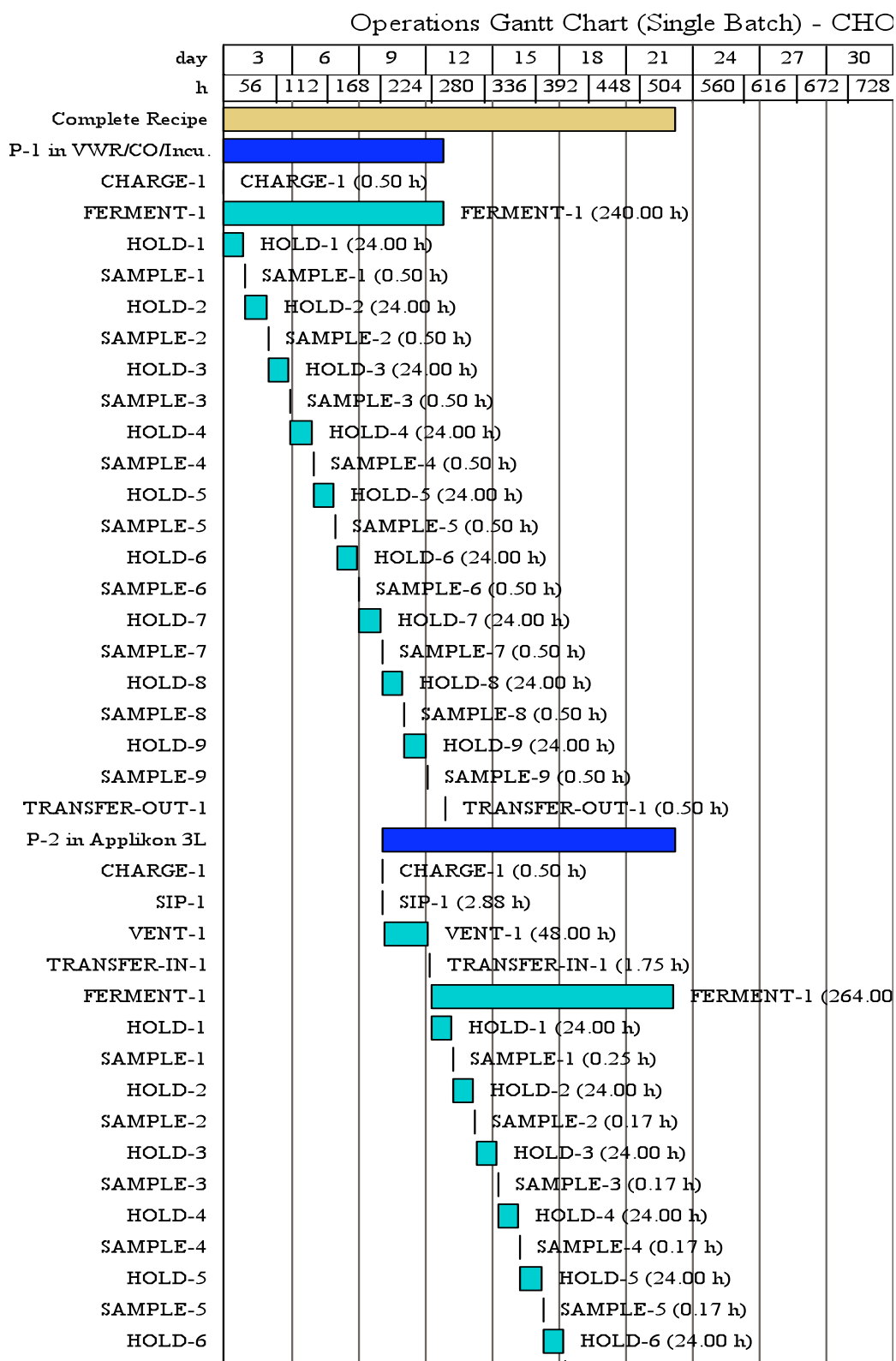


Fig 3.11. Gantt chart schedule for the CHO cell upstream process as generated by Super Pro Designer software.

3.10 References

- [1] Puck, T., Cieciura, S., Robinson, A. 1958. *The Journal for Experimental Medicine*, **108**(6):945-956.

- [2] Yin, Xiao and Dong, Zeng. 2001. *Essentials of Apoptosis*. Humana Press, 300 pp.

- [3] Sáez-Miranda, J.C., Saliceti Piazza, L., and McMillan, J.D. 2005. Measurement and analysis of intracellular ATP levels in metabolically engineered *Zymomonas mobilis* fermenting glucose and xylose mixtures. *Biotechnology Progress* **22**(2):359- 368.

4. Experimental Results and Discussion

4.1 Cell Culture Respiration Profile

In this study, the metabolism (secondary and primary) and their perturbations via over expression of anti-apoptotic molecules were monitored and analyzed to improve and establish a culture profile for Chinese hamster ovary (CHO) cells. Some of the standard measurements from samples collected in suspended cell culture were performed in equipments normally used in the biopharmaceutical industries, such as the HPLC and biochemical analyzers, among others. On the other hand, as another way to achieve a similar measurement profile, Raman spectroscopy with multivariable analysis was used to correlate the reference data to the Raman spectra. Figures 4.1-4.4 show results for the quantitative analyses made for cell density, glucose and L-lactate concentrations, and viability patterns for each culture condition. For each condition, a duplicate was performed to demonstrate reproducibility and consistency.

In order to compare pattern behavior and results, each measurement is compared through all experiments. For example, cell density was compared between all conditions giving a remarkable difference among conditions studied (Figure 4.1). L-lactate production and consumption patterns were also studied and significant differences between conditions were found (Figure 4.2). This suggests that when added to the cell culture, the apoptotic inhibitor affects or stops the gluconeogenesis pathway, among other biochemical pathway changes observed. A marked increment in L-lactate production and a constant cell density (Figures 4.2 and 4.3) and viability (Figure 4.4) instead of an increment in cell density and a viability drop through the last days of the batch (a normal pattern in cell behavior) were also observed. This suggests a change induced by the over-expression of the apoptotic molecule in the media. Lactate and cell density pattern changes (increment and constant behavior, respectively) observed under the conditions with the apoptotic molecule over-expression correlated with some studies made by Centocor [1] using a different apoptotic inhibitor and genetic modifications instead of over-expression.

The best performance for the two factors studied and four conditions involved was with the temperature range of 35 to 33°C with the over-expression of the apoptotic inhibitor. This condition provoked an alteration of the gluconeogenesis pathway (a complete inhibition) avoiding the consumption of L-lactate by the cell, but keeping the viability and cell density constant along the culture batch. As a last source of analysis for the cell behavior profile, graphs with a comparison between inhibitor over-expression and both temperature ranges (37-33°C and 35-33°C) were studied (Figure 4.5 - a and b). On the analysis of both ranges it is clearly seen that our proposed range of 35-33°C achieved more cellular stability and a better viability percent. Our explanation is that a shorter temperature shift of two degrees (35-33°C) instead of a larger one of four degrees (37-33°C), could bring a faster stabilization and adaptation of the cell to reach the hypothermia phase at 33°C, aiming towards its survival and by consequence production of more by-products rather than incrementing cell growth or reproduction.

A more complete evaluation of this performance will be included in the conclusions and recommendations chapter (Chapter 5). All cell density and viability data were obtained using a Nexcelom Cellometer in which the trypan blue exclusion tint technique was performed (Chapter 3).

Another useful comparison is the specific growth rate and cell diameter for each condition. With the first information a time of cell doubling (also known as cell doubling time) could be calculated. It is important to bring to the discussion that for cases in which the inhibitor was present the specific growth rate, the doubling time and cell diameter were widely affected. For the inhibitor addition conditions, values were lower as compare with no addition of the inhibitor. On the contrary, the cell diameter achieved values up to 15 microns, values higher with the presence of the inhibitor rather than without it (refer to tables A2 and A3 of the Appendix).

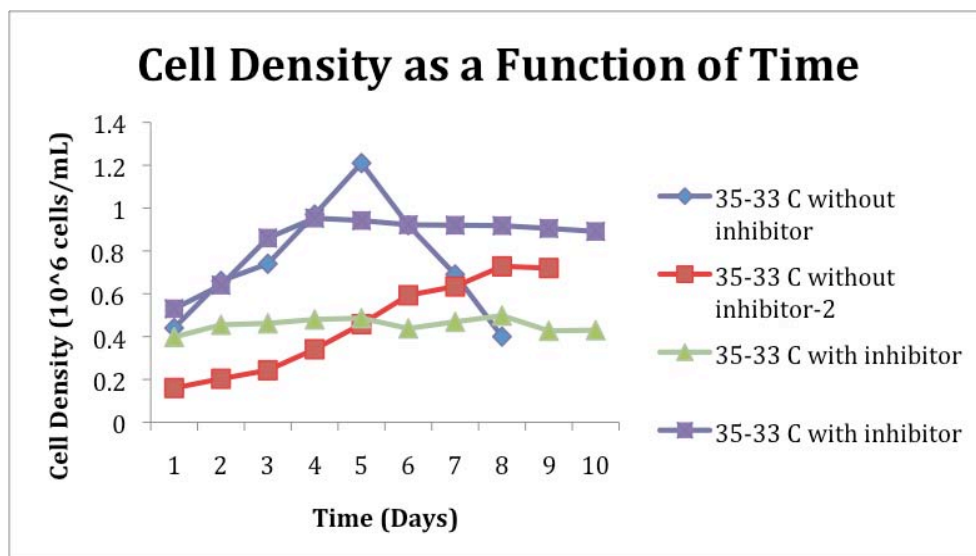
A remarkable increment (as mentioned above) in L-lactate up to approximately 35% than the normally observed in this kind of cultures affected pH ranges and increased the amount of base used and by consequence the osmolality values were higher in cases

when the inhibitor was present in the media (Table A3 of the Appendix). It is imperative to mention that a phenomenon in its earliest study designated by its researchers as a “Rising Phoenix” was observed in this work. Along with the inhibition of apoptosis, given the strategy of inhibition, caspase 3 and 7 were also locked or shut down [11]. This caspase inhibition brought a completely “turn off” of the growth process of the cell as shown on Figures 4.1 a and b. It is widely seen that since the inhibitor was present on day 3 until the run was finished, the cell density was basically constant.

4.2 Determination of Glucose, L-Lactate, Other Metabolites and Internal Cell Material using Raman Spectroscopy

The following analysis was performed to generate partial least squares models for the prediction of glucose and L-lactate concentrations in a batch reactor. Raman spectroscopy was used for the analysis of these metabolites due to the strong absorption of energy by organic molecules and the weak absorption of the hydroxide band, enabling to avoid water interference, which is the most abundant component of the media, and to reduce disturbances of this compound in the final results. It is important to mention that even when the OH band was extracted from the analysis, the spectra obtained for each sample were not completely smooth, mostly by the presence of fluorescent molecules added to the media as markers by the manufacturing company to detect pH variations.

(a)



(b)

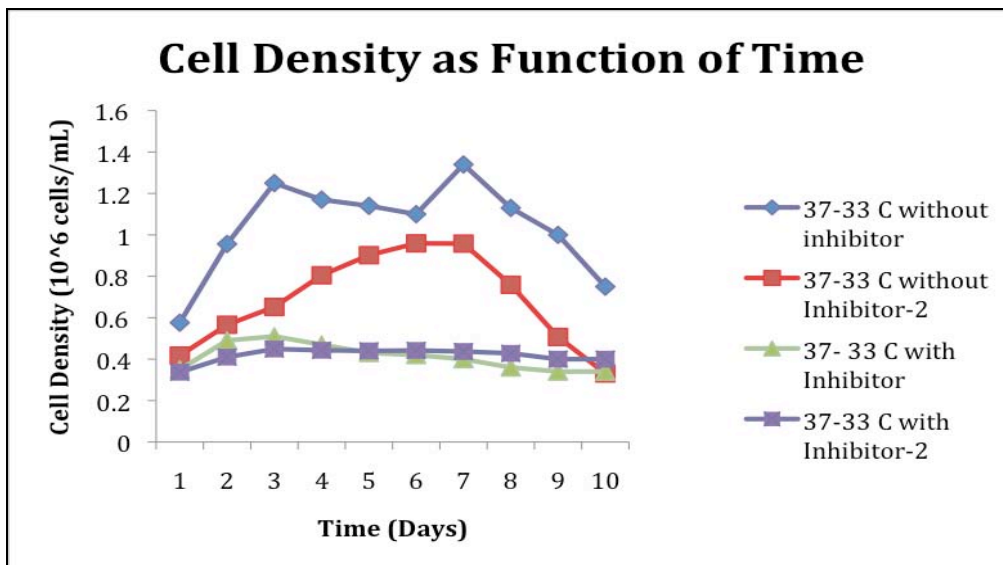
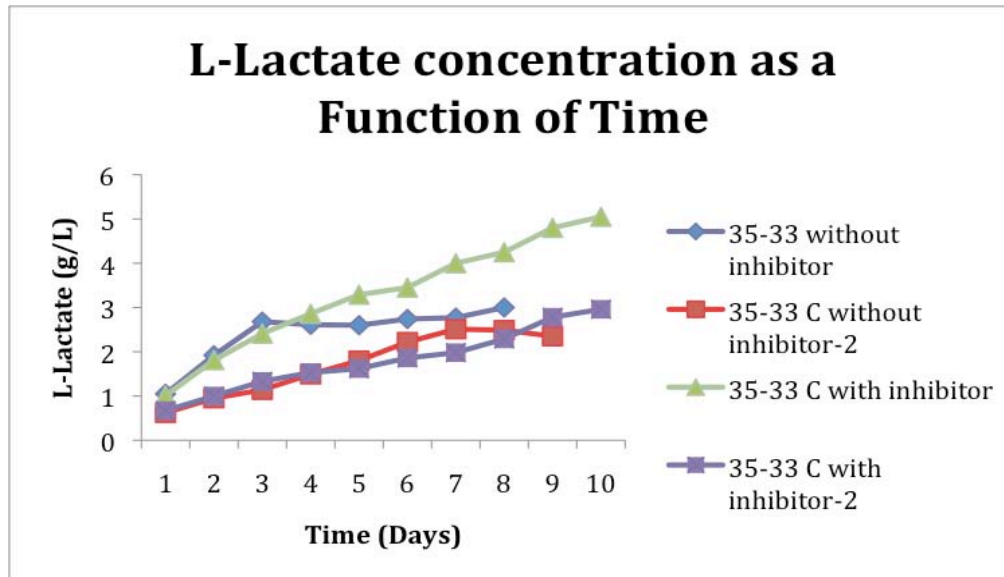


Figure 4.1. (a) Cell density measurements as a function of time, with or without inhibitor at 35-33°C temperature shift and (b) with or without inhibitor at 37-33°C temperature shift. Duplicate batch for each condition are shown.

(a)



(b)

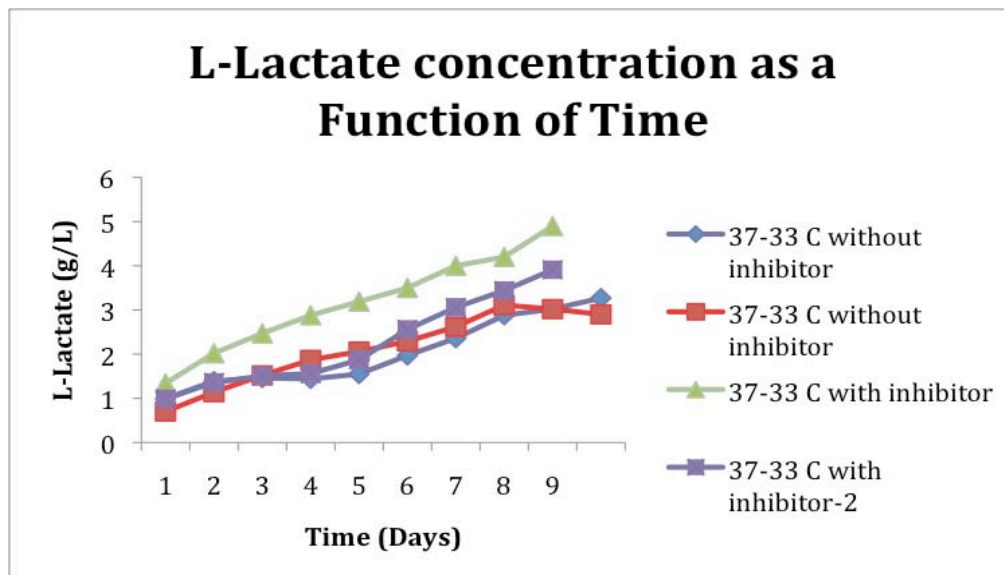
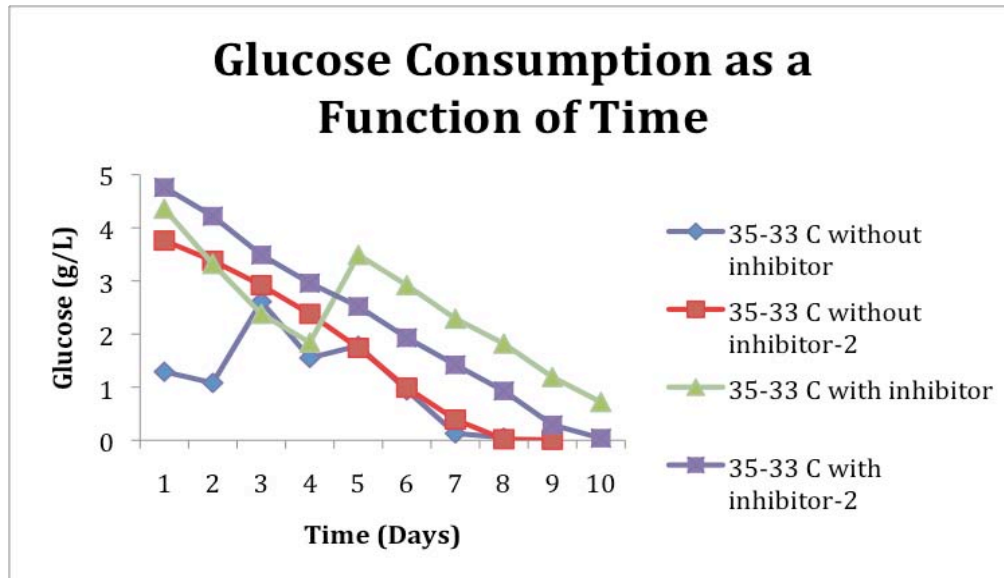


Figure 4.2. L-Lactate concentration as a function of time monitored with the YSI 2300, a biochemical analyzer. The HPLC was used for the cases in which the anti-apoptotic molecule was over-expressed. All measurements were made in the following conditions: (a) with or without inhibitor at 35-33°C temperature shift and (b) with or without inhibitor at 37-33°C temperature shift. Duplicate batch for each condition are shown.

(a)



(b)

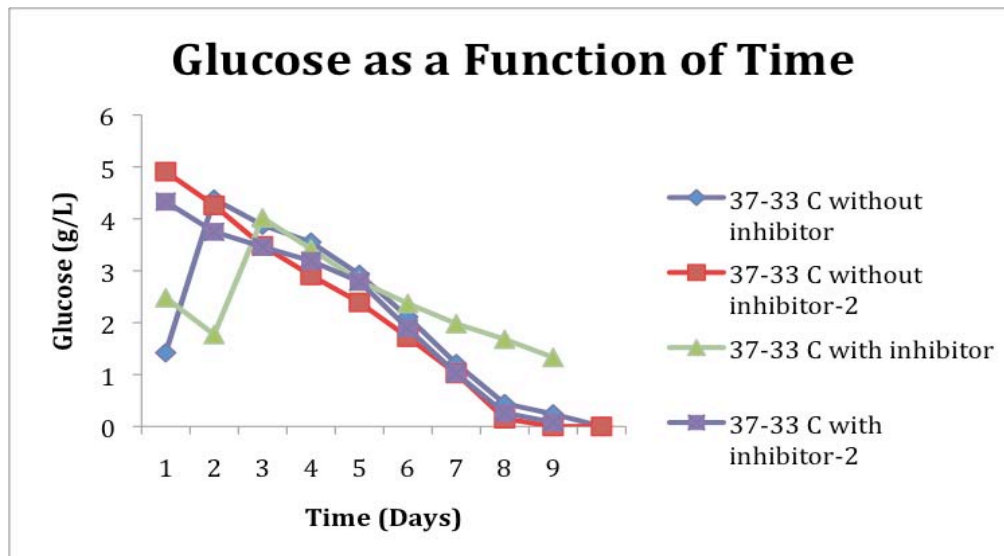
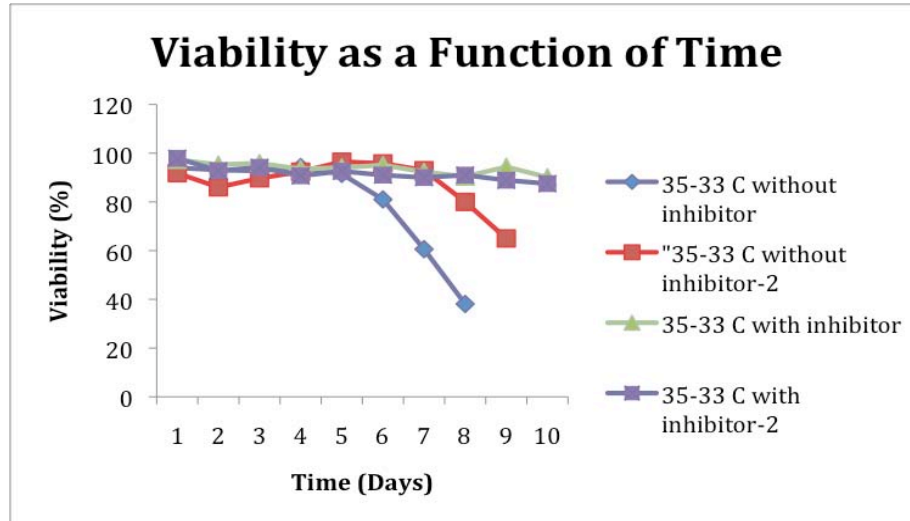


Figure 4.3. Glucose consumption as a function of time, measured using the YSI 2300 analyzer. All measurements were made in the following conditions: (a) with or without inhibitor at 35-33°C temperature shift and (b) with or without inhibitor at 37-33°C temperature shift. Duplicate batch for each condition are shown.

(a)



(b)

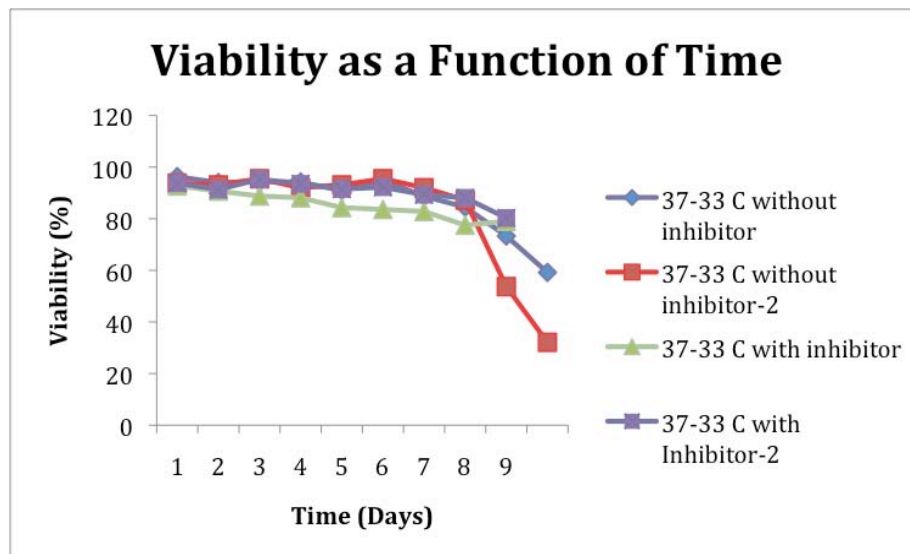
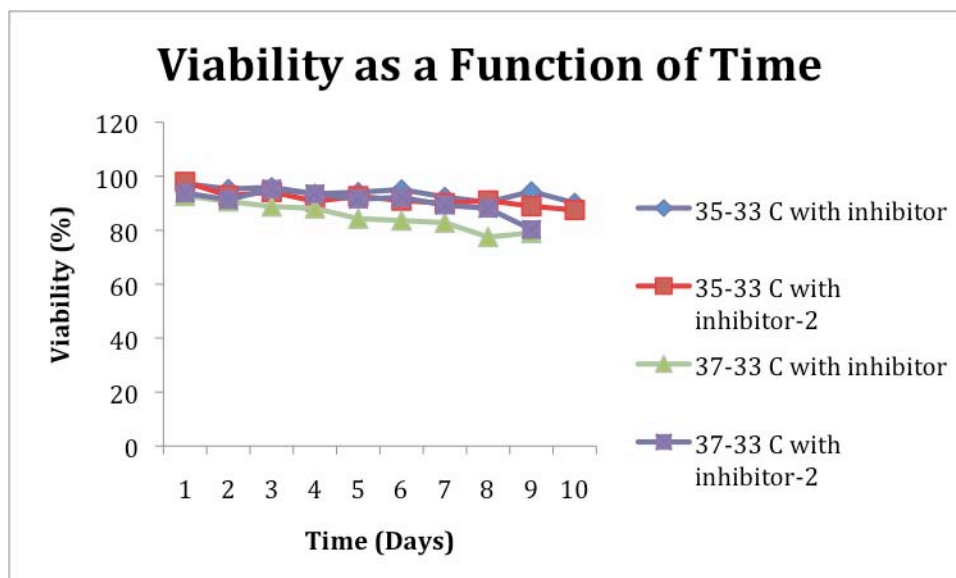


Figure 4.4. Sample measurements for all conditions and their replicate for cell viability as a function of time (a) with or without inhibitor at 35-33°C temperature shift and (b) with or without inhibitor at 37-33°C temperature shift. Duplicate batch for each condition are shown.

(a)



(b)

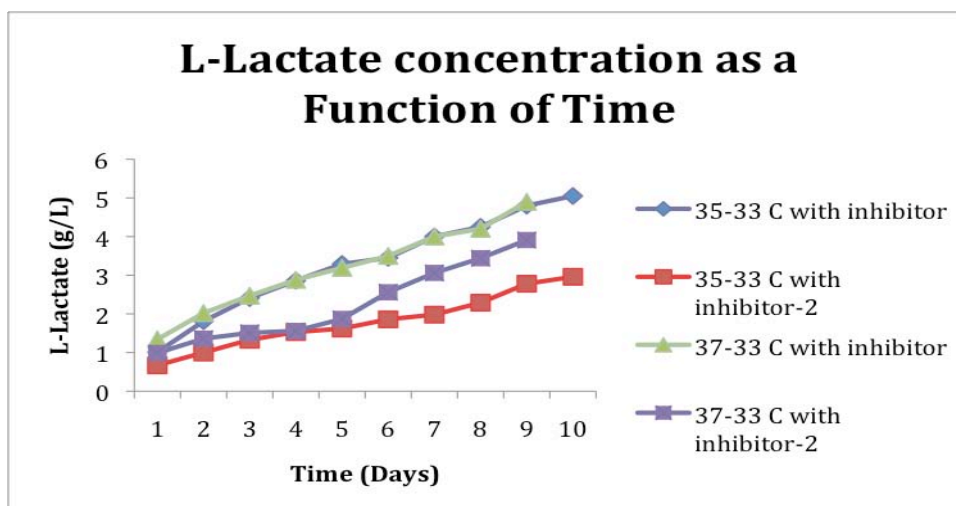


Figure 4.5. (a) Cell viability as a function of time at both temperatures ranges and (b) L-lactate concentrations at both temperatures ranges. Duplicate batch for each condition are shown.

On the other hand, reports about chemometric analysis of glucose and L-lactate or any other component, including the cells, in suspended mammalian cell culture are not abundant or practically non-existing in the literature. Over the years, scientists have studied the dynamics of anchorage mammalian cells along time using Surface Enhanced

Raman Spectroscopy (SERS), trying to understand the development of primary and secondary metabolism, and when and how the different apoptotic cascades are triggered in mammalian cells [2].

Among these studies, the predominant were the ones made with epithelial cells, human cells and CHO cells [3], being the last one the less studied, but the most important in the bio-pharmaceutical industry. Studies of these primary and secondary metabolites (glucose and L-lactate) were made by “using Raman spectroscopy as the source or tool of study, but only in pure solutions of these media components [4].” In these studies, tools such as partial least squares (PLS) for multivariate analysis were used and showed a great correlation along time. As established in the first sentences of this section, no studies using mammalian cells (specifically CHO) in suspended cell culture and Raman spectroscopy have been jointly used, neither multivariate analysis or chemometrics have been applied to model this system.

It is important to mention that our approach is focused in establishing a precedent or fundament for the adoption of this tool as a Process Analytical Technology (PAT) to achieve a better understanding of the suspended cell culture behavior along time without perturbing, drawing samples, or making any kind of invasive measurement to monitor the batch culture. Among these invasive techniques are the biochemical analyzers (such as YSI 2300, 2700, etc.), and the widely used High Performance Liquid Chromatography (HPLC) technique. Both of these techniques were used as reference methods to test the feasibility and reproducibility of the Raman. A calibration of the Raman equipment was made using pure sterile media, pure L-lactate and pure glucose solutions to differentiate relevant peaks that could represent each molecule. By the work of *Ren, et al.* [4] we can deduce that a PLS analysis could give a better understanding, given the similarity in structure of glucose and L-lactate. The work from the same authors was used as a calibration model to compare between pure solutions and the media [4].

All variations such as operational conditions and the addition or no addition of the apoptotic inhibitor were tested, and Raman spectra on a day-to-day basis for each

experiment were obtained and analyzed giving a substantial variation in concentrations among time of the glucose and L-lactate present in the samples.

4.2.1 Regions of Spectral Analysis

The selection of the spectral region to be studied is an important element of the evaluation process. In our case, association patterns related with peaks were evident among the data set, particularly in the low lambda region of the spectra ($1400-100\text{ cm}^{-1}$). The spectra were characterized mostly by a clear definition of the peaks and the change in concentrations along time, but also with non-smooth spectra given the fluorescence present in the media. Figures 4.6 to 4.9 show different replicate spectra obtained under each condition studied throughout the first to last days of each batch. A remarkable difference between concentrations for each spectrum can be seen along time for each experimental condition studied. Four conditions were set and studied. Conditions with a temperature range of $35-33^{\circ}\text{C}$ without apoptosis inhibitor and conditions with a temperature range of $37-33^{\circ}\text{C}$ without apoptosis inhibitor were focused on temperature ranges. Conditions with a temperature range of $35-33^{\circ}\text{C}$ with apoptosis inhibitor and conditions with a temperature range of $37-33^{\circ}\text{C}$ with apoptosis inhibitor were focused on the interactions (if any) between temperature ranges and the over-expression of the apoptosis inhibitor.

4.2.2 Description of the Primary Data Sets

The primary data consist of four different operational conditions studied in which two levels of temperature ranges ($35-33^{\circ}\text{C}$ and $37-33^{\circ}\text{C}$) and addition or no addition of an apoptosis inhibition were studied. Eight experiments were made, in duplicate by each condition studied and daily samples were collected and analyzed, resulting in 72 samples in total. The spectra were obtained in the $300-100\text{ cm}^{-1}$ range, but our analysis focused

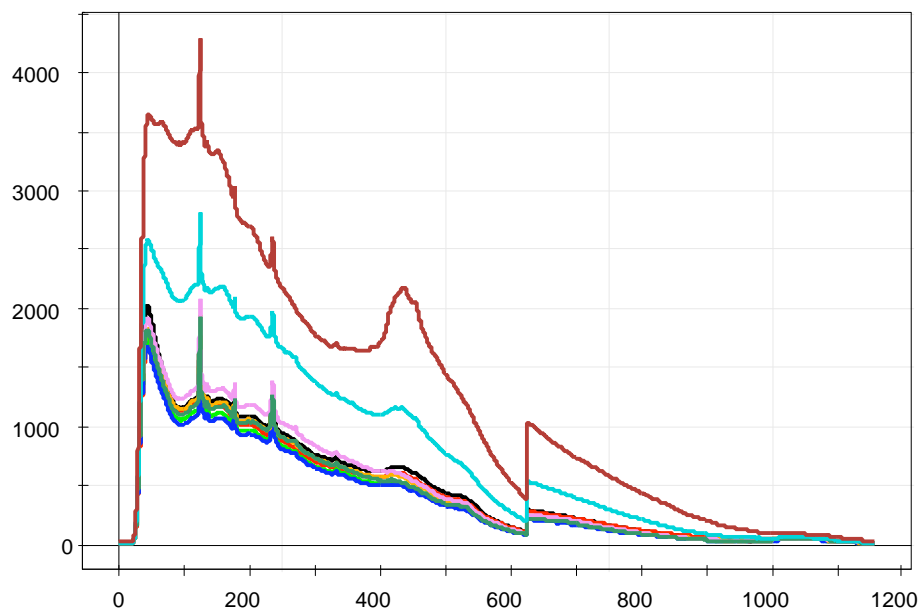


Figure 4.6. Raman spectra for suspended CHO cells culture system as seen in SIMCA Plus software. Culture days 1-9 of condition 1: 35-33°C and no inhibitor present in the media. For this case the red spectra represent day 9 and the dark blue day 1.

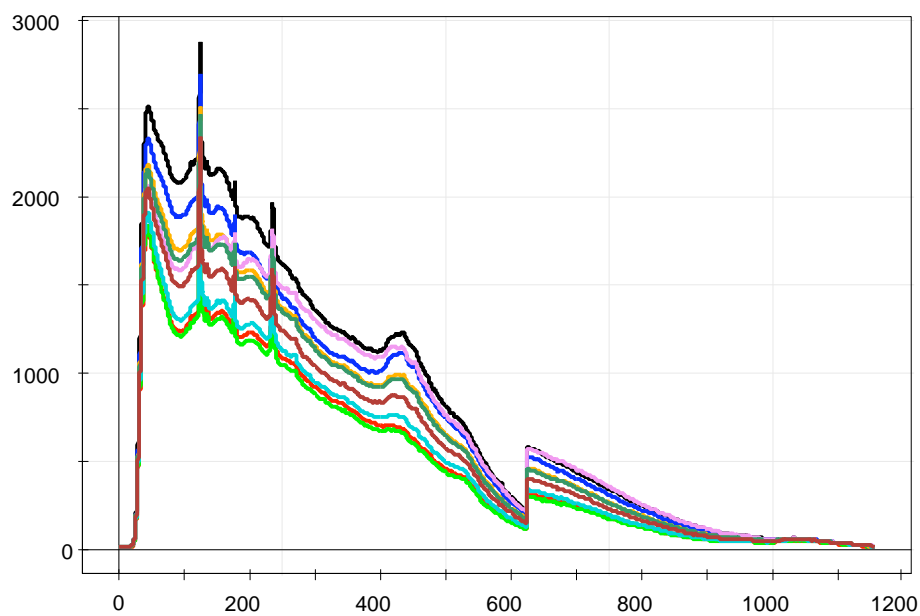


Figure 4.7. Raman Spectra for suspended CHO cells culture system as seen in SIMCA Plus software. Culture days 1-9 of condition 4: 37-33°C and no inhibitor present in the media. For this case the black spectra represent day 9 and neon green day 1.

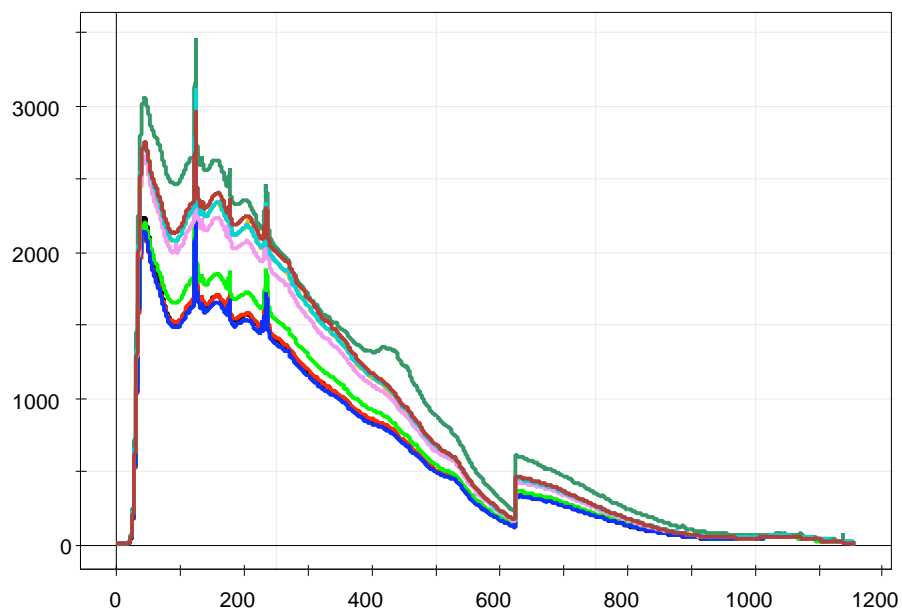


Figure 4.8. Raman Spectra for suspended CHO cells culture system as seen in SIMCA Plus software. Culture days 1-9 of condition 3: 35-33°C and the inhibitor present in the media. For this case the dark green spectra represent day 9 and royal blue day 1.

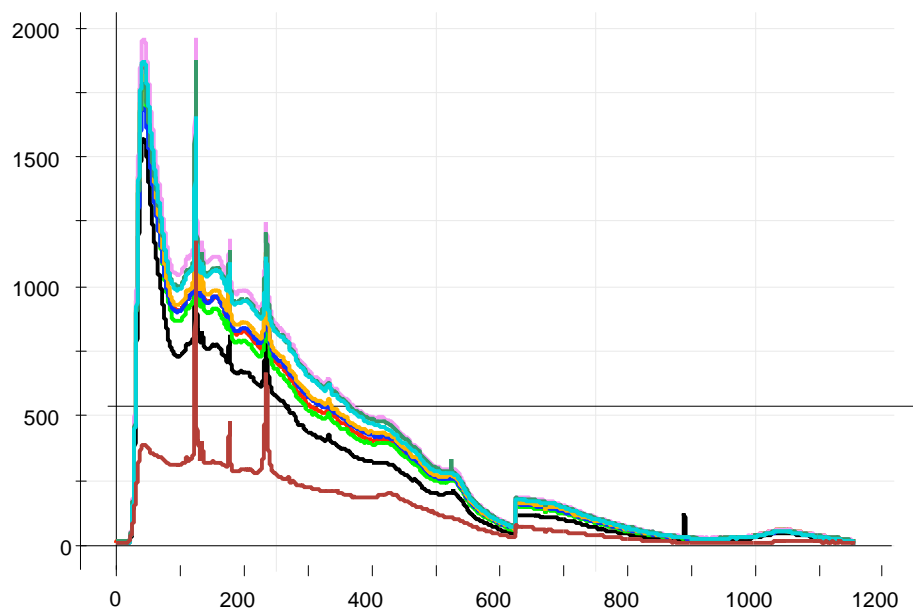


Figure 4.9. Raman Spectra for suspended CHO cells culture system as seen in SIMCA Plus software. Culture days 1-9 of condition 2; 37-33 °C and the inhibitor present in the media. For this case the pink spectra represent day 9 and dark red day 1.

in the 1400-100 cm^{-1} range of the spectra. The total “X” variables (absorbance) were approximately 11,500 points. The analysis used to differentiate between peaks consistently appearing under all conditions reduced our multivariate analysis to approximately 400 points.

4.2.3 Raw Data Evaluation

From the scrutiny of raw spectra shown in Figure 4.10, the additive and multiplicative effects are present, showing that the higher the concentration of the analytes the higher absorbance in the spectra. The Raman, as we can see, differs from other techniques such as Near Infrared (NIR) in general, because more spectral features are present for each solute and the features are narrower, with less overlap for the Raman. The dominant spectral peaks have been determined by others scientist [5]. Glucose bands are centered at 880, 1072, 1128, 1267, 1334, 1370, and 1464 cm^{-1} , corresponding to C-C stretching, C-O stretching, C-O-H bending, CH_2 twisting, CH_2 wagging, CH_2 wagging and CH_2 bending, respectively [6]. Lactate bands are centered at 855, 930, 1044, 1420, and 1457 cm^{-1} and are assigned to C-COO⁻ stretching, CH_3 rocking, C- CH_3 stretching, COO⁻ stretching, and CH_3 deformation, respectively [7].

The primary bands, distinguishing glucose are centered at the region of 1000-1100 cm^{-1} ; those for lactate are centered at the 700-900 cm^{-1} regions.

4.3 Determination of Glucose and L-Lactate Using the HPLC and the Biochemical Analyzer (YSI 2300)

Many methods are available to analyze metabolites and high-performance liquid chromatography is one of the most reliable and widely used by scientists and industry. In our case the use of this quantitative method, jointly with the YSI-2300, also known as a biochemical analyzer, were mostly to generate data as reference methods to the proposed Raman spectroscopic method. All three technologies differ mostly in the way of detecting changes of the concentrations of analytes. For HPLC, the way to separate, quantify and measure changes in compounds is through their idiosyncratic polarities and interactions with the column’s stationary phase. HPLC utilizes different types of stationary phases, a

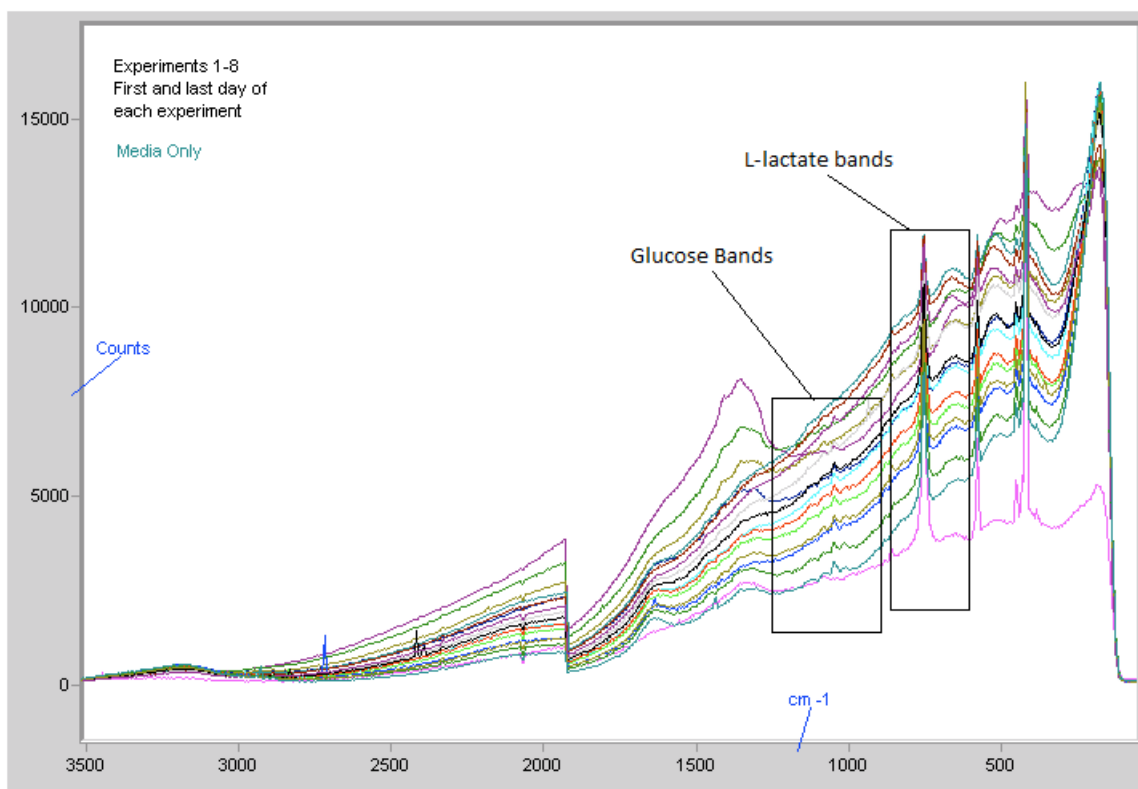


Figure 4.10. A representative example of Raman spectra obtained for day 1 and day 9 for each of the eight-batch culture performed. Graph shows Raman intensity in Absorbance Units (A.U.) as a function of the Raman shift in cm^{-1} . The regions of glucose and L-lactate bands are outlined in the Raman spectra.

pump that moves the mobile phase and analytes through the column, and a detector (refraction index) that provides a characteristic retention time for the analytes. It is important to mention that in our case the HPLC serves as a method to obtain data which we cannot get through our main comparison source, the biochemical analyzer (YSI 2300), mostly by the limitations with L-lactate concentration increment over the range of measurement accepted by the biochemical analyzer. A representative sample of measurements obtained using HPLC is shown in Figure 4.11.

On the other hand, biochemical analyzers are well used by the industry as a fast way to measure changes in concentrations of analytes if raw and fast knowledge of data is needed. although results are not as precise as those obtained from the HPLC as a control quality analysis technique. The biochemical analyzer chemistry (immobilized enzyme

technology) is more specific than the HPLC, but lacks in robustness and repeatability. The sample is aspirated by a mechanism (approximately 25 microliters) and passes through a membrane containing an immobilized enzyme. The enzymatic reaction releases oxygen peroxide that contacts a probe, generating an electric pulse that is converted by the machine to a concentration level of the substrate as g/L or mg/L. Data measured for the first four suspended CHO culture batches is shown in Table A.1 in the appendix as a representative example of the data obtained in all experiments.

For Raman spectroscopy, the interaction and energy between bonds gives a particular signal that can be used as a “finger print” in a direct correlation with the intensity of the peaks and using multivariate analysis techniques (chemometrics software) concentrations, pattern behavior and dynamic changes of the metabolites could be detected and quantified. Sample spectra of our data were discussed and shown in Figures 4.6-4.10.

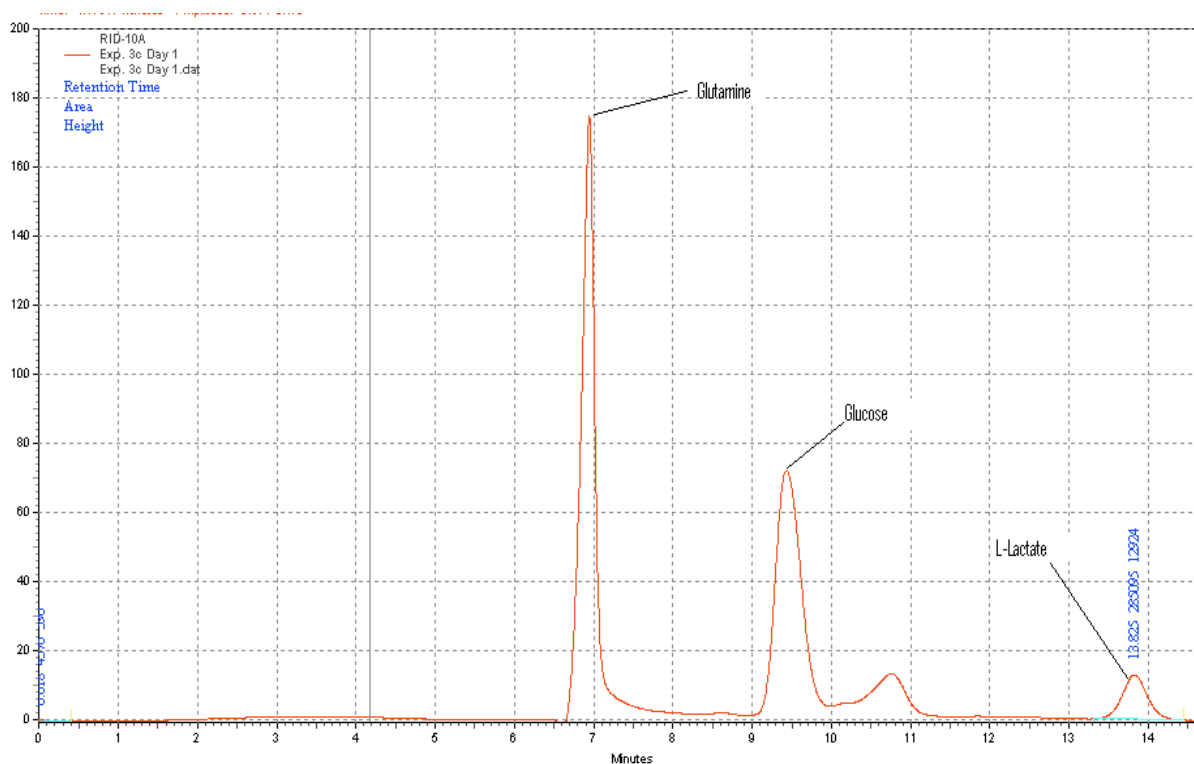


Figure 4.11. A representative chromatogram of a CHO cell culture sample using the HPLC reference method.

4.4 Suitable Fits of X/Y Variables for Glucose and L-Lactate

To identify behavior or patterns and foresee changes in cell density or primary and secondary metabolites in a quantitative or qualitative way at real-time, is one of the important goals of upstream processing in the bio-pharmaceutical industry. Many approaches to achieve these goals using different technologies are available off-line, but what if all could be executed using only a single statistical technique and one analytical technology? Partial least squares regression (PLS) is well known as one of the best techniques to achieve this goal jointly applying Raman spectroscopy. PLS regression is a statistical method that keeps some relation to principal component analysis (PCA). PLS finds a linear regression model by projecting the predicted variables and the observed variables to a new space [8].

PLS is widely used to find the fundamental relations between two axes or matrixes (X -observed variables, Y -predicted variables). A PLS model will try to find the multidimensional direction in the X space that could explain the maximum multidimensional variance direction in the Y space. This technique is particularly well matched when the matrix of predictors has more variables than the observations, in these particular cases standard regression (multiple linear regression) will fail to describe the system.

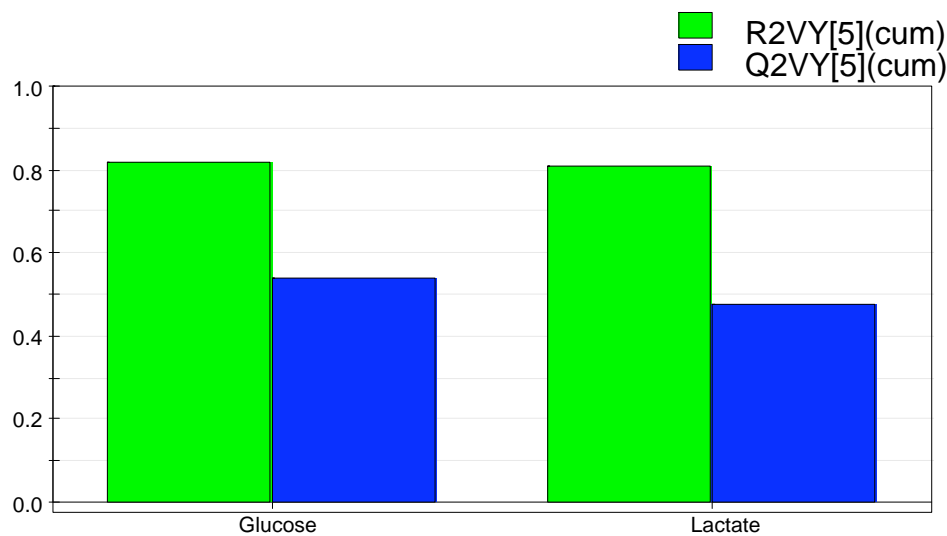
In our case of study, the PLS regression models were obtained and explained using SIMCA 11 + Software with two factors and 99% of the variance in the system, shown in Figures 4.12 to 4.14 as an example for glucose and lactate, respectively, in the ranges of more relevance. These plots basically show the cumulative R^2 and Q^2 for the Y matrix for each component. R^2 cumulative is the percent of variation for the entire Y explained by the model and Q^2 cumulative is the percent of the variation for the entire Y that can be predicted by the model. All these data interpreted as metabolites concentrations, is shown in several figures (Figures 4.1 and 4.2) for the cases in which we want to predict and validate our novel technique for glucose and L-lactate concentration measurements on the range studied in each case. It is important to bring to our discussion that given the large

amount of data obtained, examples of each analysis will be shown throughout the discussion.

Given the complexity of this kind of bio-process and the factors studied, experiments 1, 3, 5, and 7 were evaluated within the same PLS regression model; 2-8 in a different one and 4-6 in another too, in order to bring more stability and accuracy to the analysis and to create the suitable fits in X/Y variables for the proposed Raman spectroscopic technique as a process analytical technology (PAT).

Wavelength ranges analyzed were between $100\text{-}1100\text{ cm}^{-1}$, of which ranges $500\text{ to }600$, $700\text{-}800$, and $1000\text{-}1100\text{ cm}^{-1}$ were chosen to correlate the data obtained for L-lactate and glucose concentrations, respectively. Only these three ranges were choosing given the literature found mentioned in detail on chapter two. This data were analyzed using the biochemical analyzer (YSI 2300) and the HPLC as reference methods versus Raman spectra ranges for L-lactate and glucose to generate the PLS models. The range of $1000\text{-}1100\text{ cm}^{-1}$ was the most suitable for glucose (Figure 4.12). On the other hand, ranges of $500\text{-}600$ and $700\text{-}800\text{ cm}^{-1}$ were used to best represent L-lactate, as shown in Figures 4.13 and 4.14, respectively. Other ranges were obtained and analyzed, but only the ones mentioned were the most suitable for the analysis of these two important metabolites as reported in the literature about these two organic molecules. The other ranges might be analyzed as possible intracellular material, which could support our hypothesis of viability detection.

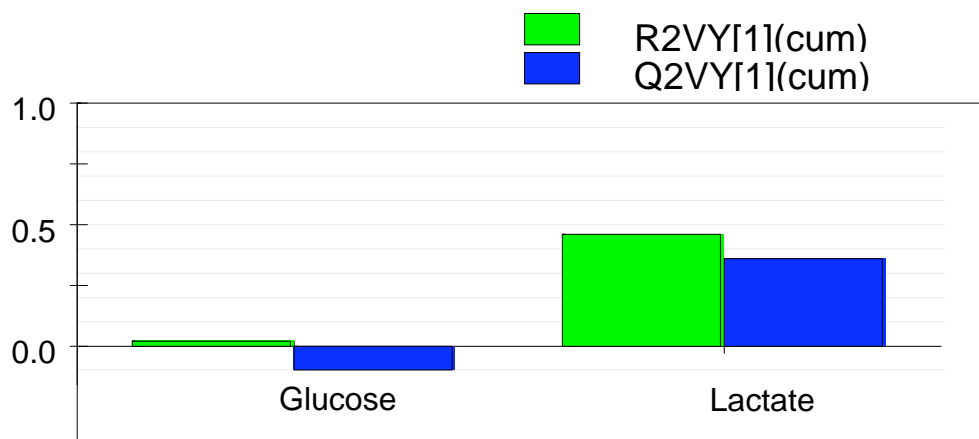
A single PLS regression of the four conditions studied in all ranges was practically impossible given the amount of data obtained and the negative impact that resulted when it was tested to the exercise proposed to validate the Raman spectroscopy technique as a PAT tool. All experiments were re-grouped by best fit by condition, avoiding data manipulation, but considering which will be the best way of analysis. Experiments with its duplicate, 1-5 and 3-7 were re-grouped to be analyzed separately in one PLS-regression, but condition and its duplicate were also analyzed separately, with the purpose to achieve a better model accuracy and precision.



SIMCA-P+ 11 - 5/4/2010 4:29:28 PM

A

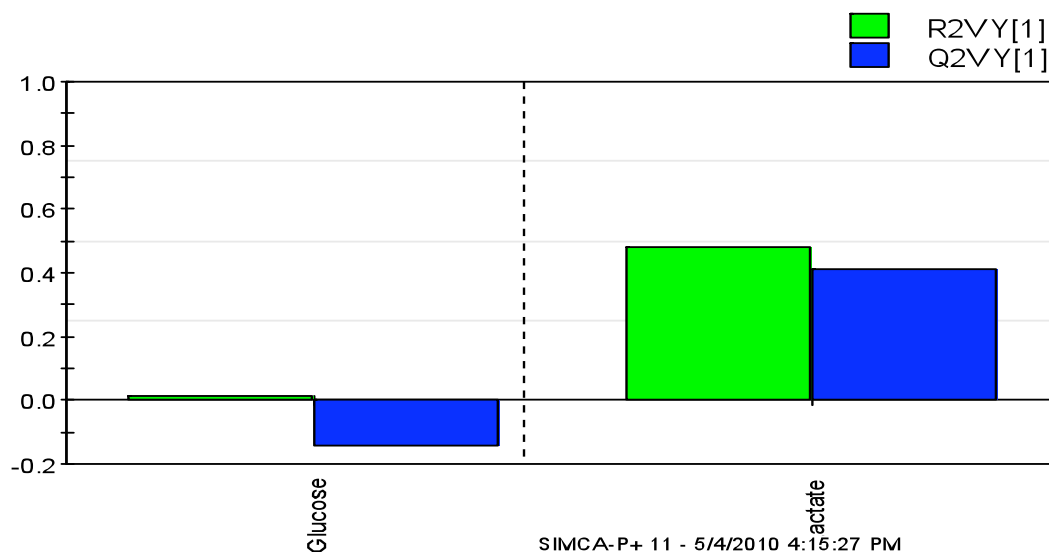
Figure 4.12. A satisfactory fit suggested for the cases 1-3-5-7 shown as A; that the components (glucose and L-lactate) find the direction in X space which get better the X-data description and provide a good correlations with the Y residuals. In other words, from the all points obtain by the Raman a satisfactory but not good correlation could be achieve between the Raman and the analyzer or the HPLC. It is important to mention that even though both components are reported in this graph, attention must be directed to glucose in this range ($1000-1100\text{ cm}^{-1}$), given that it is the suggested range to identify this component.



SIMCA-P+ 11 - 5/4/2010 4:20:34 PM

A

Figure 4.13. A satisfactory fit for L-lactate suggests a correlation between the observed values and model predicted values obtained with the Raman spectral data. This correlation between techniques could express a cross-validation suggesting one factor, L-lactate was the only component that find the direction in the X space that improve most the description of X data for this range ($500-600\text{ cm}^{-1}$).



A

Figure 4.14. Good fit is also observed for L-lactate in two of the three analyses performed for cross-validation at ranges of 700-800 cm^{-1} . This analysis could be validated with literature work that suggests this range as one of the ranges to detect characteristics peaks identifiable as L-lactate peaks.

In Figures 4.15 and 4.16 a series of t_1 vs. t_2 plots of the X scores are shown, which might be interpreted as a window into the X space. These plots show how the X conditions are located with respect to each other. The B plot of experiments 2-8 for glucose as ranges of 1000-1100 cm^{-1} show no outliers. Groups and possible patterns could be seen in the data. For the A plot the presences of two groups is clearly seen; an outliers are also shown (experiment 1 day 9).

However, in the plot for the range of 500 to 600 cm^{-1} (Figure 4.15) we could also see some points might be outliers, one sample of these possible outliers are experiment 1, day 9. Patterns and groups in the data are clearly seen also for this range but its interpretation is unknown.

To comprehend, analyze and interpret behavior or patterns from the data, we can observe the corresponding T2 range plots (Figures 4.17, 4.18 and 4.19). The T2 range plots display the distance from the origin in the model plane for each selected observation. Values larger than 95% critical limit (i.e., a significance level of 0.05) are considered as outliers and values larger than 99 % critical limit (a significance level of 0.01) should be

considered as serious. Samples for experiments 1 and 4 on days 9 and 9, respectively, are considered serious and outliers in that order. However, these data were not excluded, due to the integrity of the models obtained. If discrepancies, poor patterns and dynamics are found in the model, the presence of these outliers and serious point (at 99% confidence) should be considered.

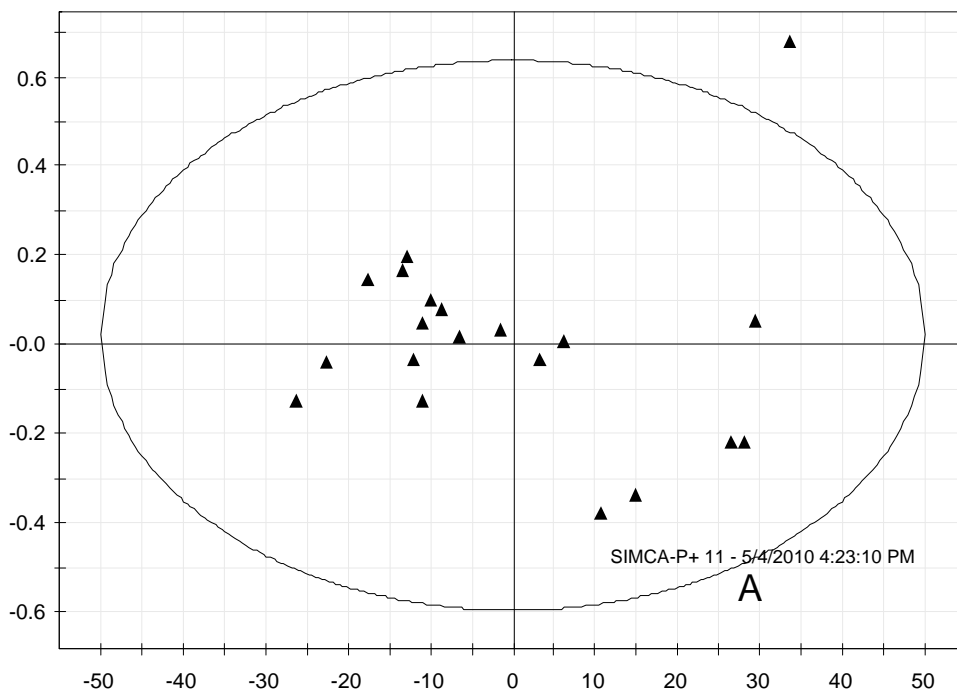


Figure 4.15. Score t_1 versus t_2 for experiments 1, 3, 5, and 7 (A) using PCA analysis.

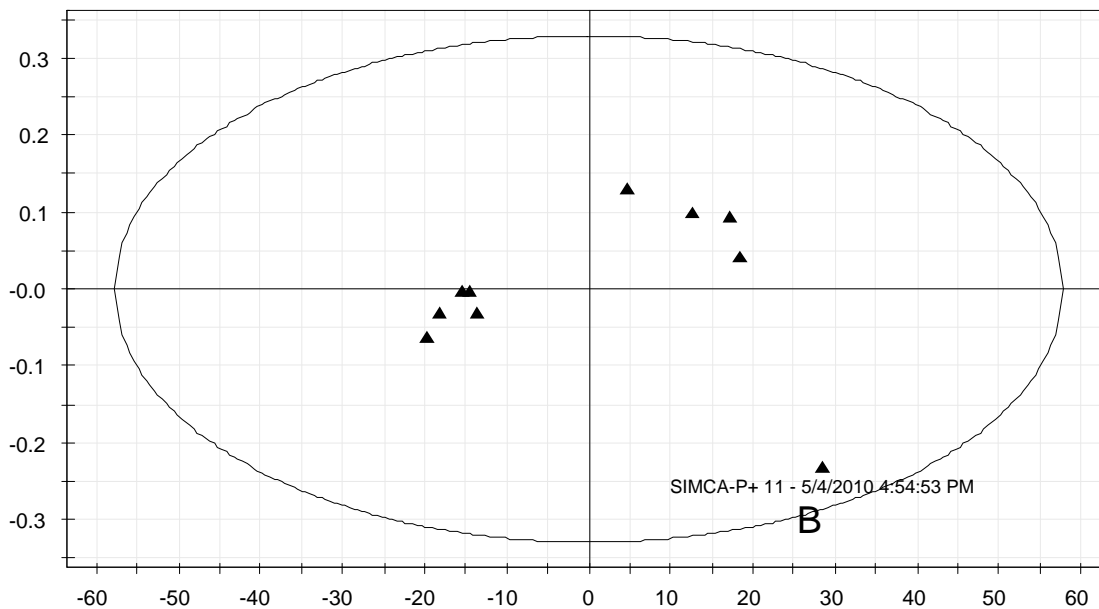


Figure 4.16. Score t_1 versus t_2 for experiments 2 and 8 (B) using PCA analysis.

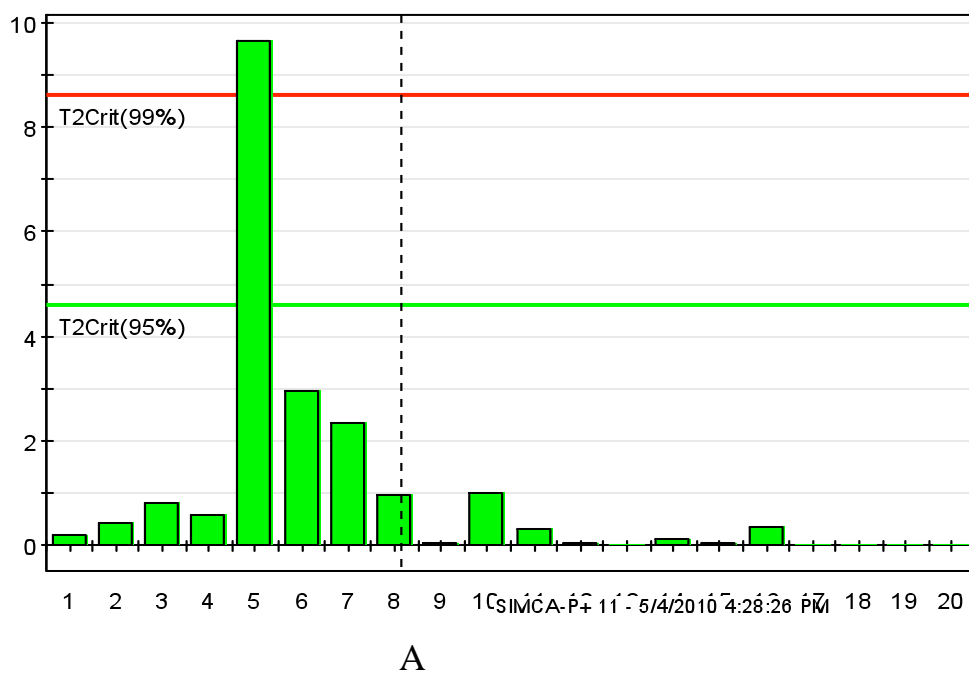
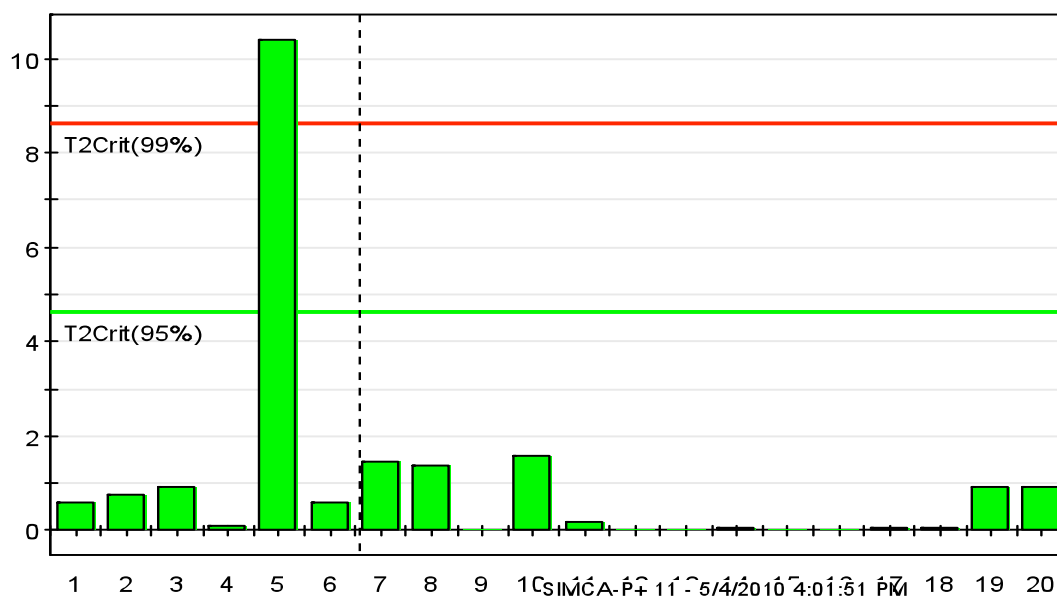
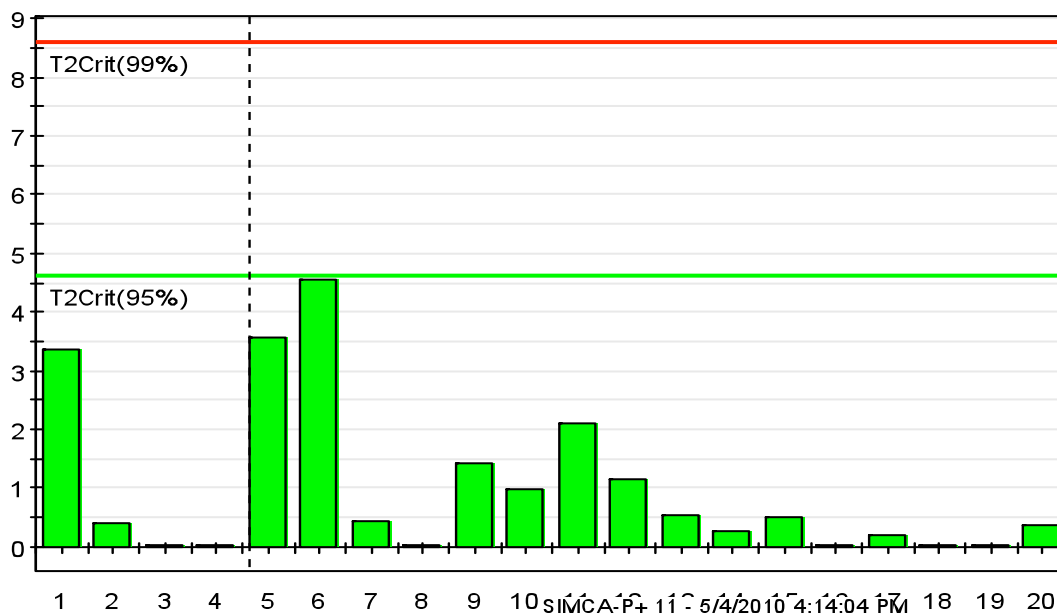


Figure 4.17. Hotelling T^2 range plots of glucose and L-lactate components containing experiments 1, 3, 5, and 7 (A) at a range of $1000\text{--}1100\text{ cm}^{-1}$.



A

Figure 4.18. Hotelling T2 range plots have L-lactate and glucose concentrations containing Experiments 1, 3, 5, and 7 (A) from range 500-600 cm^{-1} .



A

Figure 4.19. Hotelling T2 range plots of L-lactate and glucose containing experiments 1, 3, 5, and 7 (A).

As established earlier in the discussion, PLS regression is basically an extension of the multiple linear regression model. In its simplest form, a linear model specifies the relationship between a dependent variable (response) Y , and a set of predictor variables, the X 's. In our case we use PLS regression as a verification mode for our samples.

Another useful statistical tool to verify model predictions are cross validation and loadings plots. A very important step when fitting models that will be used for prediction is to verify (i.e. cross-validate) the results. In other words, to apply the current results to a new set of observations that was not used to estimate or compute the PLS model. In a way to obtain this, plots such as the predictive residual sum of square plot (PRESS) or the loading plot, can be generated, in order to choose the most favorable model that might explain the information without any noise or interruption present. Values of even days (2, 4, 6 and 8) for each CHO cells culture batch were not used to generate the model and were used for the cross-validation analysis.

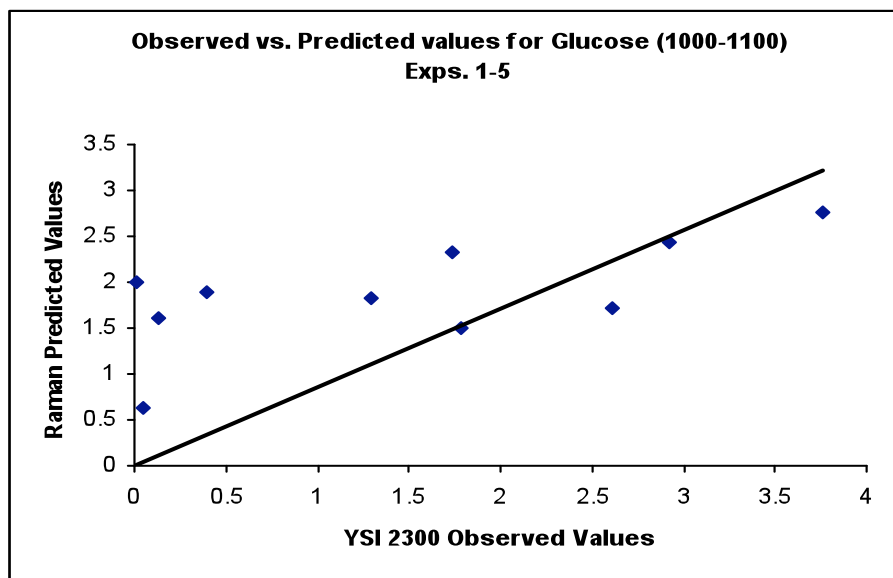
4.5 Predictions and Validation

It was stated in the first part of this chapter that one of the important goals in the biopharmaceutical industry is to predict behavior and patterns along time for new cell culture or fermentations runs, with the main objective to better understand the behavior of batches in real-time. Below is the test in which the predictive ability of the models are analyzed. Figures 4.20 to 4.22 illustrate the relationship or correlation between observed values and the predicted values by the PLS models. It is important to establish that for each of the four conditions studied individually, the majority of the experiments show a good and acceptable fit for the principal components measured (glucose and L-lactate).

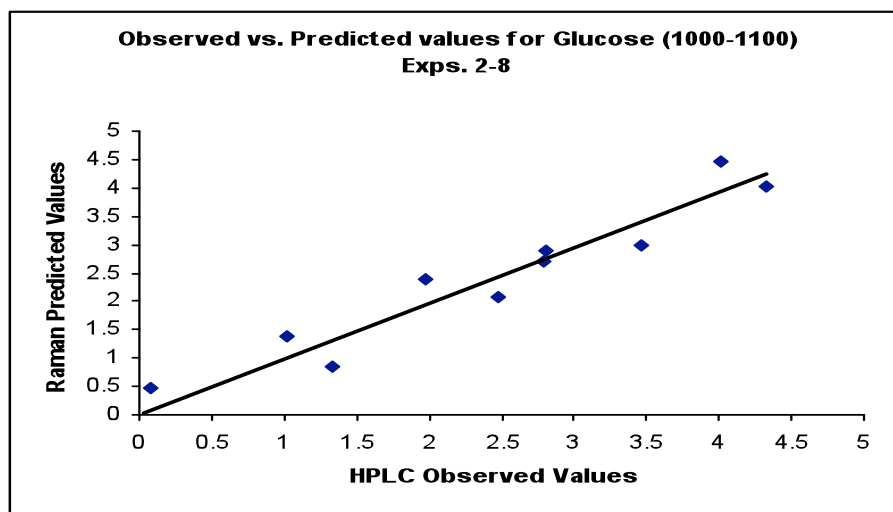
Good fits were obtained for L-lactate in the ranges of 500-600 and 700-800 cm^{-1} , coinciding with the ranges reported in the literature review. In the case of glucose, the selected range (1000-1100 cm^{-1}) was also in the range suggested by other works in which only mixtures and pure samples of both components (glucose and L-lactate) were reported to compare the reliability of Raman spectroscopy versus the near-infrared

technique [4]. A low frequency background or noise in the low lambda range was observed, given the tints present in the media used, which have fluorescence properties. However, an interference behavior is barely observed in the PLS model. The HPLC technique (used for conditions with apoptotic inhibitor) and YSI 2300, a biochemical analyzer, (used for condition without apoptotic inhibitor) were used as reference methods and compared with the model and plotted in the figures mentioned above.

(a)



(b)



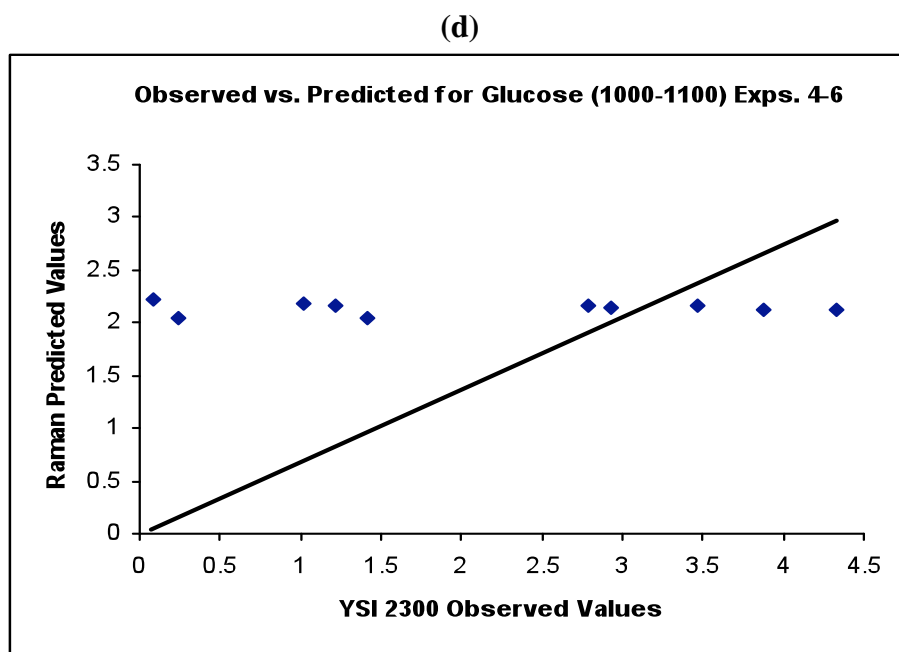
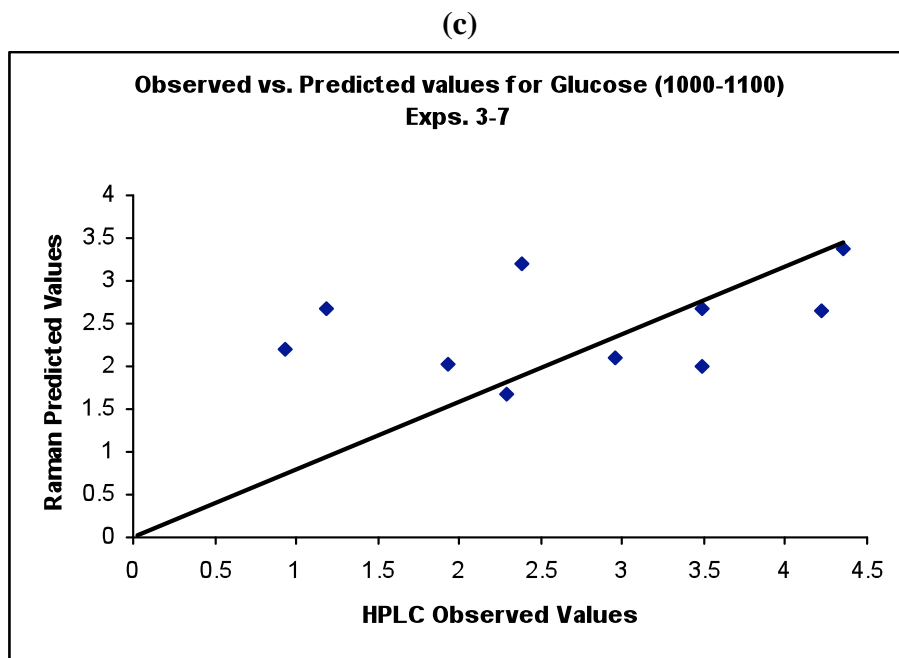
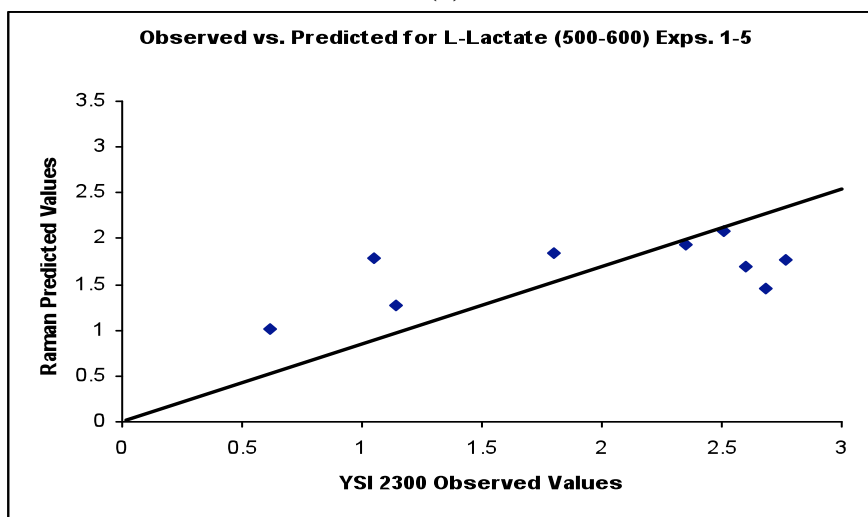
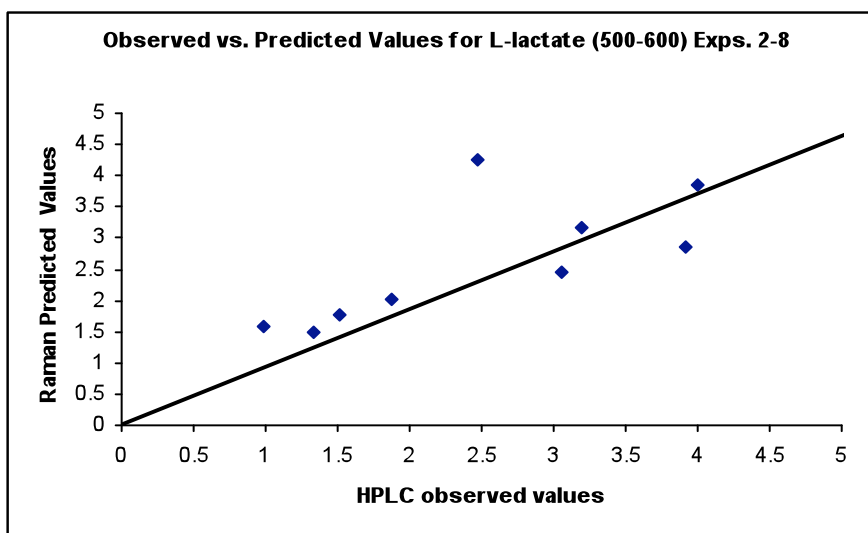


Figure 4.20. Relationship between observed and predicted values for experiments 1 & 5 (a), 2 & 8 (b), 3 & 7 (c) and 4 & 6 (d) at a 1000-1100 cm^{-1} suggested range to determine glucose concentration.

(a)



(b)



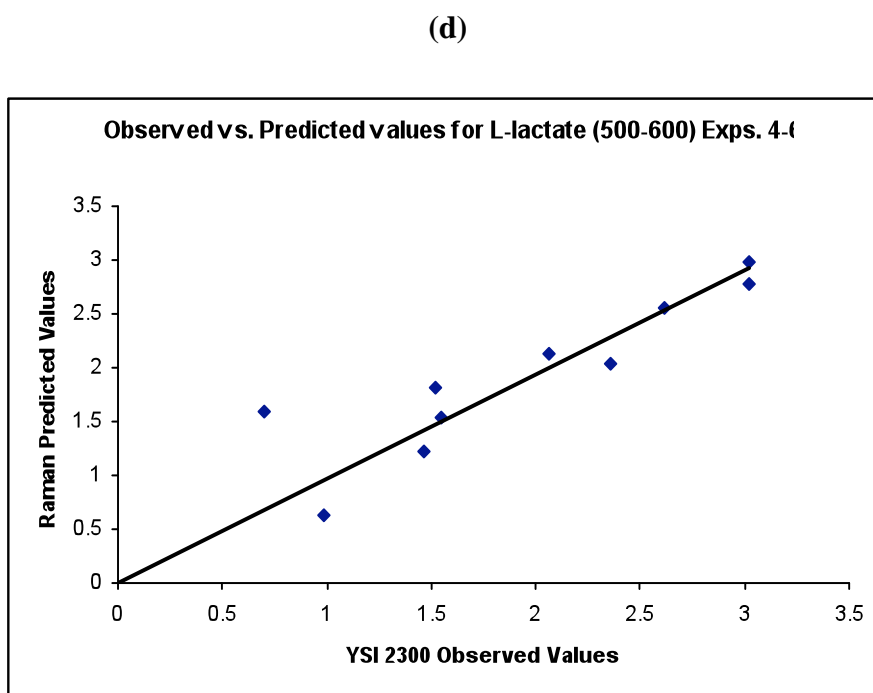
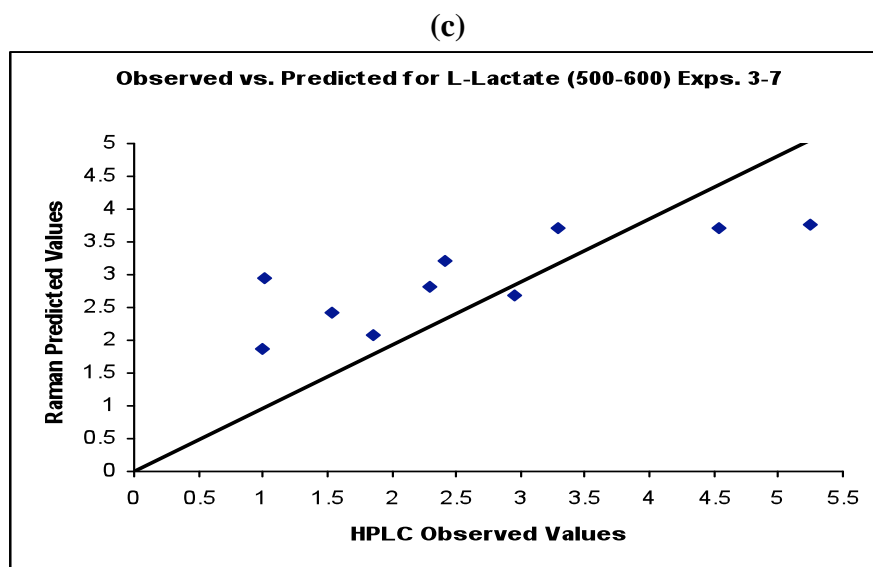
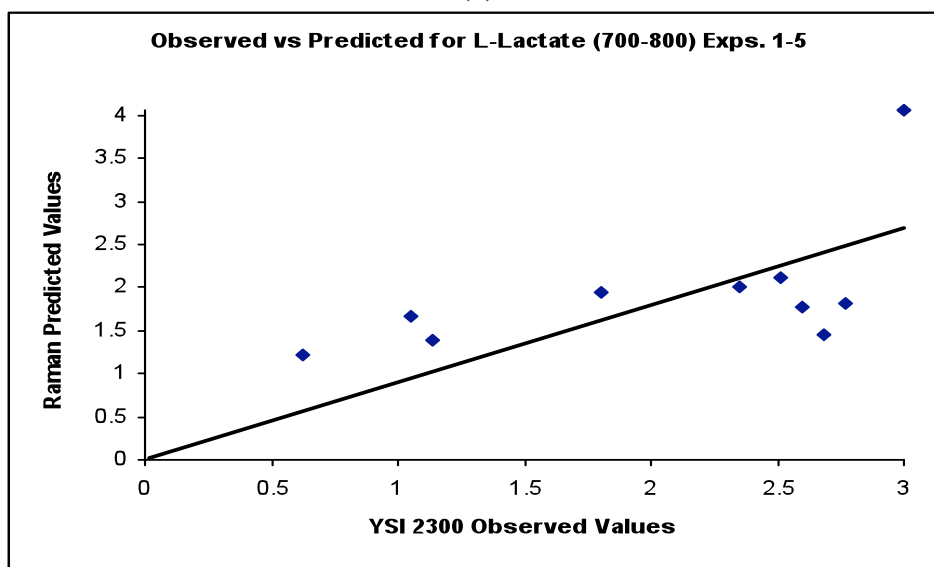
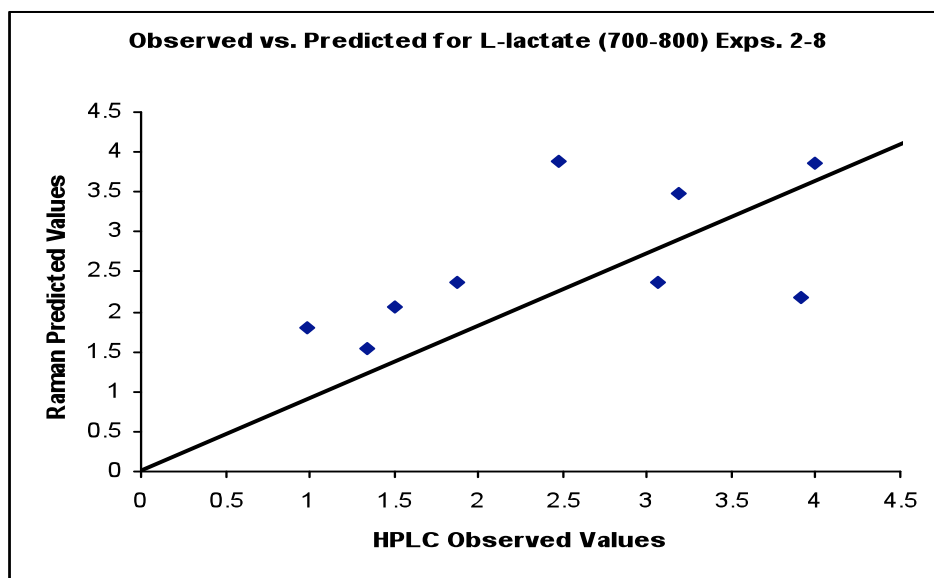


Figure 4.21. Relationship between observed and predicted values for experiments 1 & 5 (a), 2 & 8 (b), 3 & 7 (c) and 4 & 6 (d) at a range of 500-600 cm^{-1} to determine L-lactate concentration.

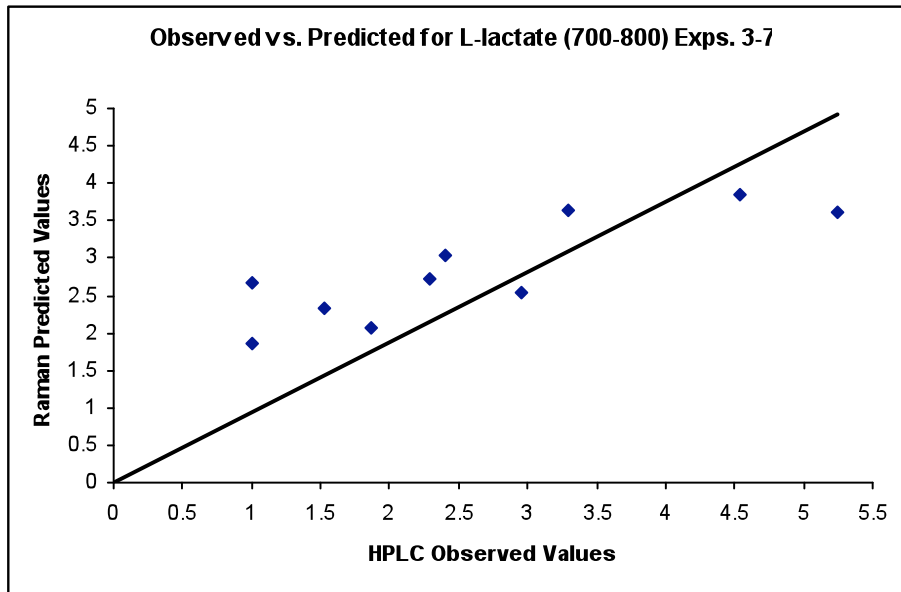
(a)



(b)



(c)



(d)

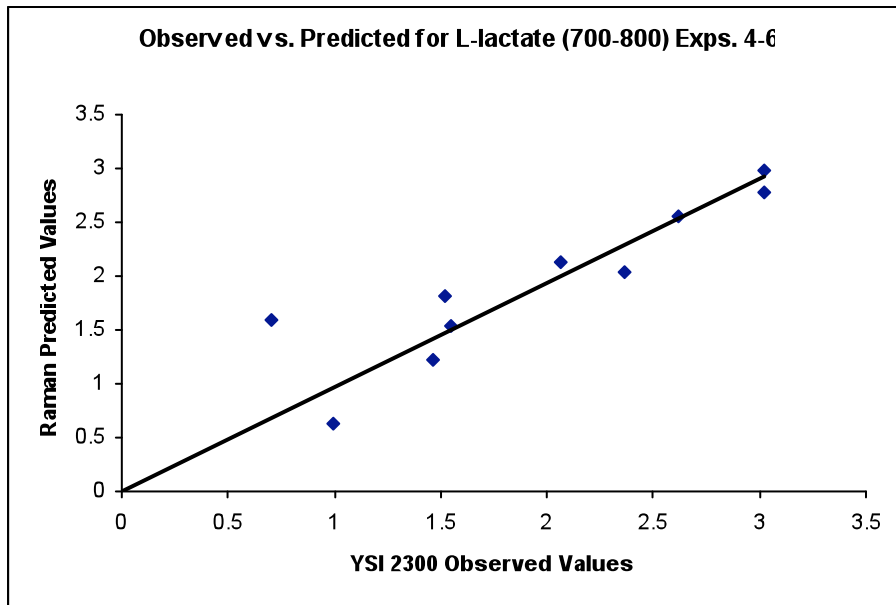


Figure 4.22. Relationship between observed and predicted values for experiments 1 & 5 (a), 2 & 8 (b), 3 & 7 (c) and 4 & 6 (d) at 700-800 cm^{-1} to determine L-lactate concentration.

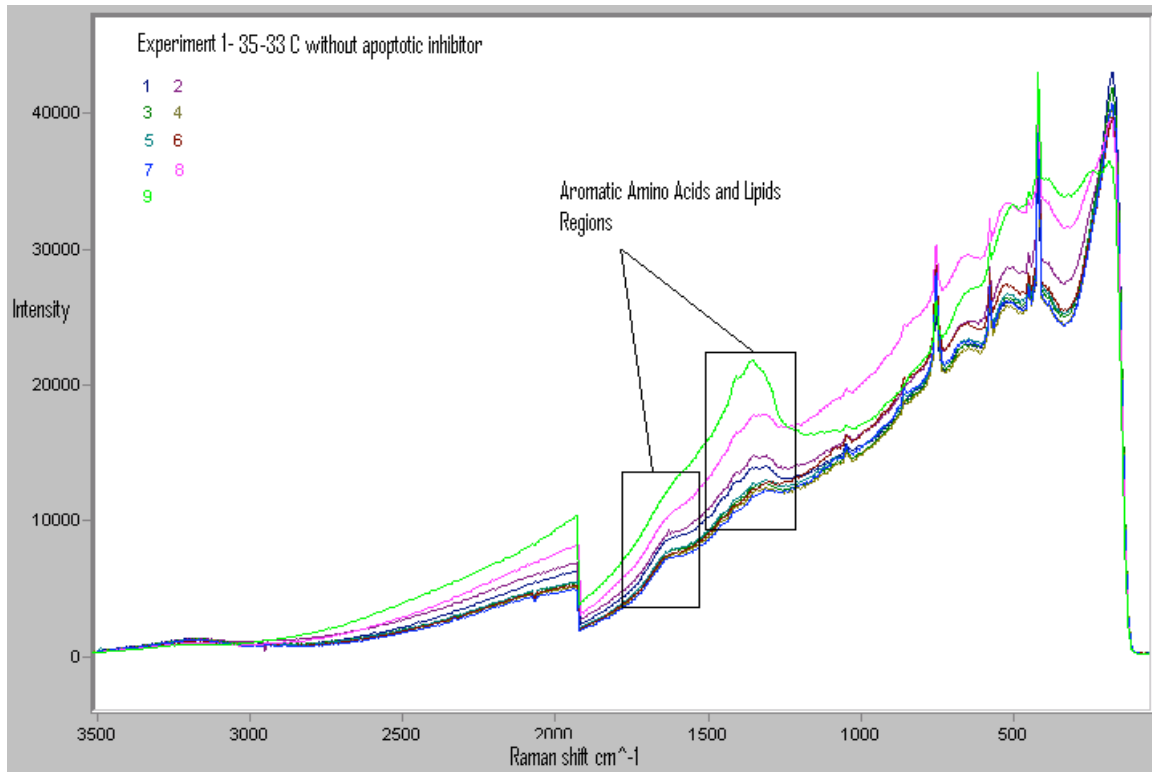
4.6 Determination of Viability using Raman Spectroscopy

Raman spectra from the four conditions and eight suspended CHO cell culture batches performed were analyzed with the purpose to find intra-cellular material such as RNA, DNA, amino acids, or lipids. The purpose of this exercise was to correlate characteristic peaks and their variation along the cell culture time with the cell viability. Given the premise that as a higher concentration of intra-cellular components is detected, the greater the possibility of cell wall rupture and consequently greater cell death, cell viability might be monitored and quantified with the Raman spectra. As shown in Figure 4.23 for the four conditions studied, the Raman spectra clearly show significant differences among the days of high viability (first culture days) as compared to the days of low viability (last culture days), as it would be expected.

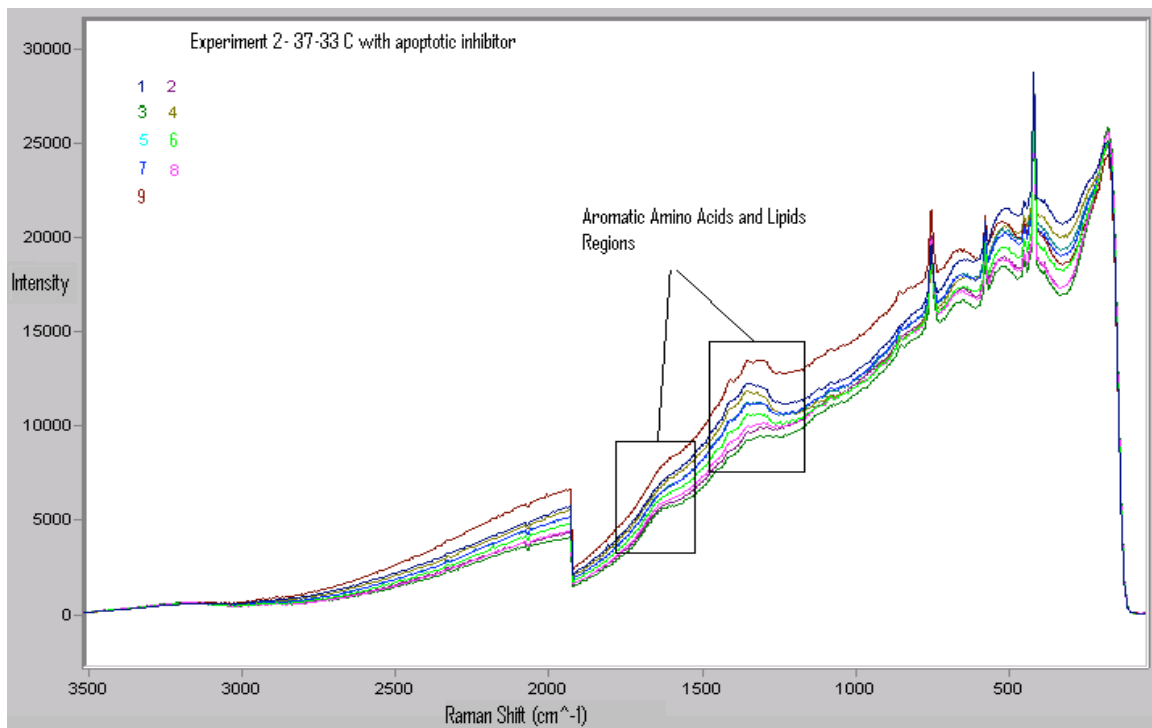
Noticeable spectral differences are observed in the range of 1350-1700 cm^{-1} , a typical area associated with protein (lipids), nucleic acids and aromatic amino acids peaks [9]. It was also suggested that these differences in the spectra are more likely to be a consequence of the cells being in different phases of their cycles. Similar observations were obtained by Mourant, et al. [10]. Certainly, the conducted experiments were not controlled to ensure that cells were at a particular phase of the cell cycle and that is why the our results can only be interpreted as an attempt to propose the Raman spectroscopy technique as a potential tool to detect in-line, analyze and quantify the spectral patterns that could be associated with the cell viability in suspended culture in future works.

There was a significant broadening and increment of the larger peaks in the range of 1351 to 1650 cm^{-1} , all of them in the lower wave number side. This could possibly indicate the presence of aromatic amino acids as a result of protein cleavage from dead cell lysis. All peaks observed that might have an intra-cellular relationship were associated with proteins, lipids, and aromatic amino acids. A decrease in these peaks even in the later days of the culture with addition of the apoptotic inhibitor (experiments 2 and 3, Figure 4.23 b and c), clearly show the effect in cell viability by the over-expression of the anti-apoptotic molecule.

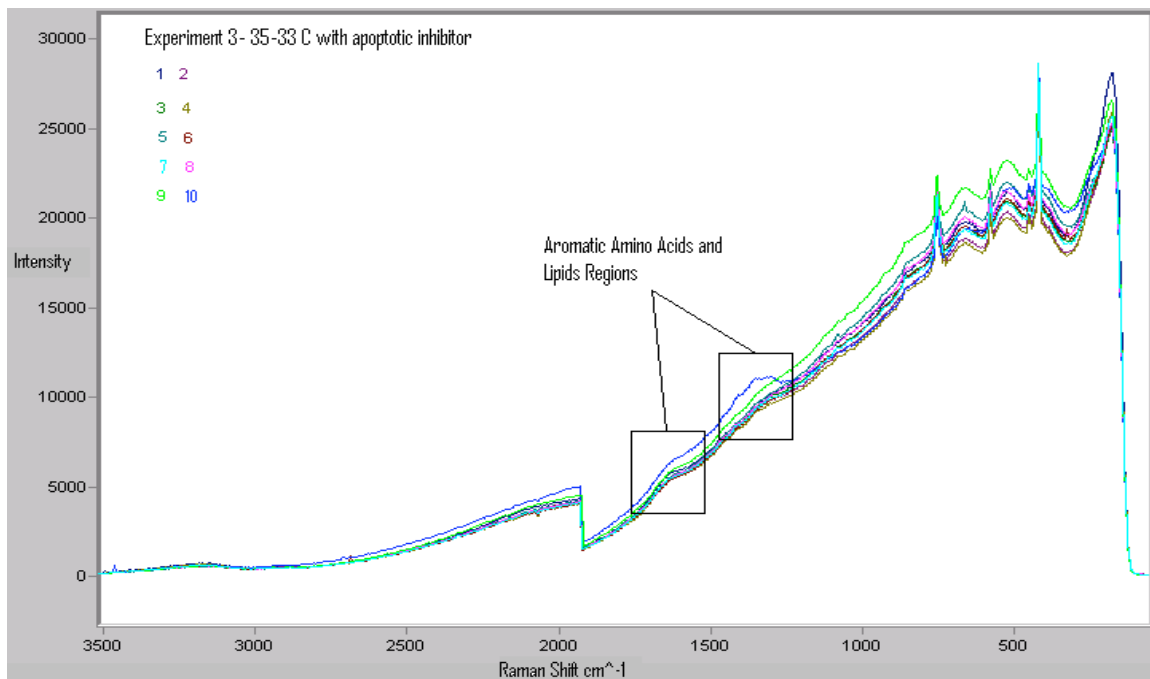
(a)



(b)



(c)



(d)

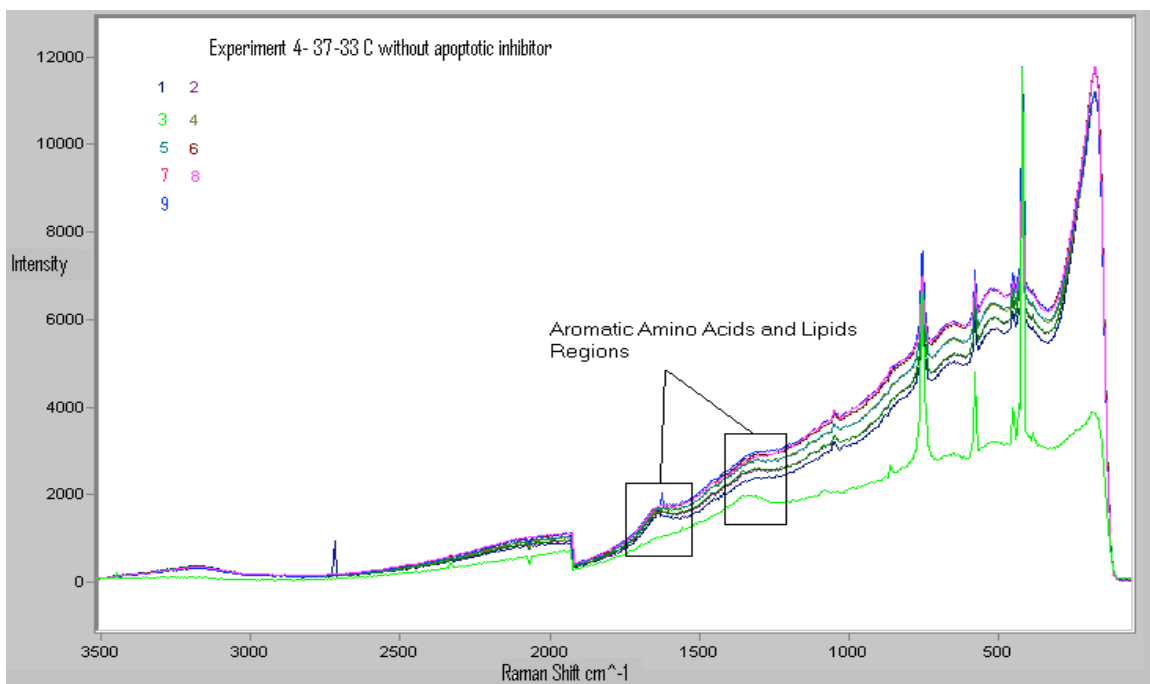


Figure 4.23. A Raman spectra of four experimental conditions. Aromatic amino acids and lipid regions are marked. Clear broadening and increase in peaks is also shown.

4.7 References

- [1] Haimanti, D., Yun-Seung, K., Dawn, E., Kinney, and Ch., Jan, D. (2009) Expression of Anti-apoptosis genes alters lactate metabolism of Chinese hamster ovary cells in culture. *Biotechnology and Bioengineering*, **103**(3):592-608.
- [2] Notingher I. (2007) Raman Spectroscopy Cell-based Biosensors. *Sensors* (7):1343-1358.
- [3] Zhang, X., Yin, H., Cooper, J., and Haswell, S. (2008) Characterization of cellular chemical dynamics using combined microfluids and Raman techniques. *Anal. Bioanal. Chem.* **390**:833-840.
- [4] Ren, M. and Arnold, M. (2007) Comparison of multivariate calibration models for glucose, urea, and lactate from NIR and Raman spectra. *Analytical and Bioanalytical Chemistry*, **387**:879-888.
- [5] Frost, R.L., Kristof, J., Rintout, L., and Klopogge, J.T. (2000) *Spectrochem. Acta A* **56**:1681-1691.
- [6] Mathlouthi, M. and Luu, D.V. (1980) Carbohydrates as raw materials. *Carbohydrates Res.* **81**:203-212.
- [7] Cassanas, G., Morssli, M., Fabregue, E., and Bardet, L. (1991) Analysis of metabolites in aqueous solutions by using laser Raman spectroscopy. *J. Raman Spectrosc.* **22**:409-413.
- [8] Montgomery, D.C. (2008) Design and Analysis of Experiments, Wiley-Inter Sciences. 680 pp.
- [9] Short, K.W., Carpenter, S., Freger, J.P., and Moursant, J.R. (2005) Raman spectroscopy detects biochemical changes due to bioliferation in mammalian cell cultures. *Biophysical Journal*, **88**:4274-4288.
- [10] Mourant, J.R., Yamanda, Y., Carpenter, S., Dominique, L., and Freyer, J.P. (2003) FTIR spectroscopy demonstrates biochemical differences in mammalian cell cultures at different growth stages. *Biophys. J.*, **85**:1938–1947.

- [11] Fang, L., Qian, H., Jiang C., Yuanlin, P., Roop, D., and Chuan, L. (2010) Apoptotic cells activate the “Phoenix Rising” Pathway to promote wound healing and Tissue Regeneration. *Sc. Signal.*, 3(**110**): 1-20.

5. Conclusions and Recommendations

5.1 High Viability Prolongation via Cytochrome C Inhibition and Best Operational Conditions

The inhibition of Cytochrome C with the over-expression of the apoptotic inhibitor in the media and two different levels of temperature shifts conditions were studied: a proposed temperature shift of 35-33°C, and the other one a process parameter usually reported in literature, a temperature shift of 37-33°C. On both temperature shift conditions, the objective was to initially adapt the cells to achieve a consistent exponential growth (35-33 or 37°C), and secondly, a temperature shift of 33°C to provoke hypothermia to reach growth stability. This final temperature level of 33°C will also push the cells into a survival state in which the only goal is to increase the production of by-products that result in L-lactate production and consumption (gluconeogenesis cycle), release of toxic agents such ammonium and finally, but not less important, to promote increase in production and secretion of a recombinant protein.

5.1.1 Conclusions

For the four cases reported and discussed in Chapter four, several data were acquired and analyzed. In the four experimental conditions variables such as cell density, viability, cell mean diameter, osmolality and glucose and L-lactate concentrations were collected. Of all data acquired the values of cell density, viability and L-lactate were primary evaluated as a source to identify if the over-expression of the anti-apoptotic molecule worked to provoked a consistent stability in viability and an increase in cell density that by consequence could extend a more healthy time to a suspended CHO cell culture bioprocess.

Of all goals mentioned related with this matter, just one of them was accomplished, the stability in viability and by consequence an increase in cell culture time with cell viability percents around 80 or higher, for both temperature ranges in which the over-expression of the anti-apoptotic was present. The best of all was the proposed range of 35-33°C at a step change of approximately 3 days to reach the hypothermic temperature (33°C). This

specific condition resulted in cell viability values of 90 or higher along the entire culture days in the bioreactor and over passed the usual stipulated days, reaching up to 12 culture days. Although this was an important success in this work, irregularities were observed in both cases in which the anti-apoptotic molecule was over-expressed. Increments in L-lactate concentration were clearly perceived, and a consistency (no higher and lower values) was found in cell density among the entire experimental runs associated to the presence of the anti-apoptotic molecule. Others changes in cell diameter were visualized and represented as Tables A.1 and A.2 in the Appendix. Of the analysis certain increment in cell diameter was observed for conditions with inhibitor addition only, being this factor the one directly affecting the cell diameter.

5.1.2 Recommendations and Future Work

As discussed earlier, eight bench-scale batches were performed with duplicate runs of four conditions mimicking industrial cell culture parameters at bench-scale. Each condition was duplicated to prove consistency and reproducibility. Even though improvements and consistency in viability were obtained, a more in-depth study must be made to determine what other metabolic pathways were affected by the over-expression of the anti-apoptotic molecule at the temperature shifts proposed and studied. Studies using molecular assays such as Western blot and ELISA could be used among others as reference methods to study the apoptotic cascade in the mitochondria that is activated by the Cytochrome C and was deactivated by the apoptotic inhibitor. Levels of each caspase could be detected by these assays and used as a deep proof of work.

It might be necessary for all conditions studied to scale up the cell culture bioreactor and determine if differences in results would be obtained. Such differences, if any, can occur for the cases of the anti-apoptotic media over-expression (by the quantities administered at bench scale versus large scale), but rarely should be seen in the temperature shifts. It is also recommended to study constant temperature levels along the entire cell culture time, such as 37, 35, and 33°C with and without anti-apoptotic over-expression to establish remarkable differences, if any. Finally the possible repercussions (if any) to the use of apoptotic inhibitors over-expressed in the media in commercial runs might be studied in

order to evaluate the effect (positive or negative) in the Downstream processing and yield of the product of interest.

5.2 Determination of Glucose and L-Lactate using Raman Spectroscopy

For the period of the work reported in section 4.3, a pronounced qualitative behavior in the suspended culture concentrations of the principal substrate and by-product (glucose and L-lactate, respectively) was observed. This was achieved modeling the spectrum obtained each day with chemometrics and its comparative performance of a cell culture batch respiration using HPLC and the Biochemical Analyzer YSI 2300 as reference methods. The ability to determine the culture dynamics without a sample pre-treatment or culture invasion, and in real time might suggest Raman spectroscopy as a powerful tool for the bioprocess monitoring with the advantage and potential of achieving a robust process control, automation, and PAT application to improve in commercial operation cost savings.

5.2.1 Conclusions

In the process of the principal substrate and by-product concentration determinations in this work, two factors were studied as ways to improve the cell culture upstream process. These factors were temperature shifts and apoptosis inhibition. Last one mentioned clearly affected the L-lactate dynamics and by consequence the gluconeogenesis cycle in the cells. All these changes were detected in a qualitative manner by the Raman spectroscopy technique used in the study. Higher cell densities are recommended through literature to get a clear spectrum related with viability.

For this case the cell concentration was never achieved, but our goals were accomplished and the technique was proven to be a powerful tool to at least identify and monitor changes in suspended cell culture dynamics. It is important to finally mention that the reliability of the model was tested for the four different conditions showing serious differences between conditions for the ranges of 500-600 and 700-800 cm^{-1} analyzed for

L-lactate, and 1000-1100 cm^{-1} for glucose, even with such differences an acceptable tendency and comparison with the routine equipment used could be established and validated. Correlations between 65 to 90% were observed.

5.2.2 Recommendations and Future Work

As discussed in previous sections, models for each condition were achieved. Calibration using culture media without the organism was done in order to distinguish between cells and metabolites. Values reported in literature for pure solutions and mixtures for L-lactate and glucose were also used to differentiate both metabolites. It could be more helpful for the Raman technique the continuous testing (more samples per day) of different conditions to search the maximum and minimum ranges of acceptable reliability for this analytical technique in suspended mammalian cell culture and get more feasible models. Another course of action is to test the technique in a large-scale environment, and test the technique in-line instead of off-line.

5.3 Determination of Intra Cellular Material and Viability using Raman Spectroscopy: a Possible Way to Determine Cell Health and Cell Viability.

Through the discussion in section 4.6, peaks with increasing intensities along time were observed between the 1400-1700 cm^{-1} . These peaks were associated in the literature as possible signals of cell death and culture instability. The ability to detect these changes in a qualitative way as a non-invasive manner, in-line, but mostly without the need to do any sample pre-treatment, makes of this technique a stronger candidate tool for the complete qualitative analysis of cell behavior in upstream bioprocesses and as a consequence being able to decrease operating costs and product instability. It is important to mention that this hypothesis on this kind of detection is still a matter of study in the field.

5.3.1 Conclusions

As discussed and shown in Chapter four the detection of the peaks that could be related with intra cellular molecules associated with apoptosis and cell instability were detected. Changes in four conditions studied were consistent with what could be expected from

them. For cases in which over-expression of the apoptosis inhibitor was involved, a reduction in peak intensity, and by consequence, a reduction in concentration, was observed for the peaks that could be associated with lipids and aromatic amino acids. On the contrary, for cases in which just temperature ranges were studied without the over-expression of the anti-apoptotic compound, an increase in peak intensity was noticed along the culture time. This could be related with the decrease in cell death but is a matter of study yet and common techniques such HPLC (to detect amino acids and lipids) and Western Blot or Elisa to monitor the levels of apoptotic molecules, should be used to prove this hypothesis. For the purpose of this work, just changes among the entire days of culture were studied in a qualitative way, which is why values of literature were used as possible “calibrators” for the detection of any intracellular molecule related with apoptosis. Only patterns and behavior of those peaks related with any intracellular molecule, in this case lipids and aromatic amino acids, were studied and differences between conditions and days were visibly shown.

5.3.2 Recommendations and Future Work

As discussed previously, a qualitative analysis of the lipids and possible aromatic amino acids was observed as reported in the available literature for mammalian cell biomolecular behavior and dynamics discussed and mentioned in section 4.6. The most important recommendation is the study of this hypothesis and results in a deeper way. More than patterns are needed to support this hypothesis in our work and others reported in the literature. Runs with more points through time, precise calibrations and reference methods with pure and mixture solutions of lipids and aromatic amino acids that could be present such as phenylalanine, for a reliable quantification of these molecules might be made. A future work should try to evaluate this additional hypothesis (aromatic amino acids and lipids detection), and identify some other peaks present and seen in the Raman spectra to acquire more knowledge on the cell dynamic in real-time.

Appendix

Table A.1 Viability for all runs with the respective cell diameters per run.

Time (Days)	Viab. 35-33 (%)	Diam. 35-33 (Microns)	Viab. 35-33 (%)	Diam. 35-33 (Microns)	Viab. 37-33 (%)	Diam. 37-33 (Microns)	Viab. 37-33 (%)	Diam. 37-33 (Microns)	Viab. 35-33 I (%)	Diam. 35-33 I (Microns)	Viab. 35-33 I (%)	Diam. 35-33 I (Microns)	Viab. 37-33 I (%)	Diam. 37-33 I (Microns)	Viab. 37-33 I (%)	Diam. 37-33 I (Microns)
1	94.0	13.9	91.8	11.4	96.3	13.0	93.8	13.6	97.3	13.0	97.9	13.8	92.7	12.1	93.8	12.9
2	93.1	12.3	86.0	13.5	94.0	12.7	93.1	13.6	95.3	13.8	92.8	13.8	90.7	12.1	91.3	13.5
3	92.7	14.9	89.7	14.2	94.4	12.8	95.5	13.3	95.9	15.0	94.2	13.2	88.8	11.8	95.3	13.9
4	94.3	14.6	92.4	14.2	94.2	13.6	92.0	14.3	93.5	13.3	90.7	14.4	88.1	12.3	93.5	14.0
5	91.5	15.0	96.5	14.2	90.9	13.9	93.1	14.3	94.1	14.1	92.6	14.5	84.3	12.4	91.5	14.3
6	81.0	13.8	95.8	14.2	94.9	14.6	95.5	14.5	95.1	15.9	91.0	14.5	83.6	12.6	92.2	15.1
7	60.6	11.4	93	14.9	88.7	15.3	92.0	14.1	92.3	14.2	90.0	14.5	82.8	13.4	89.3	15.1
8	38.1	11.8	80	15.1	84.5	14.2	87.2	13.7	90.4	14.7	91.0	14.7	78.0	14.0	88.1	15.4
9			65	14.2	73.3	14.4	53.7	12.7	94.4	16.4	90.0	15	80.0	14.3	80.3	15.4
10					59.2	13.0	32.1	12.0	90.1	17.0	89.0	15	79.0	14.3	80.0	15.5

Table A.2 Cell Density as a function of time.

Time (Days)	Cell density 35-33 (cells/mL)	Cell density 35-33 (cells/mL)	Cell density 37-33 (cells/mL)	Cell density 37-33 (cells/mL)	Cell density 35-33 I (cells/mL)	Cell density 35-33 I (cells/mL)	Cell density 37-33 I (cells/mL)	Cell density 37-33 I (cells/mL)
1	0.44	0.16	0.56	0.42	0.40	0.53	0.35	0.34
2	0.66	0.20	0.96	0.57	0.46	0.64	0.49	0.41
3	0.74	0.24	1.25	0.65	0.47	0.86	0.51	0.45
4	0.97	0.34	1.35	0.81	0.48	0.95	0.47	0.44
5	1.21	0.46	1.14	0.90	0.49	0.94	0.43	0.44
6	0.92	0.59	1.10	0.96	0.44	0.92	0.42	0.44
7	0.69	0.63	1.34	0.94	0.47	0.92	0.40	0.43
8	0.40	0.73	1.13	0.76	0.49	0.92	0.36	0.40
9		0.72	1.00	0.51	0.43	0.91	0.34	0.40
10			0.75	0.33	0.42	0.89	0.34	0.40

Table A.3 Specific growth rate (μ) and cell doubling time (t_d).

Specific Growth Rate At Day 3 (μ -cells/ml-h)	Cell doubling time (t_d -h)	Condition
0.011	63.01	35-33
0.014	49.51	35-33
0.003	231.05	37-33
0.009	77.02	37-33
0.002	346.57	35-33+I
0.004	173.29	35-33+I
0.003	231.05	37-33+I
0.001	693.15	37-33+I

Table A.4 Osmolality as a function of time.

Time (Days)	Osmo. 35-33 (mosm)	Osmo. 35-33 (mosm)	Osmo. 37-33 (mosm)	Osmo. 37-33 (mosm)	Osmo. 35-33 I (mosm)	Osmo. 35-33 I (mosm)	Osmo. 37-33 I (mosm)	Osmo. 37-33 I (mosm)
1	330	333	330	330	325	338	361	351
2	332	336	331	335	330	337	366	357
3	335	342	333	340	333	337	369	373
4	345	346	336	342	347	334	372	373
5	347	350	340	353	350	333	384	376
6	352	352	343	357	354	336	387	379
7	367	351	345	362	360	349	388	380
8	375	355	346	365	363	352	391	382
9		357	351	367	367	358	393	384
10			351	369	370	360	395	387